2009

Delay Modeling And Long-range Predictive Control Of Czochralski Growth Process

Dhaval Shah
University of Central Florida

DELAY MODELING AND LONG-RANGE PREDICTIVE CONTROL OF CZOCHRALSKI GROWTH PROCESS

by

DHAVAL SURESH SHAH
B.S. Maharaja Sayajirao University of Baroda, India, 1998
M.S. University of Central Florida, 2003

A dissertation submitted in partial fulfillment of the requirements
for the degree of Doctor of Philosophy
in the School of Electrical Engineering and Computer Science
in the College of Engineering and Computer Science
at the University of Central Florida
Orlando, Florida

Spring Term
2009

Major Professor: Christine Klemenz

ABSTRACT

This work presents the Czochralski growth dynamics as time-varying delay based model, applied to the growth of $La_3Ga_{5.5}Ta_{0.5}O_{14}$ (LGT) piezoelectric crystals.

The growth of high-quality large-diameter oxides by Czochralski technique requires the theoretical understanding and optimization of all relevant process parameters, growth conditions, and melts chemistry. Presently, proportional-integral-derivative (PID) type controllers are widely accepted for constant-diameter crystal growth by Czochralski. Such control systems, however, do not account for aspects such as the transportation delay of the heat from crucible wall to the crystal solidification front, heat radiated from the crucible wall above the melt surface, and varying melt level. During crystal growth, these time delays play a dominant role, and pose a significant challenge to the control design.

In this study, a time varying linear delay model was applied to the identification of nonlinearities of the growth dynamics. Initial results reveled the benefits of this model with actual growth results. These results were used to develop a long-range model predictive control system design. Two different control techniques using long range prediction are studied for the comparative study. Development and testing of the new control system on real time growth system are discussed in detail. The results are promising and suggest future work in this direction.

Other discussion about the problems during the crystal growth, optimization of crystal growth parameters are also studied along with the control system design.

To my parents, Suresh Shah and Kokilaben Shah, who have taught me the values of hard work, discipline and sacrifices.

ACKNOWLEDGMENTS

I would like to express my gratitude to all those who gave me the possibility to complete this work.

First, I would like to thank the Department of Electrical Engineering and Computer Sciences (EECS) of the University of Central Florida (UCF) for providing me support throughout my studies. Then, I would like to express my thanks to Dr. C. Klemenz, whose continuous encouragements and support have allowed me to perform and complete this work. During my studies, I have learned many important lessons not only in the area crystal growth but also for life from her. In particular, I can mention simplicity, hard work and optimistic attitude. I am glad that I could work in a field where I could really apply my understanding of the area of controls, and at the same time learn and contribute to advances in a field, crystal growth, so important for technological applications.

In addition, I would like to thank Dr. Malocha, Dr. Haralambous, Dr. Dhere and Dr. Schoenfeld, who served on my thesis committee and provided their support. Their comments were very helpful to the performance and improvement of this study.

I cannot thank enough to my parents, my brother and my wife, whose encouragements and sacrifices kept me focused during my study.

TABLE OF CONTENTS

LIST OF FIGURES

LIST OF TABLES

CHAPTER 1: INTRODUCTION

In this chapter, the main objective and problem statement are first discussed. Then, an introduction to the time delay system and predictive control is presented. The detailed description is presented later, in the respective chapters. An outline of the dissertation is given at the end of this chapter.

1.1 Problem statement and objective

The growth of crystals from the melt by Czochralski technique is a widely accepted and economic method to produce bulk single crystals. In this technique, the crystals are pulled from the melt using a seed crystal [1]. The temperature of the melt is kept close to the melting temperature of the material [2], and the driving force for growth is provided by the temperature gradients that exist at the growing interface. The heat from the growing interface is removed through the crystal. The efficiency of this heat removal process is governed by the thermal conductivity of the crystal material. The thermal conductivity of oxides is much lower than Si or other semiconductors. Therefore, oxides have to be pulled at a much lower rate, and this is very challenging in terms of process control. During the growth, the crystal is rotated, which produces a very complex hydrodynamic pattern in the melt and at the growing interface. This rotation also ensures a more homogeneous distribution of the temperature gradient, but at the same time, it produces localized variations of the growth rate that can lead to crystal defects such as transverse growth bands. Only a few aspects are discussed herein, but from this already,

one can easily understand that the Czochralski growth process is extremely complex and implies knowledge in a variety of fields.

The basic objective in Czochralski growth is to stabilize the growth process thermodynamically, to produce a low defect crystal with the constant diameter. This can be achieved by measuring the crystal weight as an output signal of the growth process, which is then used as a feedback to control the heating power as an input signal. Among others, the crystal quality depends on the growth stability, on the chemicals used, on the design of the furnace, on the temperature gradients in the melt and crystal-melt interface, and on the composition of the growth atmosphere [[3], [4], [5], [6]].

Presently, proportional-integral-derivative (PID) controllers in the double loop cascade structure are the most implemented industrial method to control the Czochralski growth process [[8], [9], [10], [11]]. Generally, such controllers are tuned based on the lumped-parameter linear models of the system that neglects delayed effect and nonlinearities. During the growth of oxide crystals, there is a time delay between the applied input power and the output response (growth rate or diameter). The time delay is mainly caused by the slower growth rate and the lower heat conductivity of the oxide materials compared to the semiconductor materials [4]. This time delay, if not considered during the control system design, can destabilize the process or create oscillations during the crystal growth, even for small perturbations [7].

The Czochralski process is a nonlinear process, where all the process variables and parameters are interrelated and have different time scales [1]. Therefore, there is no true steady state as the parameters keep varying during the growth. The most common variables that affect the growth process are the melt level and the crystal size. These are

continuously changing during the growth. To control such complex process, the tuning parameters need to be adjusted during the growth by some technique. For this, the gain scheduling algorithm is a better alternative, compared to PID controllers, because it considers the time-varying process parameters for the tuning. However, because of the dependence of the crystal quality on the stability of all process parameters, still a better model of the process is needed. In particular, such model needs to be able to simulate the time delay, and not just the time scales. This is required for the indirect control system design.

Although the growth process is nonlinear, the nonlinear models, described by partial differential equations, may not be applicable to real-time control systems. Finite element method can be used to solve such equations, but it is too slow to execute for the real-time control [3]. Nonlinear models are nevertheless helpful for the understanding of the crystal growth process, but they have significant limitations because various properties of the material must be known. Hence, lower order models, or reduced order models, were also proposed [[8], [9], [10], [11]]. However, once again, such models do not consider the time delay, which is a particularly critical parameter for the growth of crystals that require a very slow growth rate. In order to achieve the sufficient crystal quality (low density of defects), many oxide crystals require to be grown at very slow pull rates, typically less than 1.5mm/h. The slower the growth rate (or pull rate), the more challenging it becomes for the control system to provide the required stability.

When the growth rate is slow, the time delay in the heat and mass transport lead to poor process control. This delay can be of the order of few minutes, at the early stages of growth, and continuously changes as the growth proceeds. Besides the delay in heat

and mass transfer, the time delay is also introduced because of the way the growth rate is measured.

The objective of this research was to design a versatile computer control system that includes non-linearity and time-varying time delay, and that is optimized for the growth of oxide crystals at very slow growth rates. An adaptive Long Range Predictive Control (LRPC) of time-varying unknown time delay system is considered for the control design. The Long Range Predictive Control by model predictive technique and PID were studied for comparison. A modeling of the system drawn from the recursive root mean square (RLS) is preferred to predict the system performance in the finite horizon with varying time delay and gain.

1.2 Time delay system introduction

Time delay (TD) systems and their control systems are vast and active fields in the mathematical and control research. Some of the research and review can be found in [14]. The detailed study of the TD systems analysis, control and optimization is presented by various authors. Here, the general significance of time delay system and representation are given.

By definition, the time-delay (TD) systems are the systems in which time delays exist between the inputs (control signals) to the systems and their resulting effects (outputs) on them. This time-delay can be due to transport or measurement delays. Time-delay occurs often in various engineering fields for example electronic, mechanical, biological and chemical processes. In general, it represents the transport time or

calculation time. The mathematical representations of such processes can lead to delay-differential equation or functional differential equations [14].

Time delay systems are a compromise between the lumped parameter systems (described by the ordinary differential equations) and the distributed parameter systems (described by the partial differential equations with initial, boundary conditions and unknown parameters). Often the delay for fast acting processes can be neglected without any considerable effect, like in the motor vehicle engine. On the other hand, some slow processes cannot be modeled and realized without time delay, like crystal growth of oxides. These kinds of processes are generally distributed parameter system. Identifying exact models of these processes can be much more complicated for computational realization in real-time control system.

For such distributed parameter system, each mass or energy storage element provides the first order element in the model for simplicity [15]. Therefore, one can consider a process having N first order elements in series, each having time constant τ / N. The resulting transfer function can be represented as:

$$G(s) = \frac{1}{\left(1 + s\tau/N\right)^N} \tag{1-1}$$

Here, s is the Laplace operator. For the distributed parameter system, such as crystal growth, the value of N can be considered as infinite because each atom behaves like an individual system. The simplification can be represented as a first order (or a second order) system with pure dead time τ_d and time constant τ. This system can be described by the following equation, which is a first order time delay system.

$$G(s) = \frac{K}{(1+\tau s)} e^{-s \cdot \tau_d} \tag{1-2}$$

Here, K is the process gain. To describe this, a simulink model of order 10 is presented for better understanding in Figure 1-1. Simplified of the model can be presented as second order model with time delay of 6.5s and gain of 2 as shown in the Figure 1-2. The least square method can give more accurate model if time delay is known at priory. This model is better than the first order model presented in the lumped parameter model (shown in Figure 1-2 as transfer function 10).

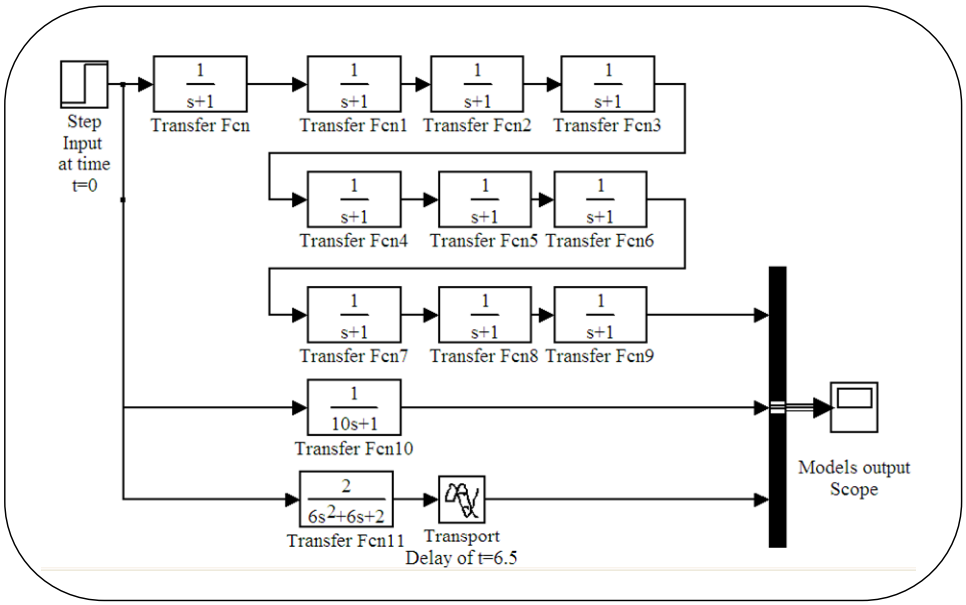

Figure 1-1: Matlab-Simulink model for transport delay

Hence, the time delay provides and acceptable model for such systems. In principle, the physical process may have several different delays; their collective effect can be simplified as single delay τ_d. For this delay system, the main difficulty in control

system design and tuning is the response lag, which may lead to unstable behavior even at the low controller gains. This limits the amount of control action possible with the presence of time delay. For example, in Crystal Growth and Epitaxial Lab (CGEL) at University of Central Florida, Microcon controller is used to control the growth process. The controller is set at the lowest possible values of P (Gain = 0.1) and I (Reset=0.001) gains for PID control of growth rate loop with sampling rate equal to 4 second.

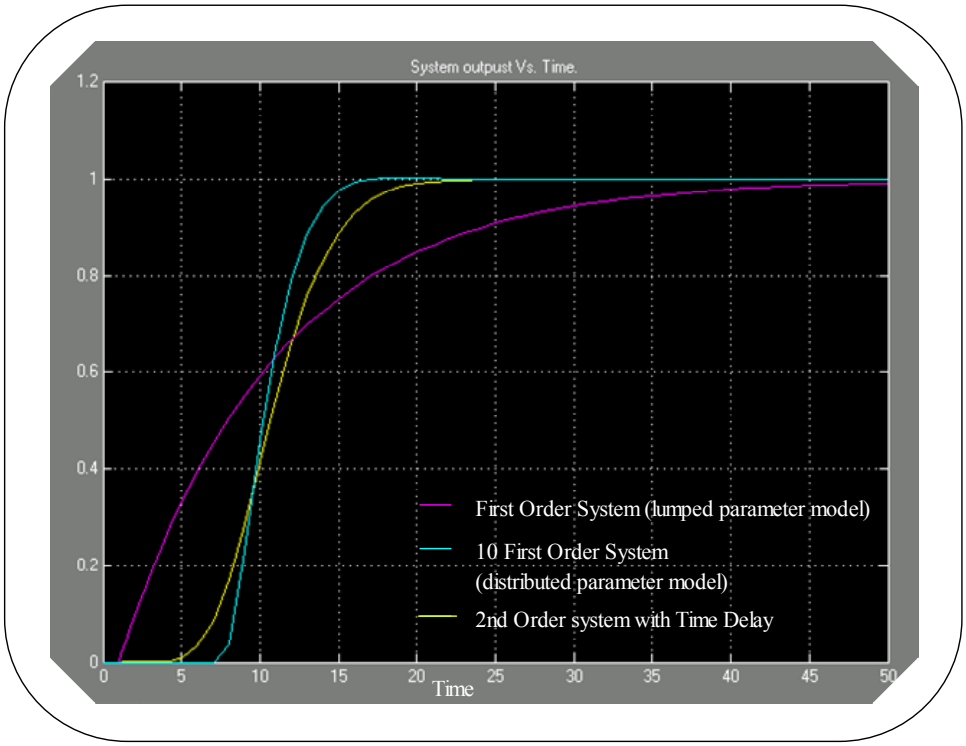

Figure 1-2: Models output for simulink models

The time-delay system can be represented as continuous time system or discrete time system. Any system has mainly two major sets of characters, namely input variables ($u(t)$) and outputs variables ($y(t)$). The third character is called state variables (n-

dimensional vectors $x(t)$ at instant of time t), which represents information of the system at time.

For continuous-time time delay system, the state at any time t is defined over an interval $[t', t]$, where t' depends on the delay present in the system. In other words, the state space of continuous-time time delay system is Banach space of continuous functions over a time-interval of length τ_d. Here, τ_d is the largest time delay in the system, mapping interval $[t-\tau_d, t]$ into R^n. For continuous-time time delay systems, the state and output equations in the general form can be represented as follows:

$$\dot{x}(t) = f(x(t),\ x(t-t_{d1}),\ \ldots,\ x(t-t_{dN}),\ u(t),\ u(t-t_{u1}),\ \ldots,\ u(t-t_{uR}),\ t)$$

$$y(t) = g(x(t),\ x(t-t_{d1}),\ \ldots,\ x(t-t_{dN}),\ u(t),\ u(t-t_{u1}),\ \ldots,\ u(t-t_{uR}),\ t)$$

(1-3)

Here, f and g are nonlinear vector valued functions. Time delay periods $t_{di} > 0,\ i = 1,\ 2,\ \ldots,\ N;$ and $t_{uj} > 0,\ j = 1,\ 2,\ \ldots,\ R$ represent the state and control delays in the system, respectively. For the discrete-time time delay system, with constant sampling period it can be represented as follows. Here, the delay is assumed to be multiple of sampling period.

$$x(k+1) = f(x(k),\ x(k-1),\ \ldots,\ x(k-N),\ u(k),\ u(k-1),\ \ldots,\ u(t-R),\ t)$$

$$y(k+1) = g(x(k),\ x(k-1),\ \ldots,\ x(k-N),\ u(k),\ u(k-1),\ \ldots,\ u(t-R),\ t)$$

(1-4)

Here, the linear discrete time time-varying delay system is considered for the crystal growth process.

1.3 Long range predictive control

The model predictive control (MPC) strategy is one of the most common control strategies is used in process industry after PID [[16], [17]]. The basic idea is to introduce the known characteristics of the process by building a suitable model [18]. The next step is designing a control system to minimize the required objective function by using the error between the prediction from this model and the actual system in the predictive horizon. The PID control action depends on past performance, but MPC control action depends on the predictive future performance [[19], [20]].

There are many advantages of the Model predictive control over the other methods. For example, it can be used to control various processes like long delay times, unstable systems, non-minimum phase systems other complex processes and for the batch process even though the process model is always varying [[16], [21]]. The predicative control performs better for the process which has a significant delay because the future dynamics and output of the system can be well-defined [[22], [23], [24]]. In self-tuning control, the control signal is calculated based on the difference of the output to the reference set point at a particular time in the future [[17], [24], [25], [26]]. However, the Long Range Predictive Control (LRPC) is intended to control the output at set point over a defined range of time in future. The detailed study of MPC is discussed in Chapter 3.

1.4 General outline

The first chapter was an introduction presenting the main objective of this study and the problem statement.

Chapter 2 is a literature review on Czochralski crystal growth using the crystal weighing technique. All aspects of the growth method, including the structure of the process control system and the measurement of various parameters are presented.

Chapter 3 relates to the Long Range Predictive Control (LRPC) technique. The general recursive least square (RLS) technique, which can be applied to identify the real-time model of the system, is discussed. The mathematical derivation of LRPC technique with the real-time implementation and parameter selection are also discussed. Identifying the time delay during the real-time is left for future work.

Chapter 4 presents the work carried out in this study to model the Czochralski crystal growth as a time delay system. The general control structure for the Czochralski growth with the LRPC technique is presented. Results are evaluated.

Chapter 5 represents the new controller structure developed during this study. It will discuss the software developed with LabVIEW. Real-time application related issues are also discussed.

In Chapter 6 the result of growth experiments, carried out by using these new control programs, are presented.

Chapter 7 is a discussion on future work, and the conclusion.

CHAPTER 2: CZOCHRALSKI GROWTH FUNDAMENTALS

In this chapter, a literature review of the Czochralski crystal growth process controlled by crystal weighing technique is presented. The growth method, control structure, and measurement of various parameters are discussed.

2.1 Introduction to Czochralski growth process

The Czochralski growth method is one of the most important melt growth techniques used to pull single crystals from their melt [1]. The technique is widely employed to grow single crystals of a variety of materials in different sizes ranging from small crystal diameters of a few mm, up to crystals with very large diameters for commercial purposes (silicon). This technique can be used for the growth of crystals over a wide range of temperature, from low-melting compounds to very high-melting temperature (yttrium silicate, for example) [[27], [28], [29], [30]]. The upper temperature limit is usually set by the melting temperature of the crucible material that is used for the growth, which is 2,400 degree Celsius for iridium. Hence, it is generally considered relatively safe to grow (oxide) crystals up to about 2,100 degree Celsius.

The basic principle of the growth technique appears to be simple, in a first approach, and the procedure is quite intuitive. The required amounts of chemicals are mixed and molten in a crucible of suitable size. The crucible is placed in proper thermal environment (insulation) in the furnace. Resistive heating or inductive heating is applied, depending on the melting temperature of the crystal to be grown. For oxides, RF heating is usually used. The crystals are grown from their congruent melt composition, which can

be different from the stoichiometric composition. The chemical preparation method may vary with different materials and growth experiments. The size of the crucible depends on the required crystal diameter and its length. For oxides, the crucible is made up of heavy metal, Iridium for high-melting oxides, or platinum if a lower growth temperature can be applied. In a typical growth experiment, the crucible containing the chemicals is heated above the melting point of the material. The chemicals are kept molten for a while until chemical and thermal stability are reached. Before the seeding, the temperature is reduced progressively and manually near the melting temperature of the crystal, ideally just above of its melting point.

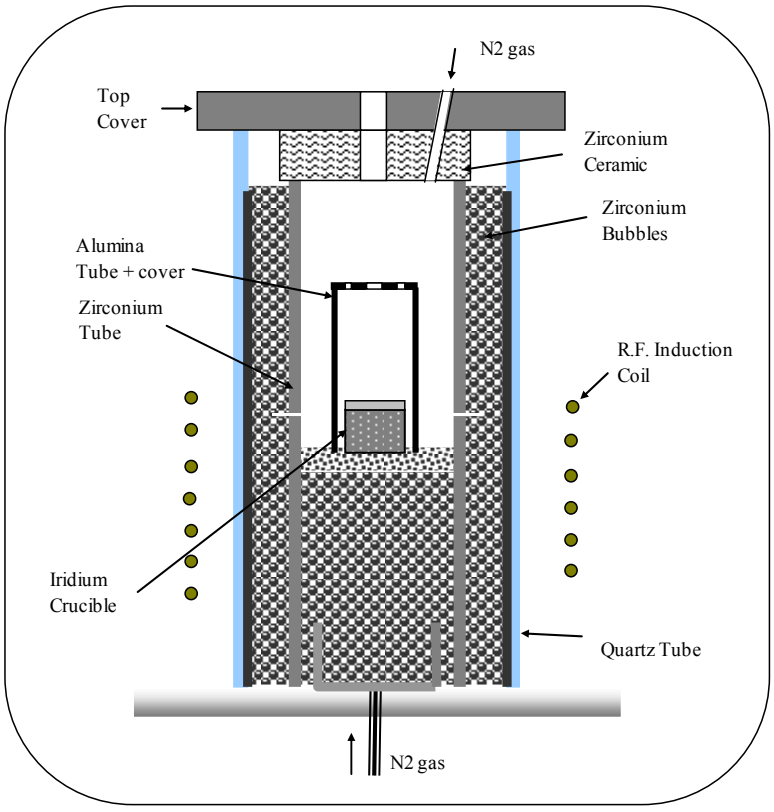

Figure 2-1: Typical crystal growth chamber at CGEL lab

The seed is prepared with required crystal orientation, polished and etched according to the desired growth orientation of the crystal. Normally, the seed is made up of the same crystal grown earlier. If it not available, platinum wire or other seed can also be used to pull a first crystal that will then be used to prepare seeds. Proper rotation rate is adjusted for seed holding mechanism to support the meniscus at the solid-liquid boundary. The seed is lowered and dipped vertically into the center of the melt, which is the coldest part of the melt surface. Once the thermal stabilization is reached, the seed is pulled out with the suitable pulling speed according to the crystal specification. Preferred pulling speed can be different for different crystal and crystal size. Crystal growth is then continued till required length of the crystal is achieved. Once it is pulled out the melt, the crystal is cooled down slowly to the atmospheric temperature to avoid thermal stress.

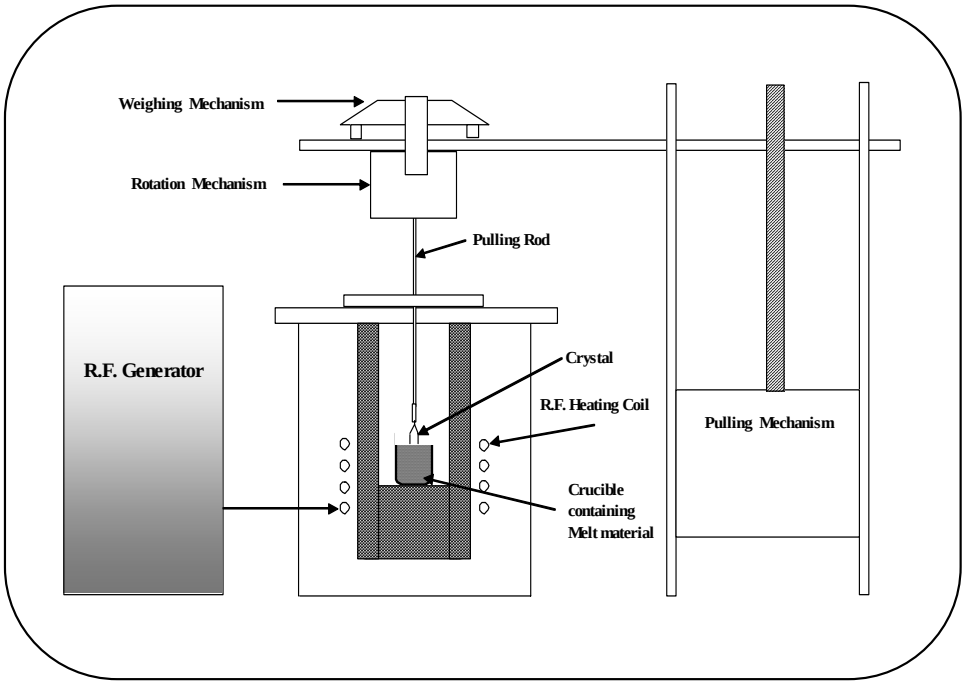

Figure 2-2: Complete Czochralski growth process

The heat conduction from melt to solid supports the crystallization front near the melt-solid boundary. The temperature of the crucible and melt, thus the temperature of the interface base, is controlled to grow the crystal of required diameter. For high temperature growth (above 1000 degree Celsius), an RF (Radio Frequency) heating system is used to heat up the crucible. The growth atmosphere is controlled depending on the crystal growth under consideration. The schematic presentation of the typical crystal growth process in the CGEL lab at UCF is shown in the Figure 2-1 and Figure 2-2.

2.2 Crystal structure

Based on the geometry of the crystal, there are mainly four crystal parts as shown in the Figure 2-4.

- In neck growth, the diameter of the crystal is reduced. For example, seed diameter reduced to 3mm diameter from initial 4.8 mm diameter. This early decrease helps to lower impurity and defects propagation from the seed to the crystal [6]. This growth is an important and difficult part of the growth. The growth process is sensitive for any perturbation. Slight change in melt temperature can lead to seed melt (disconnect from the melt) or sudden abnormal growth because of rapid crystallization. Therefore, the melt temperature during the seeding has to be suitable to support the meniscus between the melt and the crystal. During neck growth, the growth rate is in the range of the tolerance of the weighing mechanism about ± 0.1 g/sample. For example, the growth rate of oxide crystals is 0.1 g/h for 3 mm seed diameter. Therefore, applying automatic control is a challenge. Generally, the operator closely observers growth process during neck growth, which is very often done manually.

- During the cone growth, the crystal diameter is increased from the initial diameter to the final required diameter. The growth rate increment depends on the half cone angle, which represents the maximum allowable growth rate increment for the particular crystal [30]. The power of the generator is controlled in such a way to increase the crystal diameter. Initially, the growth rate is increased slowly. During the middle section, the growth rate is increased rapidly. Again, at the end of the cone growth, the growth is slowly increased for the smooth transfer to the cylinder phase. Sharp edge near this transfer is to be avoided, as this would deteriorate the crystal quality.

Figure 2-3: Abnormality during seeding

- From application point of view, the most important phase is the cylindrical phase. The crystal growth process runs for several days in this phase. During this phase, the diameter of the crystal is constant and is maintained until the crystal has reached its desired length. Also, during this phase, the thermal and fluid dynamics of the process vary because the height of the crystal increases while the melt level decreases [[31], [32]]. Thus, in this phase the process can be dynamically described as time-varying

model. The automatic control system should be adaptive with these changes [[33], [34], [35], [36]].

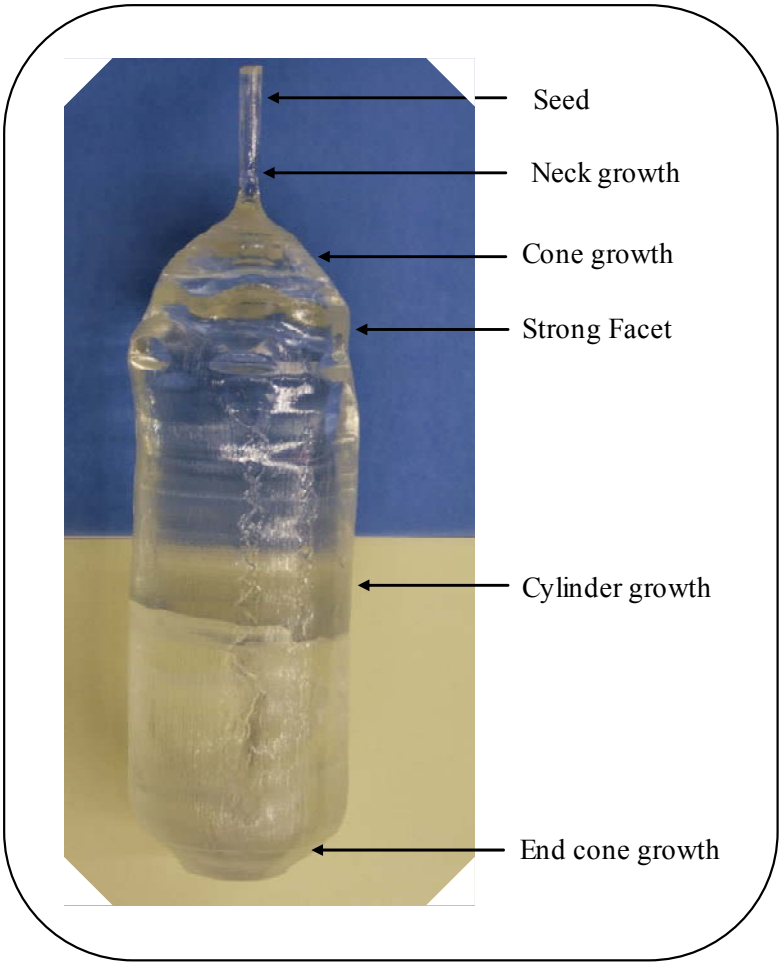

Figure 2-4: Crystal geometry

The last phase of the growth, after the crystal has reached its final length, is the end cone growth. An end cone is required in order to avoid crystal defects that would be generated if the crystal would be directly pulled out with its full diameter. Such defects could then lead to the cracking of the whole crystal through their propagation from the bottom of the crystal into its cylindrical area.

2.3 Linear dynamics of the Czochralski growth

The dynamics of the Czochralski growth process has been studied by various researchers [[1], [3], [8], [11], [31]]. The growth process can be described as a time-varying process. Nonlinear and partial differential equation based models have been presented by various researchers, but they are only applicable to the particular crystal and growth process used by the authors [[24], [25]]. The model developed in this work is independent on the crystal material, and can be used, in principle, for any Czochralski growth equipment.

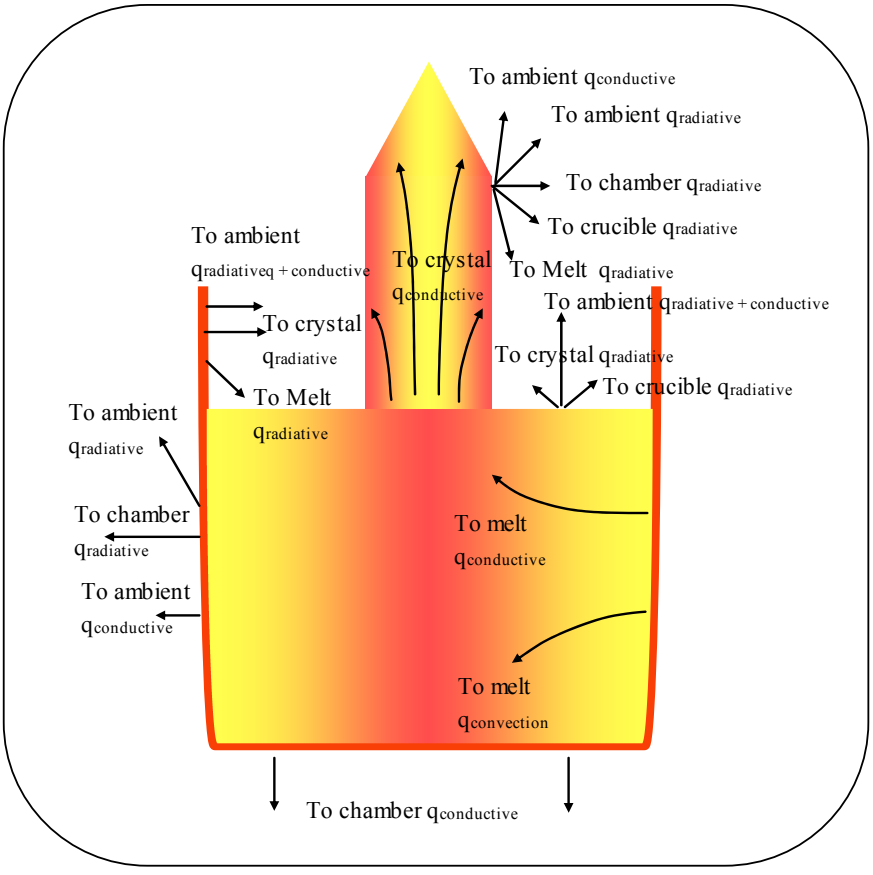

Figure 2-5: Typical heat transfer during the Czochralski growth

Here, a brief review of the linear model and the stability analysis based on perturbation analysis up to the first order is presented for further reference. A detailed discussion on the linear model can be found in [[1], [3]].

For the high temperature crystal growth like oxide crystals, the main power input of the process is R.F. heating source, which is controlled by suitable controller. A crucible's cylindrical outer surface is heated by R.F. induction from an induction coil surrounding the growth chamber. The heat transfer during the crystal growth is mainly driven by radiation and conduction between different parts of the chamber [3]. A typical heat transfer mechanism from various bodies during the growth is presented in the Figure 2-5. The complete heat and mass transfer during the growth can be presented as parabolic partial differential equation with time-varying boundary conditions and initial conditions [[3], [34], [35]]. The simulation from these equations gives a good insight of the process but that is not useful when applied for controlling the real-time process because of complex computations. In addition, this simulation requires some assumptions to simplify the simulation like infinite length of the crystal, axi-symmetry of the system and the shape of the crystallization front. Therefore, the linear model is generally preferred to design the automatic control system [[33], [34], [35]] for constant diameter.

During the heat transfer, heat from the crucible is transported from the crucible walls to the crystallization interface, by conduction, radiation and convection in the melt. At the growth interface, the heat conduction in the crystal is equal to the latent heat generation due to crystallization of material plus heat conduction from melt to crystal [1]. This heat transfer mechanism decides the base temperature of the growth interface. The base temperature of the interface decides the contact angle and the height of the

meniscus, which in turn decides the crystal diameter. Thus, this heat conduction at the growth interface defines the meniscus dynamics. However, crystal size and diameter also affects the interface temperature. The temperature of the crystallization base cannot be measured during the growth. Hence, in the weighing technique, the diameter of the crystal is estimated using the load cell or weighing mechanism [[12], [27], [28], [30]].

2.3.1 Meniscus dynamics

The crystal radius (r_c) is a function of the meniscus height (h), contact angle (θ_L) between solid-liquid and the base temperature at the solid-liquid interface (T_B). Figure 2-6 represents a general schematic of the meniscus supported by a growing crystal. Suppose that some perturbation in the thermal stability leads to increase in the height of the meniscus. This leads to decrease the contact angle so that the radius of the crystal also decreases [1]. This decrease in the radius helps to increase height further. Thus, crystal pulling is inherently unstable process. The same is true if perturbation leads to decrease in meniscus height. However, there is a unique meniscus height, corresponding to a unique input power for which the crystal grows at required radius at particular pulling speed. The material properties play an important role for deciding the contact angle and the height of the meniscus for the particular radius. The relationship between meniscus height, contacting angle and crystal radius can be presented as Laplace-Young equation [1]. The detail study of the thermal and the fluid dynamics of the process can be found in [3]. However, only the first order perturbation model is enough to describe the model as explained in [1]. In other words, radius is not only the

parameter that changes with the base temperature. Base temperature changes heat and mass transfer at the crystallization interface.

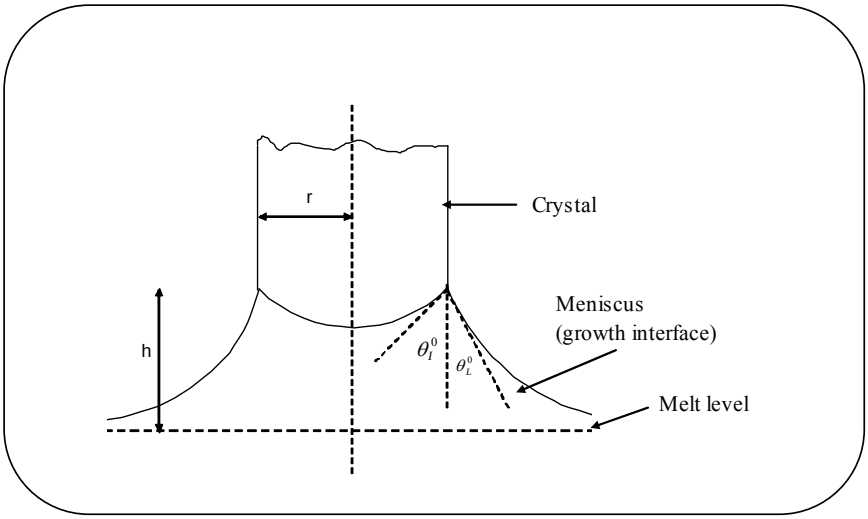

Figure 2-6: Schematic representation of meniscus at the growth interface

2.3.2 Effect of base temperature to the crystal radius

Using approximation of the Laplace-young model, perturbation theory, eliminating meniscus height change and contact angle change, the effect of the base temperature to the crystal radius can be represented by the second order transfer function as follows:

$$\frac{r_c(s)}{T_B(s)} = -\frac{C}{(s^2 + As + B)}$$

$$A = \frac{k_L G_L^0}{h_0 L} - \frac{v_0 h_0^2}{r_0^2 \sqrt{2\beta} \cos\theta_L^0}$$

$$B = \frac{v_0}{L r_0 \cos\theta_L^0}\left(\frac{k_S G_S^0 (1-\sin\theta_L^0)}{h_0} - \frac{h_0 k_L G_L^0}{r_0\sqrt{2\beta}}\right)$$

$$C = \frac{2k_L v_0 (1-\sin\theta_L^0)}{h_0^2 L \cos\theta_L^0}$$

k_L, k_S = Thermal conductivities of liquid and solid respectively

G_L^0, G_S^0 = Axial temperatue gradient in liquid and solid respectively

v_0 = Axial growth rate or actual pulling speed

h_0 = Initial meniscus height

r_0 = Initial radius of the crystal

β = Laplace constant

θ_L^0 = Characterisitc material conatact angle

(2-1)

In above equation, the negative sign is due the fact that any increases in the base temperature cause the crystal diameter to decrease eventually and vice versa.

In addition, the actual pulling speed should include the rate of change of the melt level (h_m).

$$v_0 = v_p - \dot{h}_m$$

These equations are drawn according to linear perturbation theory with the assumptions of semi-infinite crystal cylinder and the interface temperature equals to melting temperature T_m of the material.

In actual crystal growth process, change in the base temperature does not change the radius immediately. Due to the heat conduction inside the crystal and the shape of present interface, it takes some time (time delay) to change the radius effectively. This time delay depends not only on crystal diameter and temperature change but also on the length of the crystal, the crystal position in the melt, the shape of the interface and the surrounding environment [3]. Therefore, the process can be represented as time delay, or

so called second order lag plus delay, in the above equation. The final radius is reached when the heat transfer across the interface becomes stable.

2.3.3 Effect of power on the base temperature

As described earlier, the input to the process is the power supplied to the crucible outer wall by R.F. induction coil surrounding the growth chamber. The power change delivered to the crucible changes the melt temperature gradient, which is difficult to measure and quantify at real-time. Generally, the melt temperature is assumed constant and equal to the base temperature of the interface T_B. In addition, for high temperature growth process, the radiation is the main source of the heat transfer.

From energy transfer balance equation in the melt, the transfer function of the power supplied to the base temperature can be presented as follows:

$$\frac{T_B(s)}{P(s)} = \frac{1}{(m_h C_h + m_L C_L)s + \alpha}$$

Where, $\alpha = \dfrac{4P_0}{(m_h C_h + m_L C_L)T_0}$

$m_h, m_L =$ Mass of heater (in this case it is crucible) and melt respectively

$C_h, C_L =$ Specific heat of the heater (crucible) and the melt respectively

$P_0 =$ Steady state input power

$T_0 =$ Steady state melt temperature

(2-2)

Again, this equation is drawn by applying linear perturbation theory approximated up to the first order. As the crystal grows, the melt level changes due to the mass of melt

m_L decreases. As a result, the process parameters keep varying. In other words, the melt level change not only causes the melt and crucible temperature to vary, but also causes the Eigen-structure of the model to change with time [1]. In actual process, the transport delay of heat from crucible to the base of the meniscus has to be considered, specifically for the oxide crystals growth, due to the large thermal capacitances within the system. In perturbation analysis up to the first order, this delay is neglected by ignoring thermal gradient in to the melt.

However, this delay can destabilize the process and process may oscillate if the tight control is provided. To avoid this, the tuning parameter can be reduced by compromising performance, which becomes sluggish. Although, this analysis is valid, in general, up to certain temporal frequencies as described in [1] but for the oxide crystal, unlike silicon crystal, the low thermal diffusivity can create large delay. This delay is not negligible. This time delay depends on the melt level and flow pattern in the melt [3]. The flow pattern can be different for the different crystal and the rotation rate. Hence, the complete model of the crystal growth process is described as time-varying time-delay model instead of linear time-varying system. In this study, the effect of this time delay is considered to design proper controller structure.

The overall transfer function of the process is obtained by combining two-transfer function equations: (2-1) and (2-2). The transfer function has three time-varying poles. The total delay can be considered as combined delay.

2.3.4 Dynamic relation of radius to weight

Several techniques for measuring the crystal radius during the growth are proposed and are in application today but one of the most widely accepted is the crystal

weighing technique or the differential weight mode technique. In this method, the weight change of the growing crystal is measured as a measure of radius. However, the relationship between the weight signal and the radius is little complicated and can be drawn by force on the load cell. The force experienced by the load cell on which the pull rod and the crystal are suspended, is comprised of four units.

The static weight of the pull-rod $(m_0 g)$, the crystal already grown $\left(\int_0^t \rho_S g \pi r^2 v dt\right)$, contribution due to the vertically resolved unit of surface tension force (γ) exerted along the length of the three-phase boundary $(2\pi r(\gamma_0 - \gamma_\theta \theta_S))$ and the weight of the supported meniscus $(\pi r^2 \rho_L g h)$. The measured force by weighing mechanism is thus:

$$F(t) = m_0 g + \int_0^t \rho_S g \pi r^2 v_p dt + \pi r^2 \rho_L g h + 2\pi r(\gamma_0 - \gamma_\theta \Theta_S)$$

m_0 = Mass of the pull rode and the crystal at instance t = 0

γ_0, γ_θ = Component of the surface tension force at the three phase boudary

ρ_S, ρ_L = Desnsity of the solid and the melt respectively

(2-3)

Again, after applying the linear perturbation theory, the transfer function for the radius to the weight change ($\dot{W}$, growth rate in g/h) can be presented as follows:

$$\frac{\dot{W}(s)}{r(s)} = 1 + \eta s - \lambda s^2$$

Where, $\eta = \left[2\left(\rho_L h_0 + \gamma_0 / r_c g\right) - (\rho_S - \rho_L) h_a\right] / 2\rho_S v_0$

$$\lambda = \left[2\gamma_\theta / r_c g - (\rho_S - \rho_L)h_\theta\right] / 2\rho_S v_0^2$$

(2-4)

Overall transfer function from the heater power to the crystal weight change can be expressed as follows:

$$H(s) = \frac{\dot{W}(s)}{P(s)} = \frac{K(s+z_1)(s+z_2)}{(s+p_1)(s+p_2)(s+p_3)}$$

(2-5)

Therefore, the linear model of the Czochralski crystal growth process by the differential mode weighing technique is represented by the transfer function of three poles and two zeros. The closed loop control system is designed based on this model for designing PID controller [12]. From these equations, there is a critical value of the crystal radius, for right-hand side poles, below which the stability can be achieved. The stability is reached by the thermal redistribution after perturbation in power. Detail stability analysis and discussion can be found in [1].

2.3.5 Time delay model

In this research, this transfer function is considered with the time delay τ_d and can be represented as follows:

$$H_D(s) = H(s) \cdot e^{-s\tau_d}$$

(2-6)

The measurement delay can also contribute to this delay. This delay depends on various parameters of the process for example the melt level and the crystal size. As these parameters keep varying, this delay keeps varying too. The complete process can be

described as the time-varying delay system. Therefore, the real-time identification of such a model has to include the continuous identification of this time delay at every step of the control action.

2.4 Literature review: crystal growth process

From literature review, it is obvious that the Czochralski growth has various nonlinearity and uncertainties that should be considered during the control system design. The most general and important characteristics are described as follows:

- The crystal growth process is nonlinear [[1], [3]]. In other words, altering one of the process parameter can have both direct and indirect effect on other process parameters as well as future parameters like the pulling speed and the rotation rate. The simple example is a change of the heater power, which affects not only the temperature at the base of the interface but also temperature gradient in melt, crystal and growth environment. All these parameters contribute to decide the quality of the crystal by defect and distribution of impurities [7].
- The crystal shape including the interface shape changes with the time [[37], [38]]. This effect is due to the changing heat transfer in the melt, crystal and changing temperature field across the interface. The interface shape can also influence the weight signal, which normally assumes a flat interface.
- The growth interface shape can be flat, concave or convex. There is an ideal rotation rate for particular crystal to have flat growth interface [[15], [39], [40]]. The induced forced convection, caused by the crystal rotation, in the melt can be a dominant effect on the heat transfer. However, with the melt level changes this rotation rate can

destabilize the growth. Therefore, the rotation rate is kept well under the limit of the ideal rotation rate for flat interface. This low rotation causes the convex shape of the interface. In other words, crystal grows like an iceberg floating on the melt. However, this can lead to slower measurement response due to buoyancy effect on the crystal. In this condition, the diameter calculated from the weight change, or growth rate, is larger than the actual diameter of the growing crystal. In oxide crystals growth, the calculated diameter can be about 20% bigger than actual diameter.

- The power required for the constant diameter crystal growth varies with the change in dynamics [1]. It is presented that initial power requirement is high compared to midsection. However, at the end again, the power requirement is high, mainly due to decreased melt to crucible contact area.
- The required power for similar diameter crystal changes with each growth due to the change in crucible, crystal, crucible position, crystal size, growth process design and time [[5], [6], [34]]. In other words, no two growth processes are identical even for the same material.
- The design of the crystal growth furnace is carried out before the real growth. Furnace structure and related parameters, like temperature gradient inside the chamber, play a dominant role for the quality and the stability of the growth process [[41], [42]].
- Many oxide crystals grown form the melt have low growth rates [[7], [42]]. The longtime of stabilization of the growth parameters makes them sensitive to any perturbation. Therefore, for the controller to be applicable for a single class of

crystals, it should have a structure to compensate or consider this long lag typical to each crystal growth.

- The controller should be able to keep up with several phases of the crystal growth process including proper cooling and heating stage. The manual to automatic change over is necessary for control signal [36].
- The second derivative of the weight signal can be analyzed for a proper control action. This can help to reduce the time delay or help to find out the suitable direction for prediction of the system output [[1], [43]].
- The crucible, melt and crystal time constants are coupled with one another [9].
- Some unknown and unpredictable perturbations may arise during the growth, for example the generation of facet plane at the interface or parallel to the growth direction [44]. Such effects can influence the predictive value of the output. Facet formation can sometime be controlled by adjusting the rotation rate of the crystal, specifically in oxide crystal. Additive or dopant can also affect facet formation.
- The thermal stress on the crystal during the growth is presented as a main source of dislocation formation and multiplication [[4], [6]]. The mathematical representation of such a mechanism is not available to predict the generation of higher dislocation density. However, it is obvious that the lesser the thermal stress is, the lower the dislocation density will be. Dislocations can also propagate from the seed region into the crystal and continue to propagate along the entire crystal length.
- The starting melt composition and the seed orientation can also influence the Czochralski growth [5].

- The large size crystals are more sensitive to any perturbation than small size crystals. Extra care has to be taken during the control design of such crystal growth [7].
- The ratio of the melt depth to the crucible height is presented as a most pronounced effect on the thermal oscillation in the melt and the crystal [[3], [29]]. This can change the heat transfer time from the crucible to the melt interface. The change of the input power required for constant diameter can be related to this ratio. Other parameters like the cooling water, the grid voltage and the frequency and the growth atmosphere can also affect the crystal growth [[36], [43]].

2.5 Cascade controller structure

Although there are various control structures proposed, a cascade control structure is widely used for many years, as shown in [[12], [36], [43]]. The basic structure of it is shown in the Figure 2-7. There are two control variables (one for each loop), the temperature and the growth rate, but only one control signal input to the process i.e. generator power. The rotation rate and the pulling speed are generally kept constant for oxide crystals. The first loop consists of an inner temperature control loop (loop-2 or secondary loop) nested within an outer growth rate control loop (loop-1 or primary loop). The primary loop determines the change of temperature set point ΔT_s to the secondary loop. It consists of measuring and filtering of weight and calculating the growth rate of the crystal. It compares the actual growth rate to the required reference-growth rate, which is calculated from the initial diameter, the final diameter, the half cone angle, the pulling rate and the crucible diameter. This growth rate error is converted to proper adjustment of temperature ΔT_s by controller of primary loop. The update rate of the

growth rate cycle depends on the controller structure, diameter (range of temperature change for diameter change) and material.

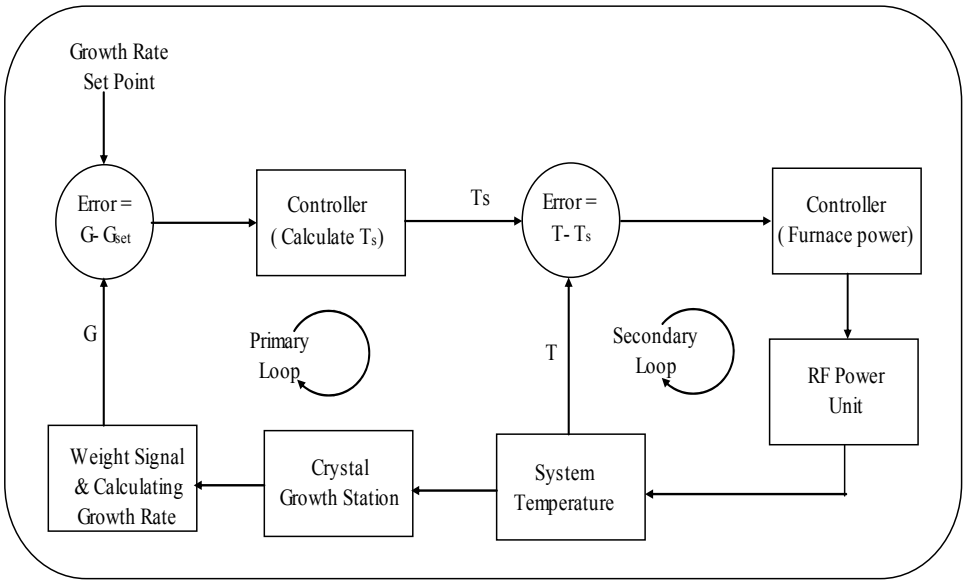

Figure 2-7: Cascade control structure

Loop-2, secondary loop, mainly works for controlling the required temperature. It measures the present temperature of the process T. This temperature is compared to the required temperature based on the loop-1 temperature adjustment and the initial temperature T_i. This error signal is used to create proper control signal u for the heating unit (in this case R.F. Generator) by the controller. The generator adjusts the power based on the control signal. Therefore, the heating of the crucible changes to adjust the required temperature for required growth.

The secondary loop can be fast, the control signal updates every few ms, where as for the primary loop, control signal updates every few seconds [43]. This structure is also good for manual to automatic changeover if manual interruption is needed [[10], [43],

[45]]. For example, during the initial stage of the seeding and the small diameter growth, an operator is needed to make the manual temperature changes. During this time only secondary loop (loop-2) is in action. In other words, Loop-1 is not adjusting any temperature $\Delta T_s = 0$ and it is open and operator changes temperature manually. This flexibility is important for the practical implementation of the growth with out any perturbation. However, for our growth system, we do not measure the temperature of the growth system but we measure the power output of the R.F. generator. The current transformer on the outgoing bus heats up the resistance depending on the current supplied to the induction furnace. The temperature of this resistance is measured as a signal of the output of the generator.

2.6 Parameter measurement

This section shows the basic equations for various variables, which are used to calculate the radius, height of the crystal and growth rate of the crystal [[1], [27], [28], [36]].

Let δt be the time for which small amount of crystal, volume δV, is grown during the cylindrical portion. Here, it is assumed that during this time the radius of the crystal (r_c) and the pulling rate (v_p) are constant. In addition, it is assumed that the density of the solid is equal to the density of the liquid ($\rho_S = \rho_L$) for simplicity of the calculation. It is assumed that material is homogeneous and there is not enough material loss because of vaporization during the crystal growth process. Hence, the volume gained by the

crystal due to pulling is $\delta V_1 = \pi r^2 v_P \delta t$ and the volume gained by the crystal gains due to melt drop δh is $\delta V_2 = \pi r^2 \delta h$. In addition, one can write from material balance equation:

$$\delta M = \rho_S (\delta V_1 + \delta V_2) = \rho_L \pi R^2 \delta h \tag{2-7}$$

Where, $R =$ Crucible Radius

Simplifying, these three equations by removing δh gives the change of weight in time, i.e. growth rate for cylindrical growth is represented.

$$\dot{W} = \frac{\delta W}{\delta t} = \frac{\pi \rho_S \rho_L v_P r_c^2 R^2}{\rho_L R^2 - \rho_S r_c^2} = \pi \rho v_P \frac{r_c^2 R^2}{R^2 - r_c^2}. \tag{2-8}$$

This equation is presented in [1].

From this, the approximate present radius of the crystal r_c can be represented as:

$$r_{c_i} = \sqrt{\frac{\dot{W} \cdot R^2}{\dot{W} + \pi \rho v_P R^2}}$$

The total height change of the crystal (or actual pulling speed) is (pulling speed + melt level drop $\dot{H}_m$) as follows:

$$\dot{H}_i = \frac{H_t - H_0}{\delta t} = v_P + \dot{H}_m = v_P + \frac{\dot{W}}{\pi \rho_L R^2}$$

The present crystal size and the melt level can be obtained by integrating the above two equations with growth time.

The above equation is for both cylindrical and cone growth for slowly growing crystals because the effect of melt level drop due to the cone is very small compared to melt level drop due to the crystal.

CHAPTER 3: LONG-RANGE PREDICTIVE CONTROL

Here, literature review of Long Range Predictive Control (LRPC) strategy is presented. The recursive least square model identification is introduced to calculate the model at real-time. Various parameters selection and implementation for the LRPC are also discussed.

3.1 General introduction to long range prediction control

As described earlier in chapter 1, the LRPC technique is two steps process. First step is to identify the process model followed by multistep cost function minimization to identify proper control action. Here, step refers to time steps over which the cost function is minimized as shown in following Figure 3-1. The cost function for predictive can be single step or multistep function. Single step cost function model predictive control (MPC) is called self-tuning control (STC). Whereas, the multistep cost functions MPC is known as Long-range predictive controllers (LRPC) [16]. Here, the predictive horizon is being extended over multiple steps into the future. STC can provide stable control provided some prior assumptions about the process are satisfied. However, improper choice of the model order and time-delay can destabilize STC [[46], [47]]. Although, the performance of these LRPC depends on the design parameters, LRPC can provide satisfactory control under these conditions. There are various classes of LRPC depending on the model like pulse response, step response and generalized predictive control (GPC) [24]. Here, GPC is considered for modeling.

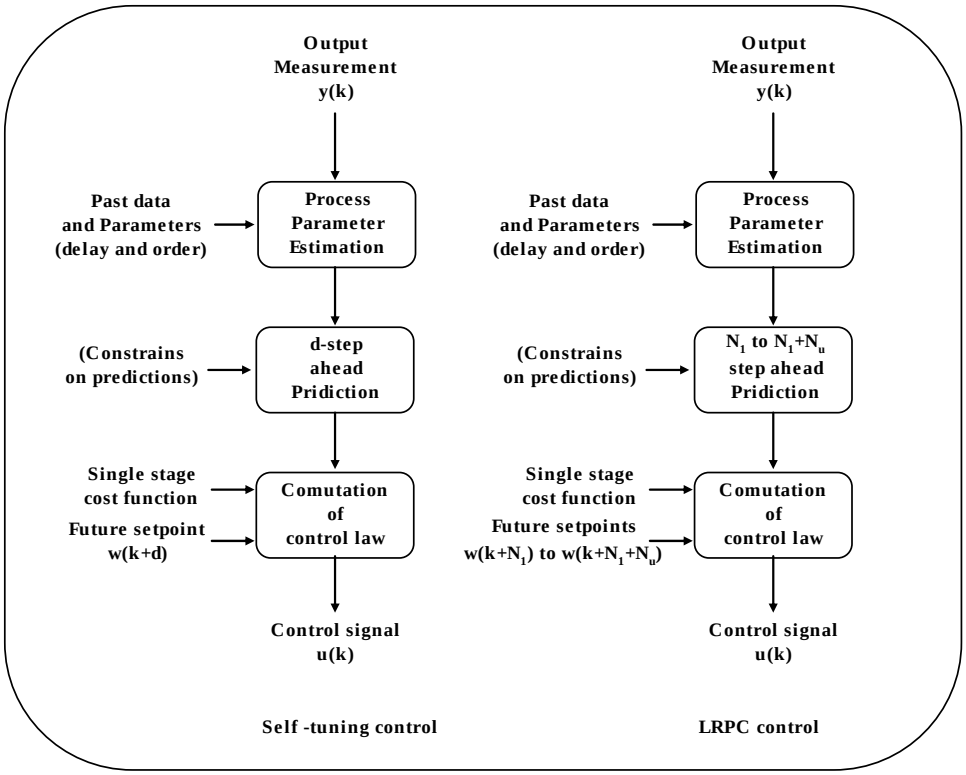

Figure 3-1: Comparison between STC and LRPC technique

3.2 The recursive least square technique

The recursive least square (RLS) model identification technique is described in this section.

3.2.1 Process model identification fundamentals

Predicting the system performance requires mathematical modeling of the process. Later, this prediction can be used to predict the process output, which is compared with the required output in designing model predictive control. Steps for identification of such model include selection of the model, calculation and validation of the model [18]. The prior information and knowledge about the process is helpful for

selecting the model and model order. For real-life application, the selected model has to incorporate noise, disturbance and error due to measurement and unidentified dynamics. In addition, such model has to be designed to adapt with the process parameter changes with the time.

However, the complete and exact representation of real-life process is not possible due to many reasons. Mainly, the measured data may not be rich enough to model required characteristics of the process. Also, the order of the input and output model for the given process may not be known or identified; and the transport delay between input and output may not be constant or known for modeling [[47], [48], [49]].

There are various kinds of discrete (for sampled data system) model available to represent the process depending on the properties of the process [[50], [51]]. Widely accepted, autoregressive integrated moving average with exogenous input (also called controlled ARIMA (CARIMA)) model for the system with time varying delay and parameters can be described as follows:

$$A(z^{-1})y(k) = B(z^{-1})u(k-d)) + C(z^{-1})e(k)/(1-z^{-1})$$

$$A(z^{-1}) = 1 - a_1(k)z^{-1} - ..... - a_{n_a}(k)z^{-n_a}$$

$$B(z^{-1}) = b_0(k) + b_1(k)z^{-1} + ... + b_{n_b}(k)z^{-n_b}$$

$$C(z^{-1}) = c_0(k) + c_1(k)z^{-1} + ... + c_{n_c}(k)z^{-n_c} \qquad (3\text{-}1)$$

Here, z is a descrete time delay operator (z-transform operator).

k is a sampling instance.

Here, $a_1(k),...a_{n_a}(k), b_0(k),...b_{n_b}(k), c_0(k),...c_{n_c}(k)$ are system parameters.

$u(k), y(k), e(k)$ are controlled input, process output and noise, respectively.

d is the minimum time delay in input and can be varying with time.

This model can also be represented in matrix form as follows:

$$y(k) = h^T(k)\theta(k) + e(k)$$

Where, $\theta(k) = \left[a_1(k)\ a_2(k)\ \ ...\ \ a_{n_a}(k)\ b_1(k)\ \ b_2(k)\ ...\ \ b_{n_b}(k) \right]$ and

$$h(k) = \left[-y(k-1)\ \ -y(k-2)\ ...\ \ -y(k-n_a)\ u(k-d)\ u(k-d-1)\ ...\ u(k-d-n_b) \right]^T$$

(3-2)

This model is also called multiple liner regression models because the input and the output parameters are linear [[16], [49]].

3.2.2 Recursive least square error technique

If the measurements are available from $k-m+1$ to k sample (for last m data sets) then CARIMA model can be represented as a linear multiple regression model.

$$Y(k) = H^T(k)\theta(k) + \xi(k)$$

$$\begin{bmatrix} y(k) \\ y(k-1) \\ : \\ y(k-m+1) \end{bmatrix} = \begin{bmatrix} h^T(k) \\ h^T(k-1) \\ : \\ h^T(k-m+1) \end{bmatrix} \theta(k) + \begin{bmatrix} e(k) \\ e(k-1) \\ : \\ e(k-m+1) \end{bmatrix}$$

(3-3)

The main objective of the least square technique is to select data sets to minimize the cost function J_I at k^{th} instant.

$$J_I(k,\theta) = \frac{1}{2}\sum_{i=0}^{m-1}(y(k-i) - h(k-i)\theta(k-i))^2 = \frac{1}{2}\xi^T\xi = \left[Y - H\theta\right]^T\left[Y - H\theta\right]$$

(3-4)

The minimum value of J with respect to θ leads to following control law :

$$\hat{\theta}(k+1) = \hat{\theta}(k) + K(k+1)\left(y(k+1) - h^T(k+1)\hat{\theta}(k)\right)$$

$$K(k+1) = \frac{P(k)h(k+1)}{\left[\sigma^2 + h^T(k+1)P(k)h^T(k+1)\right]}$$

$$P(k+1) = \left[\sigma^2 I - K(k)h^T(k+1)\right]P(k)$$

(3-5)

Here, $K(k+1)$ is called the Kalman estimator gain matrix and $P(k+1)$ is called the covariance matrix represented as follows:

$$K(k+1) = P(k+)h(k+1)$$

$$P(k) = \left[H^T(k)H(k)\right]^{-1}\sigma^2$$

3.3 Introduction to long range predictive control

Among other LRPC techniques, the Generalized Model Predictive control (GPC) based technique considers an input output model with noise and delay [[24], [25]]. Therefore, it is suitable for real-time processes.

3.3.1 Long range predictive control technique

Most single input and output processes with noise can be explained by CARIMA model as discussed before:

$$A(z^{-1})y(k) = B(z^{-1})u(k-d) + C(z^{-1})e(k)/(1-z^{-1})$$

If noise is assumed to be normal (white), then $C(z^{-1}) = 1$.

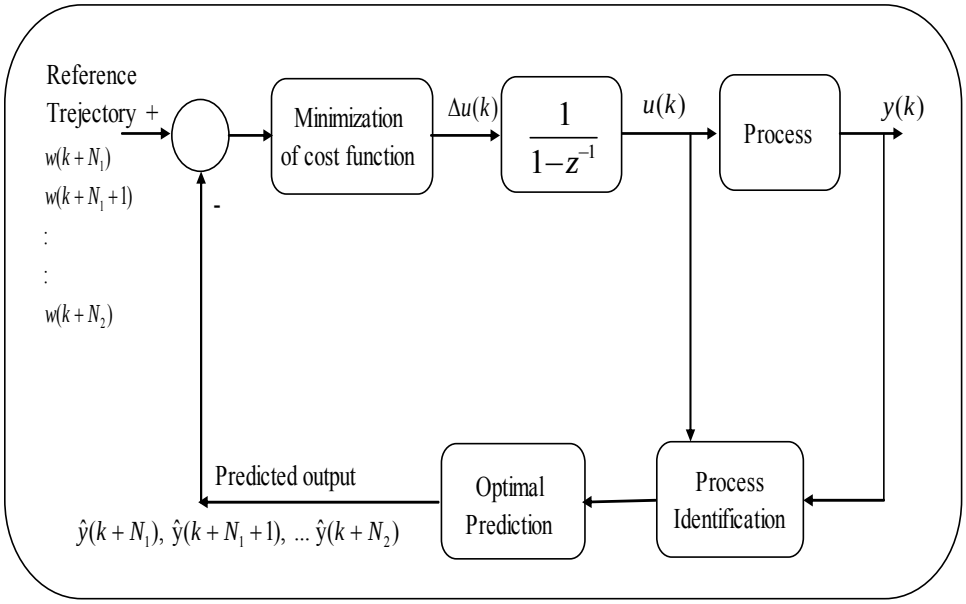

Figure 3-2: The structure of LRPC technique

The basic GPC structure is shown in above Figure 3-2. The GPC algorithm consists of applying the control sequence that minimizes a multistage cost function. This cost function is quadratic function of the predicted output deviation from the desired or reference output. This cost function is comprised of:

- The future horizon over which the cost function is minimized for control signal.
- The type and cost of the control increments penalized to minimize the cost function.
- The future set point sequence or trajectory of the output.

$$J_C(k, N_1,\ N_2,\ N_u) = \sum_{i=N_1}^{N_2} \delta(j)\left(\hat{y}(k+i \mid k) - w(k+i)\right)^2 + \sum_{i=1}^{N_u} \lambda(j)\left(\Delta u(k+i-1)\right)^2 \qquad (3\text{-}6)$$

Here, $\hat{y}(k+i\,|\,k)$ is an optimum i-step ahead prediction of the system output from the data measured up to sample k. Integers N_1 and N_2 are the minimum and maximum costing horizons. Here, $\delta(j)$ and $\lambda(j)$ are weighting sequences for the performance. $w(k+i)$ is the future reference trajectory. The choice of this performance criterion influences largely on the quality of the control. The control criterion can be modeled as per required closed loop criterion of the system.

The objective is to calculate the future control sequence $u(k),\ u(k+1),\ \ldots u(k+N_u)$ to drive the plant future output $y(k+N_1)$, $\mathrm{y}(k+N_1+1)$ … $\mathrm{y}(k+N_2)$ to the corresponding reference trajectory $w(k+N_1)$, $\mathrm{w}(k+N_1+1)$, … $\mathrm{w}(k+N_2)$ by minimizing the control cost function $J_C(k, N_1, N_2, N_u)$. The Diophantine equation is useful to calculate the output prediction. It is presented as:

$$1 = E_i(z^{-1})\tilde{A}(z^{-1}) + z^{-i}F_i(z^{-1}) \qquad \text{with } \tilde{A}(z^{-1}) = \Delta A(z^{-1}) \text{ and } \Delta = 1 - z^{-1}$$

$$\Rightarrow \frac{1}{\tilde{A}(z^{-1})} = E_i(z^{-1}) + \frac{z^{-i}F_i(z^{-1})}{\tilde{A}(z^{-1})}$$

(3-7)

The equation (3-1) is multiplied by $\Delta E_i(z^{-1})z^i$, using the above equation and simplifying; the output the prediction $(\hat{y}(k+i))$ can be written as:

$$\hat{y}(k+i) = F_i(z^{-1})y(k) + E_i(z^{-1})B(z^{-1})\Delta u(k+i-d-1) + E_i(z^{-1})e(k+i)$$

Canceling the white noise, the best prediction of $y(k+i)$ can be represented as:

$$\hat{y}(k+i) = G_i(z^{-1})\Delta u(k+i-d-1) + F_i(z^{-1})y(k)$$

with $G_i(z^{-1}) = E_i(z^{-1})B(z^{-1})$

(3-8)

Here, the Diophantine polynomials $E_i(z^{-1})$ and $F_i(z^{-1})$ are obtained by one divided by $\tilde{A}(z^{-1})$ until the remainder of the division can be factorized as $z^{-i}F_i(z^{-1})$:

$$F_i(z^{-1}) = f_{i,0} + f_{i,1}z^{-1} + \ ... \ + f_{i,n_a}z^{-n_a}$$

$$E_i(z^{-1}) = e_{i,0} + e_{i,1}z^{-1} + \ ... \ + e_{i,i-1}z^{-(i-1)}$$

Similarly, for i+1:

$$F_{i+1}(z^{-1}) = f_{i+1,0} + f_{i+1,1}z^{-1} + \ ... \ + f_{i+1,n_a}z^{-n_a}$$

$$\text{with } f_{i+1,j} = f_{i,j+1} - f_{i,0}\tilde{a}_{j+1} \text{ for } j = 0 \ ... \ n_a - 1 \tag{3-9}$$

$$E_{i+1}(z^{-1}) = E_i(z^{-1}) + e_{i+1,i}z^{-i} \qquad \text{with } e_{i+1,i} = f_{i,0}$$

With above equations, $G_i(z^{-1})$ can be calculated recursively:

$$G_{i+1}(z^{-1}) = E_{i+1}(z^{-1})B(z^{-1}) = \left(E_i(z^{-1}) + e_{i+1,i}z^{-i}\right)B(z^{-1}) = G_i(z^{-1}) + f_{i,o}z^{-i}B(z^{-1}) \tag{3-10}$$

I.e. the first j coefficient of $G_{i+1}(z^{-1})$ are identical with $G_i(z^{-1})$ and the remaining coefficient is given by

$$g_{i+1,j+1}(z^{-1}) = g_{i,j+1}(z^{-1}) + f_{i,o}b_j \qquad \text{with } j = 0 \ ... \ n_b$$

Here, because of the dead time of d sampling period, the output of the system can only be influenced by the input signal after sampling period $d+1$. Therefore, the most suitable values of horizons can be defined by $N_1 = d+1,\ N_2 = d+N \ and \ N_u = N$. With this, the set of optimal output predictions can be represented by:

$$\hat{y}(k+d+1\,|\,k) = G_{d+1}\Delta u(k)(z^{-1}) + F_{d+1}y(k)$$

$$\hat{y}(k+d+2\,|\,k) = G_{d+2}\Delta u(k+1)(z^{-1}) + F_{d+2}y(k)$$

:

$$\hat{y}(k+d+N\,|\,k) = G_{d+N}\Delta u(k+N-1)(z^{-1}) + F_{d+N}y(k)$$

Further simplification in the matrix form can lead to:

$$Y = GU + F(z^{-1})y(k) + G'(z^{-1})\Delta u(k-1) = GU + \zeta$$

$$G = \begin{bmatrix} g_0 & 0 & .. & 0 \\ g_1 & g_0 & .. & 0 \\ : & : & : & 0 \\ g_{N-1} & g_{N-2} & .. & g_0 \end{bmatrix} \text{ and } G' = \begin{bmatrix} \left(G_{d+1} - g_0\right)z \\ \left(G_{d+1} - g_0 - g_0 z^{-1}\right)z^2 \\ : \\ \left(G_{d+1} - g_0 - g_0 z^{-1} - \ \ldots \ - g_{N-1}z^{-(N-1)}\right)z^N \end{bmatrix}$$

$$Y = \begin{bmatrix} \hat{y}(k+d+1\,|\,k) \\ \hat{y}(k+d+2\,|\,k) \\ : \\ \hat{y}(k+d+N\,|\,k) \end{bmatrix},\ U = \begin{bmatrix} \Delta u(k) \\ \Delta u(k+1) \\ : \\ \Delta u(k+N-1) \end{bmatrix},\ F(z^{-1}) = \begin{bmatrix} F_{d+1}(z^{-1}) \\ F_{d+2}(z^{-1}) \\ : \\ F_{d+N}(z^{-1}) \end{bmatrix}$$

If all the initial conditions are zero $(y(k) = 0,\ \Delta u(k-1) = 0)$, the free response function ζ is also zero. If the unit step is applied at time $k = 1$ then the free response can be calculated recursively as

$$\zeta_{i+1} = z(1 - \tilde{A}(z^{-1}))\zeta_i + B(z^{-1})\Delta u(k-d+i)$$

with $\zeta_0 = y(k)$ and $\Delta u(k+i) = 0$ for i ≥ 0

The objective function from the equation (3-6) can be expressed as follows:

$$J_C = (GU + \zeta - W)^T(GU + \zeta - W) + \lambda U^T U$$

$$W = \left[w(k+d+1) \quad w(k+d+2) \quad .... \quad w(k+d+N)\right]^T$$

In another form:

$$J_C = \frac{1}{2}U^T HU + \mathrm{B}^T U + \zeta_0$$

Where, $H = 2(G^T G + \lambda I)$

$\mathrm{B}^T = 2(\zeta - W)G$

$\zeta_0 = (\zeta - W)^T (\zeta - W)$

Making the gradient of J_C for the minimum value of J_C (without any constraints on the control signal) leads to the required control sequence or control vector.

$$U = -H^{-1}\mathrm{B} = (GG + \lambda I)^{-1} G^T (W - \zeta)$$

However, the control signal required to send the process is only the first element of vector U.

$\Delta u(k) = K(W - \zeta)$ with $K = (GG + \lambda I)^{-1} G^T$

And the optimal control law becomes $u(k) = u(k-1) + \Delta u(k)$

(3-11)

In other words, if there is no error in predicted output, no further control change is necessary. The solution of GPC involves the inversion of $N \times N$ matrix K, which could be numerically difficult to compute in real-time. For simplicity, noise considered here is white. If noise is colored, the pre-filter can also be included in the system model.

Stability analysis and closed loop relationship are presented in the paper [53]. The stability can be guaranteed if the tuning parameters ($\lambda(j)$ and $\delta(j)$) are correctly chosen. However, it is difficult to prove the clear dependencies of these parameters on stability. The pre-filter for input and output measurement is suggested to improve the stability at high frequency. It also helps to improve robust stability. High frequency disturbances can

occur mainly because of the modeling error and immeasurable high frequency disturbances. This filter can be modeled to make the complete control system open loop stable.

3.3.2 Design parameter for LRPC technique

Some of the important design considerations or parameters for this control technique are as follows [[16], [24], [25]]:

- Starting horizon (N_1), also called minimum cost horizon, should be equal to the maximum time-delay between the input and the output. In other words, the error before this horizon has no importance. The underestimated time delay $(N_1 > d)$ leads to the nonminimum-phase response of the system. Therefore, the overestimated is always preferred but there is no reason for N_1 to be less than the time-delay. For $N_1 < d$, the value of λ has to be such that the matrix $(GG + \lambda I)$ is invertible because first rows till $N_1 = d$ of the matrix G are zero.
- Length of the horizon $(N = N_2 - N_1)$ should be long enough to include the rise time of the process. For the non-minimum phase system, it has to be longer until the process output gives positive response with the control signal.
- Length of the control horizon N_u defines the region where the process should reach required output. After this region the control action is zero, i.e. $\Delta u(k + j - 1) = 0$ for $j > N_u$.
- Generally $N = N_u$, so that the matrix G has full rank and the inverse of $(GG + \lambda I)$ exists.

- The weighting coefficients $\delta(j)$ and $\lambda(j)$ are sequences that consider future behavior. These values can be constant or exponential along the horizon. These values can be used to tune control for particular process.
- The reference trajectory $w(k)$ or set point sequence is used for some systems. In the crystal growth process, the reference trajectory can be represented the required diameter of the crystal. However, the reference trajectory does not necessarily have to be the real reference $r(k+i)$. It is normally the smoothed or the low-passed filtered set point.

  $$w(k+i) = \alpha w(k+i-1) + (1-\alpha) r(k+i) \qquad \alpha > 0$$

- In other words, auxiliary output can be derived from the set point, which is equivalent to placing the closed loop pole by selecting the proper function $\Psi(z^{-1})$.

  $$\psi(k) = \Psi(z^{-1}) y(k)$$

3.3.3 Constraints

The real-time process has some range for measurement and output. The controller discussed above has unlimited range, which is not possible for actual process. Sensors and actuators have limited ranges and slew rates (sometime have dead time). Economically, also, there are some constraints that have to be considered during the design of control, like range and speed, for the product is quality. For example, similar to other batch processes in crystal growth, most of the quality of the crystal requires some of the variables, like rate of change of temperature and diameter, to be under specified limits. Violating this may cause crystal meltdown or defects generation. Control systems,

especially Long Range Predictive Control, used for longtime delay system, are more prone for constraints violations and proper correction has to be considered.

Application and optimization of these constraints depends on the process that will be attended to during the actual control system design [[16], [22], [23], [51]].

Some of the most common constraints are explained here.

- Band limited constraints: The controlled parameters have to follow the required output within some band and can be represented as $\underline{y}(k) \le y(k) \le \overline{y}(k)$.
- Input constraints: The input or control signals have magnitude limits and can be expressed as $\underline{U}(k) \le u(k) \le \overline{U}(k)$.
- Slew rate constraints: The control signal can only increase or decrease with certain speed due to mechanical or other limitations and can be represented as $\underline{u}(k) \le u(k) - u(k-1) \le \overline{u}(k)$
- There can be other constraints on the process like overshoot constraints, monotonic behavior, nonminimum phase, actuator nonlinearities.

Handling such constrains during the control system design is complicated and computationally challenging. The main challenge introducing these constraints in control action and find out the control signal that can also minimizes the cost function.

In this work, these constraints and their application for the crystal growth process is considered for control. The main challenge is real-time implementation of such constraints on the control signal. Constraint reduction, feasibility and management also have to be studied to further improve the control system.

CHAPTER 4: SYSTEM STRUCTURE AND MOTIVATION

This chapter is divided into two sections. First is system parameter, which represents the present control related structure. The second part presents the initial research and results carried out with this structure to study the time delay and model identification of Czochralski growth process.

4.1 System structure and control parameter

This section is mainly focused on the present growth system structure and growth parameters.

4.1.1 Furnace structure and instrumentation

The complete furnace structure is typical and includes power unit, growth chamber, motors and controller units as shown in Figure 2-2.

- A 10 KHz, 50KW AC power generator provides controlled induction heating to the crucible. The controller unit controls the generator power. The generator power output is measured by a thermocouple, which measures the temperature of a load resister. The current transformer, connected at generator output side, powers this resistance. In other words, the thermocouple temperature is a measure of the power delivered to the furnace.
- The rotation motor and pulling motors are adjusted according to the required specification before the growth starts. Both motors are servomotors and powered by servo controllers.

- A digital scale measures the weight of the growing crystal. The digital weight signal is transferred by a serial link to the computer. The maximum weight limit for this unit is 5 Kg with the tolerance of ± 0.1 g.

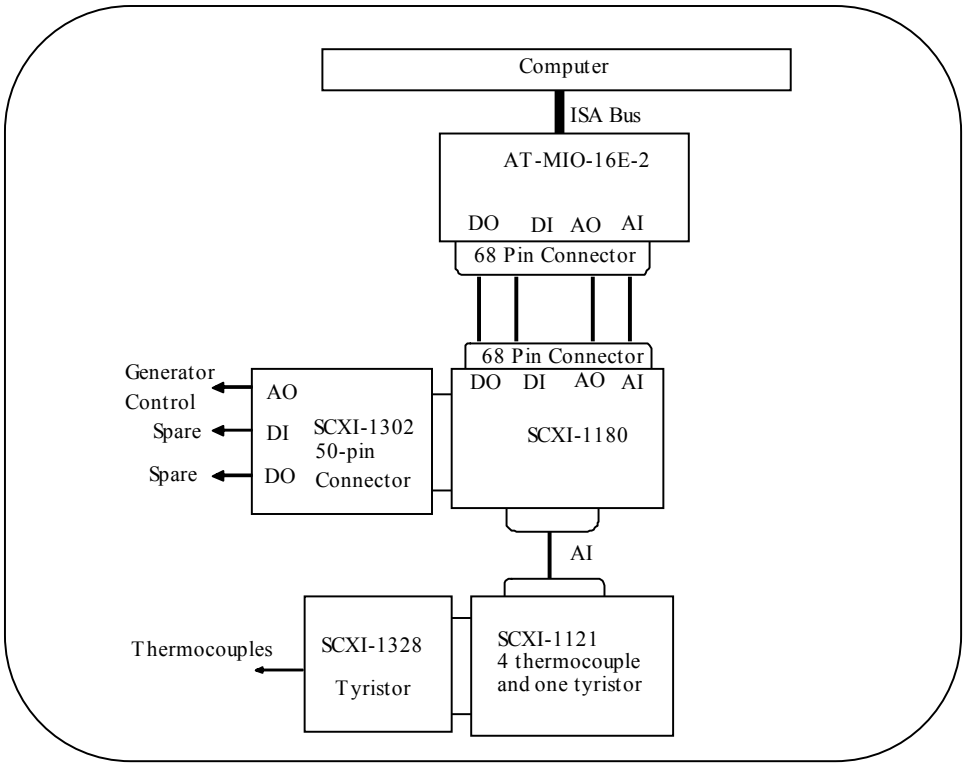

Figure 4-1: Control and Instrumentation diagram

Presently, there are two control systems used during the crystal growth in the Laboratory. The first one has a Quick Basic program that computes growth rate from last 300-filtered weight signals. The corresponding growth signal is converted to analog signal. The MicRicon controller reads this signal and compares to the set point, programmed as per requirement. Double loop cascade PID control algorithm is used to control the generator output as discussed earlier. There are mainly two drawbacks of this control structure. The gain and reset of the PI controllers are set at the lowest possible

values and tuning these PI values is not possible during the growth. Therefore, the controller response is sluggish against disturbances.

The other system is having similar control structure. However, model reference adaptive controller (MRAC) is designed to control the growth system instead of PID. The reference models for the controllers are optimized during the controller design. The exponential decaying is used for controlling crystal growth loop to compensate the delayed effect. The complete control structure is described in [45]. LABVIEW program with various National Instrument cards are used to design the controller unit. Control and instrumentation diagram for this system is presented in Figure 4-1. The complete electrical and instrumentation details are presented in APPENDIX-A. This second control system was used to carry out initial test for modeling crystal growth system.

4.1.2 Present control system of Czochralski growth

Figure 4-2 represents present control system that was used to test the Czochralski growth later discussed in this chapter. Typical two loop cascade structure as discussed in Section-2.5 is controlled by Model reference adaptive control (MRAC) technique.

Every two seconds, the weight signal was measured and filtered for the growth rate calculation. Because of the slow growth rate, the last 300 weight signals were used to calculate the effective growth rate of the crystal and to reduce the signal to noise ratio (which increases due to the weight differentiation) in the loop-1. The loop-1 controller calculates the change in power at every four seconds from the error between this measured growth rate and the required growth rate. The required growth rate is being calculated from output of the reference crystal growth model. The loop-2 controller controls the RF generator according to the change in power from the loop-1 feedback of

required power change. The process parameters were recorded every four seconds and used after the growth for the system analysis. These data are used later for the process identification by recursive least square estimation technique with the ARMA model by LABVIEW Program.

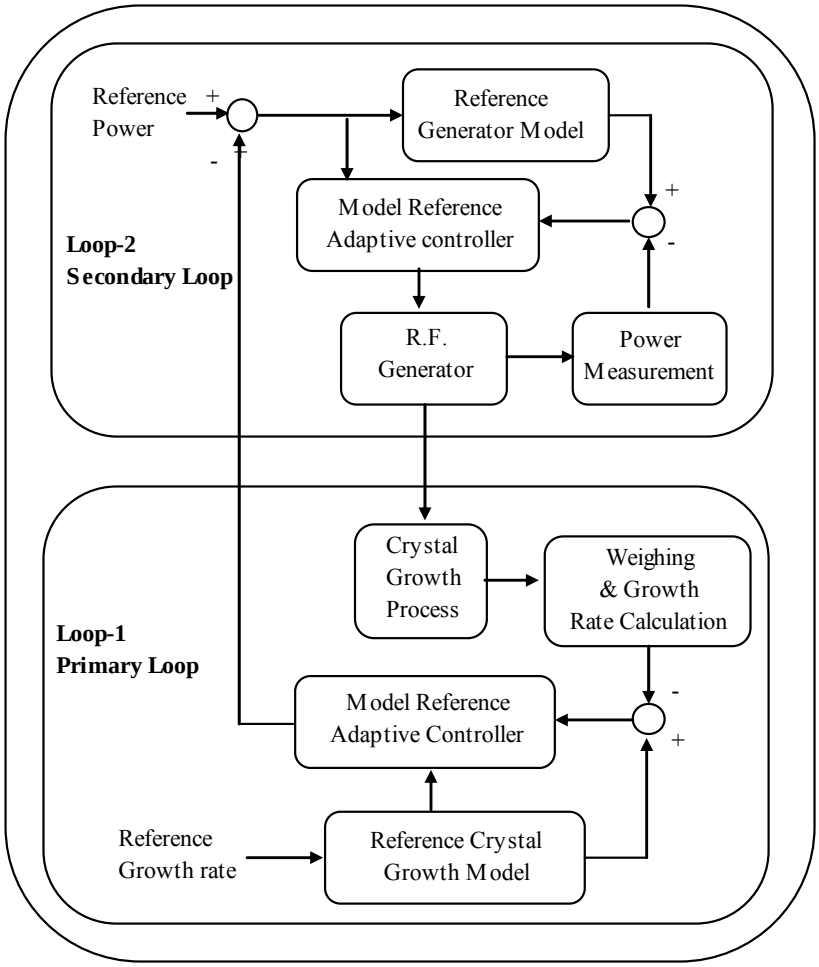

Figure 4-2: Model reference adaptive control in cascade structure

4.1.3 Calculation of growth rate from weight signal

The weighing scale has tolerance of ± 0.1 g even though it has inbuilt weight filter. The growth rate for oxide crystals also falls in this range. Hence, it is required to

filter out this noise and calculate the effective growth rate. Following digital filter reduces the noise to ± 0.01 g.

$$H(z) = \frac{1}{1 - e^{-0.5} z^{-1}} \tag{4-1}$$

The effective growth rate is calculated from last 300 weight (W_i) samples ($N = 300$) by following formula. The weight of the crystal was measured at every 4 second. In other words, the growth rate is calculated from measurements of last 20 minutes.

$$G.R. = \left[\frac{6}{N(N+1)} \cdot \sum_{i=1}^{N} (N - 2 \cdot i + 1) \cdot W_{N-i+1} \right] \times \frac{3600}{N \cdot T_s} \tag{4-2}$$

4.1.4 Growth rate set point for cone and cylindrical part

During cylindrical growth, required diameter of the crystal is constant. The set point growth rate from this diameter can be calculated from Equation (2-8). To find the ratio of the densities, we cooled down the LGT melt in the crucible by shutting off the generator power. It created a void in the center with a small entrance on the top of the melt surface because the melt solidified quickly near the crucible and at melt surface as shown in following Figure 4-3. The volume of this void was measured and compared to the melt volume. The estimated density of the melt was found to be 5.63 g/cm^3. The density of the solid material is 6.15 g/cm^3. In other words, the density of the melt is about 8.5% lower than solid. These densities will be considered with Equation (2-8) to calculate the growth rate during the cylindrical crystal growth. This is very crucial to accurately

calculating and controlling the diameter of the crystal. However, it is not considered for test discussed later in this chapter.

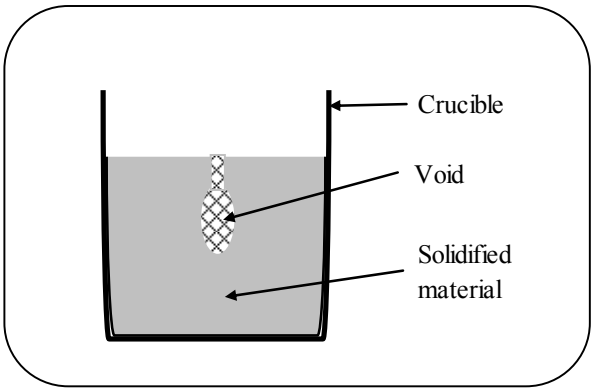

Figure 4-3: Effect of sudden cooling on the melt

Equation (2-8) can't be directly applied during the cone growth, where the diameter changes from the seed diameter (initial diameter) to the cylindrical diameter (final diameter). The preferred ramp of the diameter increase in cone phase is described in terms of half cone angle, which is an angle between the centerline and ramp line. However, it is desired to have smooth curve without and sharp edges that can create defects in the growing crystal. The normal method is to design a sine wave or design a half cosine wave and superimpose on the actual ramp according to half cone angle. This method increases the rate of change of diameter in the center of the cone growth. This is again undesirable as it may affect the crystal quality. A power function (x^n) is designed, which not only reduces the sharp edges but also preserves the maximum rate change of diameter given by the half cone angle. However, total time of the cone growth is increased. Here, doing this, the power (n) can be selected from 1 to 5. The set point of the growth rate initially follows the power curve (rate is increasing) but when it reaches

the maximum ramp, it will follow the straight line according to cone half angle until the end curve (rate is decreasing). At this point, it starts following the end curve.

The calculation is carried out in three steps for the set point diameter during cone growth as follows.

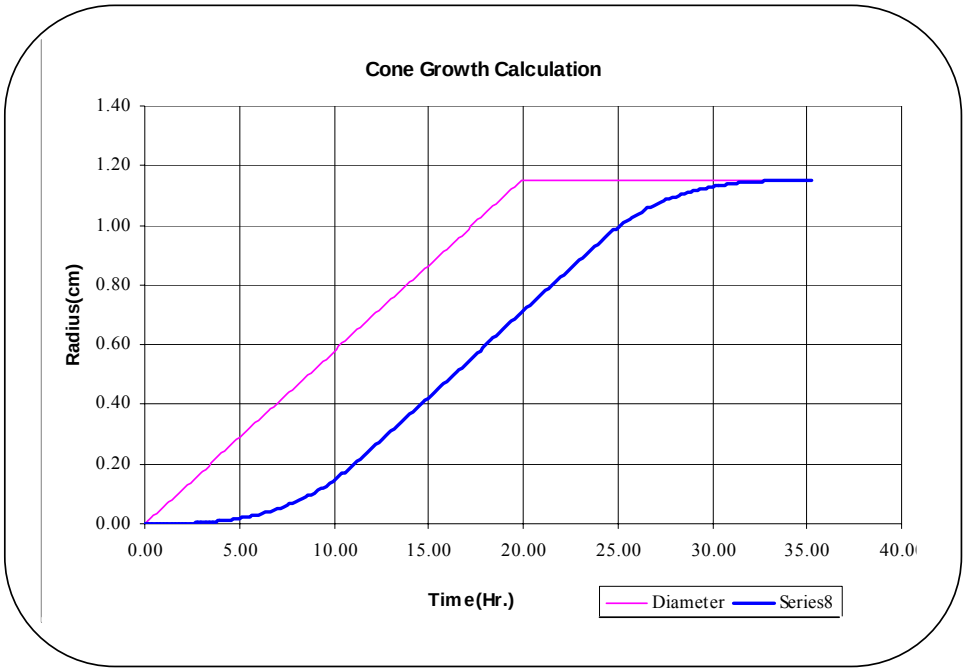

Figure 4-4: Set point of radius for cone growth

- First step is to calculate all parameters for straight-line effective radius change, slope of the straight line, total time for the straight line and set point radius for line curve.

  Effective radius change: $r_e = (Cylindrical\ \ diamter - Seed\ \ diamter)/2$

  Slope of the straight line: $\dot{r}_e = (pulling\ \ speed) \cdot \tan(half\ \ cone\ \ angle)$

  Total time for the straight line: $T_{line} = r_e / \dot{r}_e$

  Set point of the crystal radius at time t: $r_l(t) = \dot{r}_e \cdot t$

- Second step is to find out the power function and related parameters.

  Power function representation: $r_c(t) = \left(t/T_{line}\right)^n \cdot r_e$

  Time when the power function reaches maximum slope $t_{Slope} = T_{line} \Big/ \sqrt[n-1]{n}$

  Total time for the cone growth: $T_{power} = T_{line}\left[1 + 2\left(n^{-1/n-1} - n^{-n/n-1}\right)\right]$

  Power function radius at $t = t_{Slope}$ is $r_c(t_{Slope}) = r_e \cdot n^{-n/n-1}$

  Line function radius at $t = t_{Slope}$: $r_l(t_{Slope}) = r_e \cdot n^{-1/n-1}$

- Set point of the radius derived from above equations

  For $t \le t_{Slope}$: $r_{sp}(t) = r_c(t) + seed\ radius$

  For $T_{power} - t_{Slope} \ge t \ge t_{Slope}$ is $r_{sp}(t) = r_l(t) - r_l(t_{Slope}) + r_c(t_{Slope}) + seed\ radius$

  For $T_{power} \ge t \ge T_{power} - t_{Slope}$: $r_{sp}(t) = r_e\left(1 - \left(\frac{T_{power} - t}{T_{line}}\right)^n\right) + seed\ radius$

  For $t \ge T_{power}$: $r_{sp}(t) = Cylindrical\ radius$

  The growth rate set point is then calculated from this radius according to Equation (2-8).

4.2 Time delay modeling of Czochralski growth process

In this study, the approach considered to model the growth process is different from what has been commonly applied. Our approach includes the effect of system parameters variation, and the time delay. Here, a time delay based time varying linear model is used to model the Czochralski growth of oxide crystals at low growth rates (≤ 2mm/h). This model considers the heat and mass transport delay in the process. In other

words, the time delay is considered as time-varying parameter as the growth advances. The effect of the system parameters on the time delay was studied. Initially, a direct model reference adaptive controller was employed as discussed in earlier section.

In this study, impulse perturbation and step perturbation were first applied to the input power during the growth. Results showed a time delay between the input power change and the output growth rate change. From these results, we derived a suitable cycle time (reciprocal frequency) and amplitude of sinusoidal perturbations that were then applied to the power. Results were analyzed to study the relation between the time delay and the melt level drop. Such time delay represents not only the process delay because of heat-mass transfer from crucible wall to the crystal interface. It also represents the phase lag because of the weight signal and differential of the weight signal. In other words, when the weight signal is differentiated, the controller needs a sample of hundreds of measurements (typ. value for low growth rates) for calculating the effective growth rate. This causes the delay due to measurement lag. Both, the process time delay and the measurement lag, can't be identified independently from the crystal weight change measurements. Therefore the effective time delay observed represents the combination both effects. Above results, not only revealed the time delay, they were also used to identify constrains of the control, to preserve the quality of the crystal during the growth. In particular, the tolerable limits (bounds) of the control signal and its rate of change were determined.

4.2.1 Experimental setup

For all experiments, the crystal pulling rate and rotation rate were set at 2 mm/h, and 32 rpm, respectively. The required diameter of the cylindrical part of the crystal was

33 mm. An iridium crucible of 51mm height and internal diameter was used. The crystals were grown in nitrogen atmosphere. Various crystal growth experiments were carried out with different rotation rate in order to achieve the optimum rotation rate for the flat interface as shown in following figure.

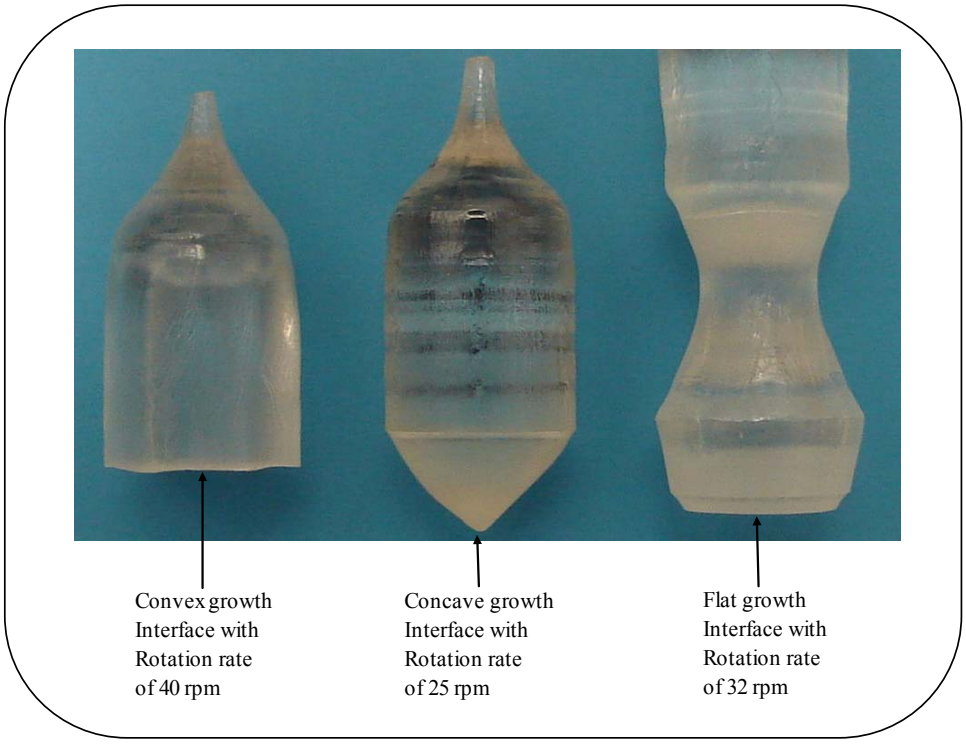

Figure 4-5: Interface shape for LGT crystals

In all growth experiments, the crystals were first grown with automatic control up to their cylindrical diameter. Once stable growth of a given cylindrical height was achieved, loop-1 was stopped. From that moment on, the generator output power (Figure 4-2) was only controlled by loop-2. The first test was carried out to measure the effect of constant power to the crystal diameter as growth proceeds and melt level drops discussed in next section. After that, the controlled perturbations in the form of impulse, step or

sinusoidal were applied on the output power. Impulse test and a step response test were carried out during the growth of Crystal-1. The sinusoidal response tests were carried out during the growth of Crystal-2 and Crystal-3 (Figure 4-6).

Figure 4-6: A: Impulse response; B: Step response; C: Sinusoidal response

The input power supplied during seeding was used as arbitrary choice to normalize the power change and express it in percentage. To express growth process as a positive response system, the percentage change in power was inverted (multiplied by (-1)). By doing this, the positive percentage of power change leads to a positive percentage

of change in growth rate. Similarly, the growth rate required for the cylindrical growth was used as arbitrary choice to normalize the growth rate change and express it in percentage. For the modeling purpose, the percentage change in the power (not the power) was considered as an input of the growth process, and the percentage change in the growth rate was considered as an output of the growth process. Such normalizations are useful for process model identification, because they reduce to dimensionless input and output and can therefore be applied and compared to any Czochralski growth. This input-output model was different from the work carried out in, where the power signal and the weight error signal was considered as in input and output of the growth process respectively.

4.2.2 Crystal growth at constant power

As described earlier Czochralski growth process is a batch process. R.F. generator heats up the crucible by induction heating. This heat conducts mainly into the melt to maintain the heat transfer across the growth interface. However, as the crystal grows the melt level decreases. This causes change in power requirement for the same growth rate at different melt level. To represent what is the effect constant power during the growth process, an experiment was carried out. Crystal was first grown to cylindrical diameter in automatic mode. Once the process reached stability, the manual power mode was run by switching off all automatic control. That means constant power was provided to the crucible after that. The resultant crystal is presented earlier in Figure 2-3. The results are presented in following figures.

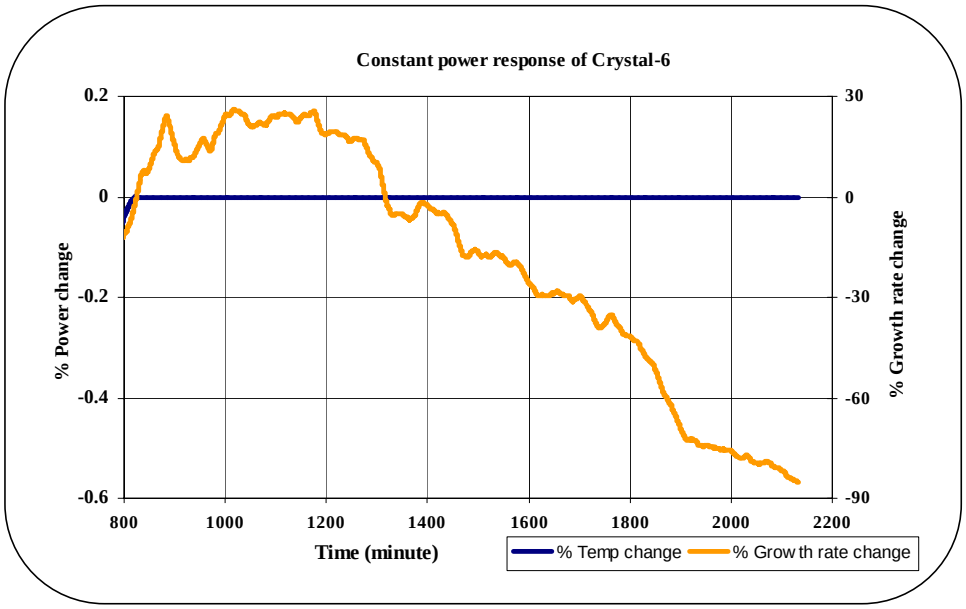

Figure 4-7: Effect of melt level drop on power requirement

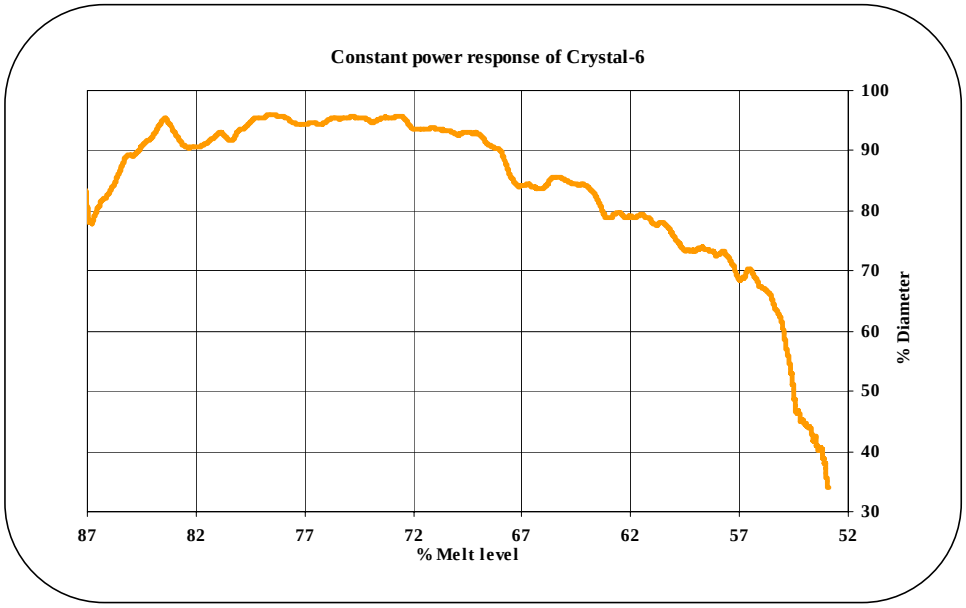

Figure 4-8: Diameter vs. melt level for constant power growth

From above figure, one can see that initially the diameter increases from 87% melt level to 75% of the melt level. However, after 70% melt level, the diameter keeps decreasing. At around 57% of the melt level crystal growth becomes unstable and diameter decreases rapidly. From this result, one can say that initially power required for same diameter increases but once the critical melt level reaches the power required for same diameter growth decreases rapidly. The control structure should have adaptation as growth proceeds.

4.2.3 Impulse test and step test for Crystal-1

The impulse test represents the relation of the output ($y(k)$, the percentage change in growth rate) with the input impulse ($\delta(k)$, the percentage change in power) applied at time in the time domain. The relation of the output to the input can be represented as time-domain convolution integral. In discrete time domain, it is a convolution summation and represented as follows with $h(k)$ as the impulse transfer function:

$$y(k) = \sum_{i=T_I}^{T_S+T_I} h(k)\delta(k-i)$$

For the non-delayed system, the initial response time T_I is zero and the output response of the system appears as soon as the system is exited with the input. However, for time delayed system T_I is not zero. In other words, the output response of the system appears after some time. This delay is called the time delay of the system. Here, after settling time T_S, the input has no affect on the output and output settles at its original value.

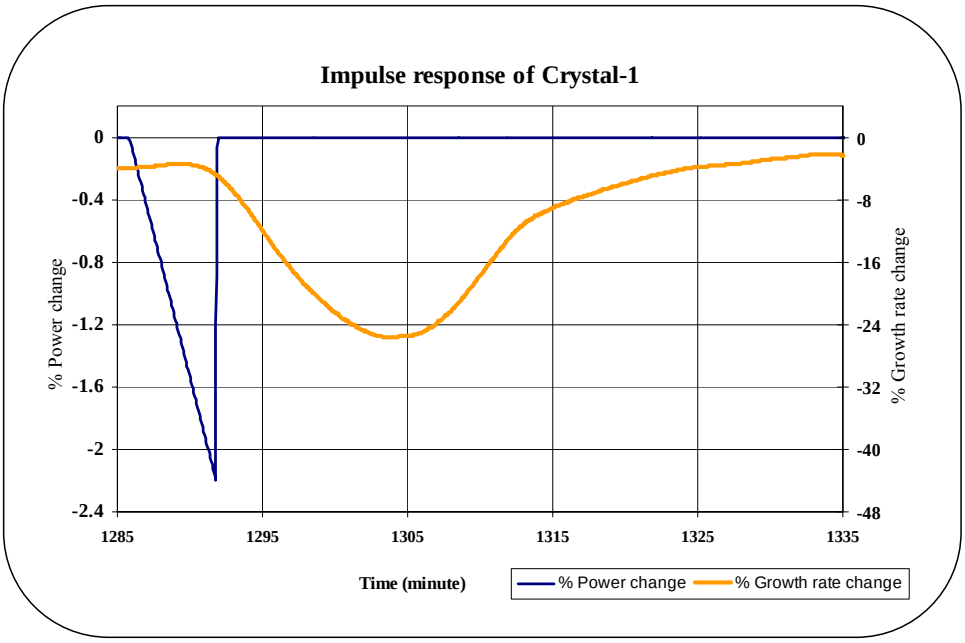

Figure 4-9: Impulse test on Crystal-1

In Figure 4-9, the result of the impulse response test is presented. It represents the significant amount of time delay in the crystal growth process. Although the value of the time delay depends on the amplitude of the impulse applied during the growth, for the limited input power change, the time delay in the output remains bounded in some range. Here, only 2.2% of power change was applied from $t = 1285.87$ minute to $t = 1291.87$ minute. The growth rate was decreased to about 25%. The growth rate came back to initial state after about 50 minutes (Figure 4-6 A). The time delay and settling time was observed to be about 6 minutes and 44 minutes respectively. These results are important for the control system design.

4.2.4 Step test for Crystal-1

Similarly, the step test was carried out on the Crystal-1 as shown in Figure 4-6 B and Figure 4-10. The step response test is the first time integral of a unit impulse occurring at the same time. In other words, in time-domain representation, a step change in input $u(k)$ is similar to the train of impulse occurring at each sampling time. Therefore, the system never converges to its original state but settles to a new output value (new growth rate). The relation of the input and the output can be described with transfer function $S(k)$ as follows.

$$y(k) = \sum_{i=T_I}^{\infty} S(k)u(k-i)$$

In Figure 4-10, the result of the step response test is presented. Here, only 1% of power change was applied at time $t = 1538.20$ minute. The system had time delay of about 4-minute whereas the settling time with new growth rate was about 150 minutes. The time delay was less compared to the impulse response test because the energy supplied (power x time) to the furnace is higher than impulse response test. Here, only 1% power change was enough to change the measured growth rate to about 75%. It represents the importance of advanced adaptive control system during for the growth process. Such large power change should be avoided during the actual growth. Hence, the maximum percentage change in power has to be considered as constrain on the control to preserve the growth stability. Also, from the Figure 4-6 B, one could see that this change had led the generation of the defects and deterioration of crystal quality.

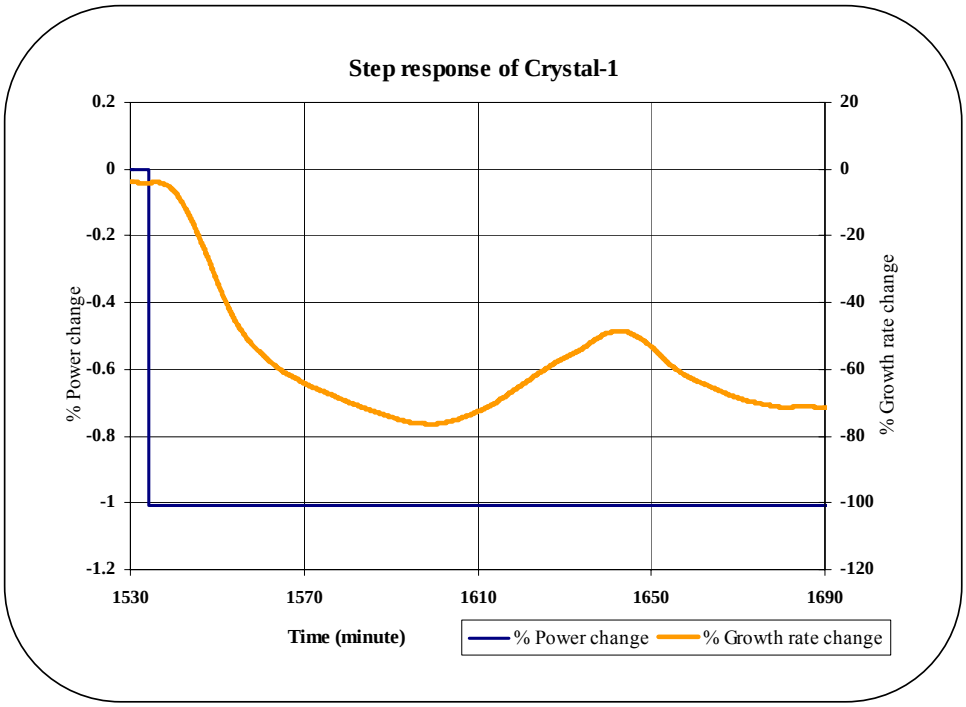

Figure 4-10: Step test on Crystal-1

This can also be seen in the Figure 4-10 as an abnormal increase in growth rate. To preserve the crystal quality during the growth, the rate of change control signal (or skew rate) during the certain period of time has to be considered as constrain on the control signal. The value of this constraint depends on the type of crystal growth. As an example, for LGT crystals, if grown with the similar specification, the maximum percentage change should be less than 1% and the maximum skew rate should be as per the half cone angle set during the cone growth. The effectiveness of such control system will be studied later.

4.2.5 Sinusoidal test for Crystal-2 and Crystal-3.

The sinusoidal tests were carried out to identify the effects of system parameters, especially the melt level and the crystal size, on the time delay during the growth of Crystal-2 and Crystal-3. The sinusoidal perturbation in the input power was applied after the stable cylindrical growth is reached. The sinusoidal signal had the time-varying amplitude and the cycle time. The amplitude and the cycle time for both the sinusoidal tests were linearly decreasing from maximum to minimum values as Figure 4-11 and Figure 4-12. The choice of the maximum and minimum values of the amplitude and the cycle time depend largely on the expertise of the operator and should be drawn such that the crystal growth remains stable during the perturbation.

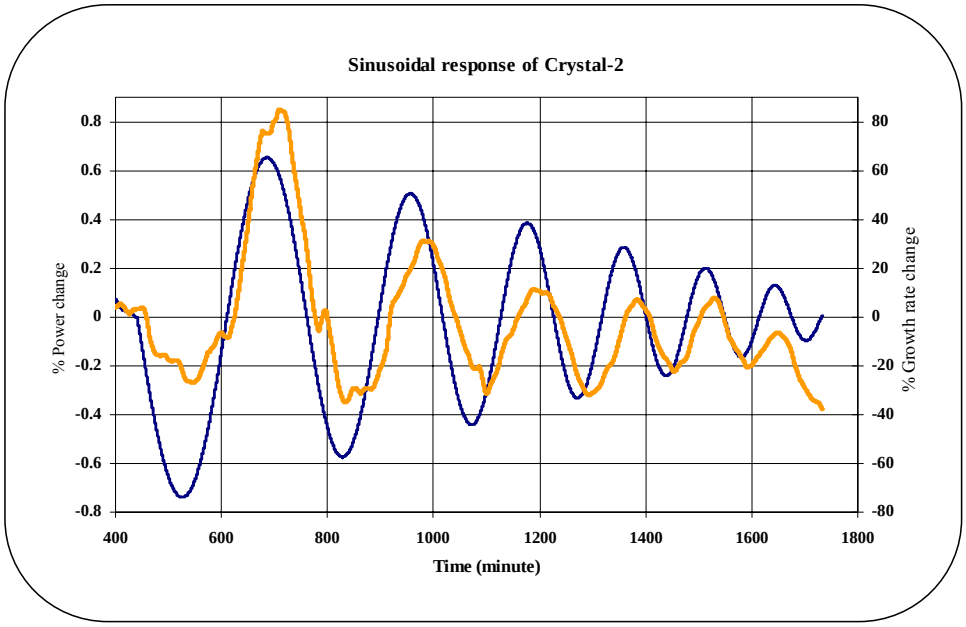

Figure 4-11: Sinusoidal response for Crystal-2

For Crystal-2, the starting amplitude and the cycle time were +0.94% and 8 h/cycle respectively. For Crystal-3, the starting amplitude and the cycle time were +0.71% and 7 h/cycle. For both crystal growths, the minimum value for the amplitude and the cycle time were zero and 3 h/cycle respectively. The total time for the sinusoidal response test was 24 h.

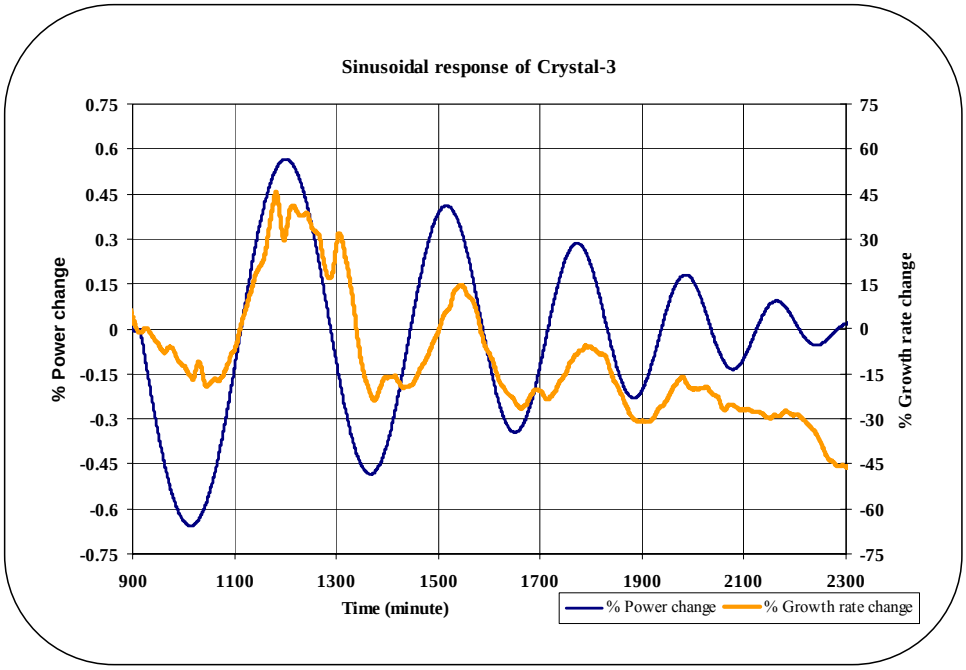

Figure 4-12: Sinusoidal response for Crystal-3

For the Crystal-1 and Crystal-2, estimated time delay between each peak and zero crossing of the input (percentage change power) and the output (percentage change growth rate) was calculated from the recoded data. For example from Figure 4-13 and Figure 4-14, the time delay for Crystal-2 at 4^{th} peak and 5^{th} zero were observed to be about 26 minute and 25 minute respectively. In addition, from the recoded data, the initial melt level was used to normalize the calculated melt level drop at particular time

and express it in percentage. Similarly, the final length of the crystal was used to normalize the calculated crystal size at particular time and express it in percentage. In Table 4-1, the percentage melt level drop, the percentage crystal size and the corresponding time delay for each event is presented.

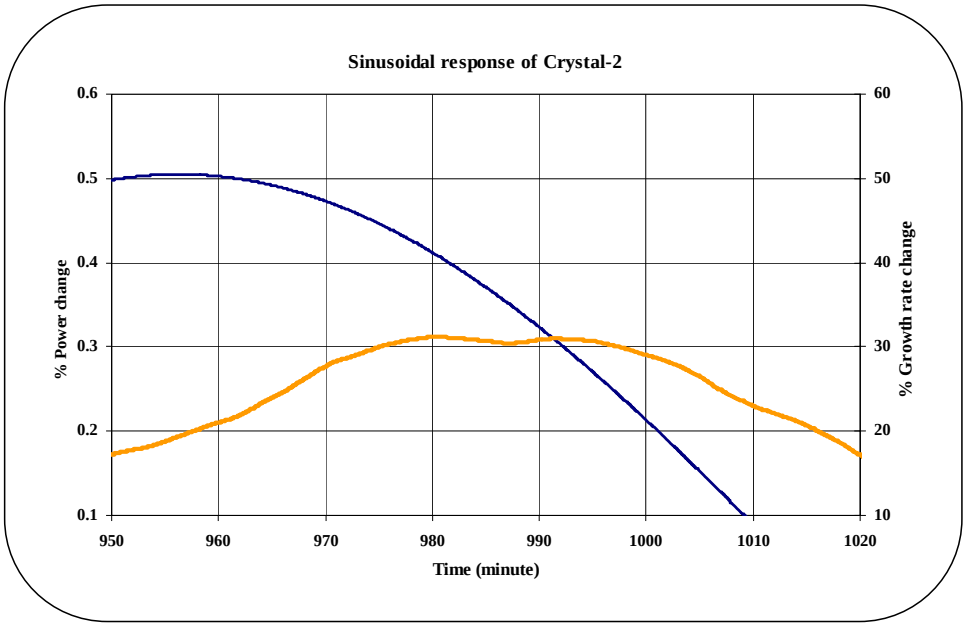

Figure 4-13: Time delay for Crystal-2 at 4th peak

It was observed that the Crystal-2 was unstable after 6th peak and crystal diameter was rapidly decreasing (Figure 4-11 and Figure 4-12). Therefore, data after, this peak has not been considered for time delay analysis. The melt level drop was only from 22% to 51% during this time. For Crystal-3, due to the early disturbance during the neck growth the crystal growth was unstable after 4th peak time. From Figure 4-12 for Crystal-3, the time delay up to the 4th peak can be observed but due to the noise and disturbances these data couldn't be analyzed for the time delay.

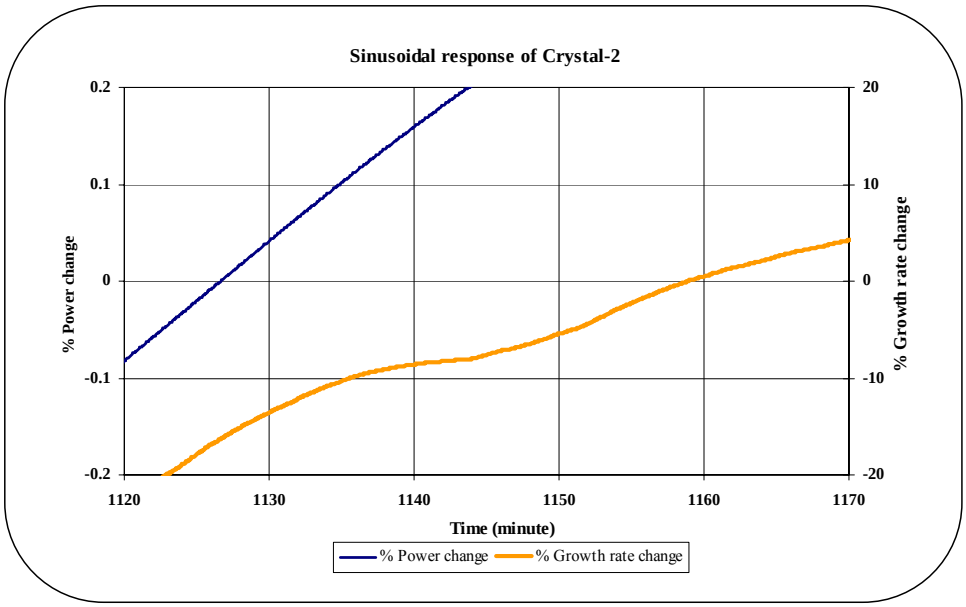

Figure 4-14: Time delay for Crystal-2 at 5th zero

Further tests are required to observe the effect on time delay during the entire crystal growth process. However, from Table 4-1, it is clear that the time delay varies as the crystal growth advances. The time delay increases as the melt level drops (and crystal size increases). In Figure 4-15, the relations are also presented by exponential trend lines. Therefore, the time delay can be considered as a function of melt level drop for the modeling purpose. In other words, the suitable model of Czochralski is time-varying delay model.

Table 4-1: Time delay, melt level and crystal size Crystal-2

The measurment of time delay for Crystal-2			
Event	**Melt drop (%)**	**Crystal size Size (%)**	**Time delay (min)**
1st zero	21.98	26.24	11.73
1st peak	24.75	30.69	13.71
2nd zero	27.54	35.05	14.34
2 nd peak	32.01	39.87	16.06
3rd zero	36.32	44.58	17.27
3rd peak	38.47	48.05	19.97
4th zero	40.45	51.48	22.26
4th peak	43.14	55.00	26.13
5th zero	45.87	58.42	25.00
5th peak	47.70	61.33	28.48
6th zero	49.50	64.21	32.54
6th peak	51.49	66.94	32.40

Heat-mass transfer can explain such increase in time delay. As the melt level drops, the contact area of the crucible and the melt decreases. Hence, the effective power delivered to the melt (so to the growth interface) decreases. This effect causes the increase in time delay. In addition, as the crystal size increases the heat conduction inside the crystal increases. In addition, the upper part of the crystal is increasingly at a lower temperature due to the configuration of the thermal insulation around and above the crucible. In other words, the heat loss increases with the crystal size. Hence, the change in power required for the appropriate change in the growth interface temperature-gradient increases. The time required to reach stability also increases. The crystal growth response becomes sluggish. Thus, the time delay increases because of both the melt level and crystal size. However, any one of the parameter is enough to describe the effect on time

delay, as they (the melt level and the crystal size) are interrelated. One can also consider multiplying the both parameters to model the time delay. These results are important in designing the control system.

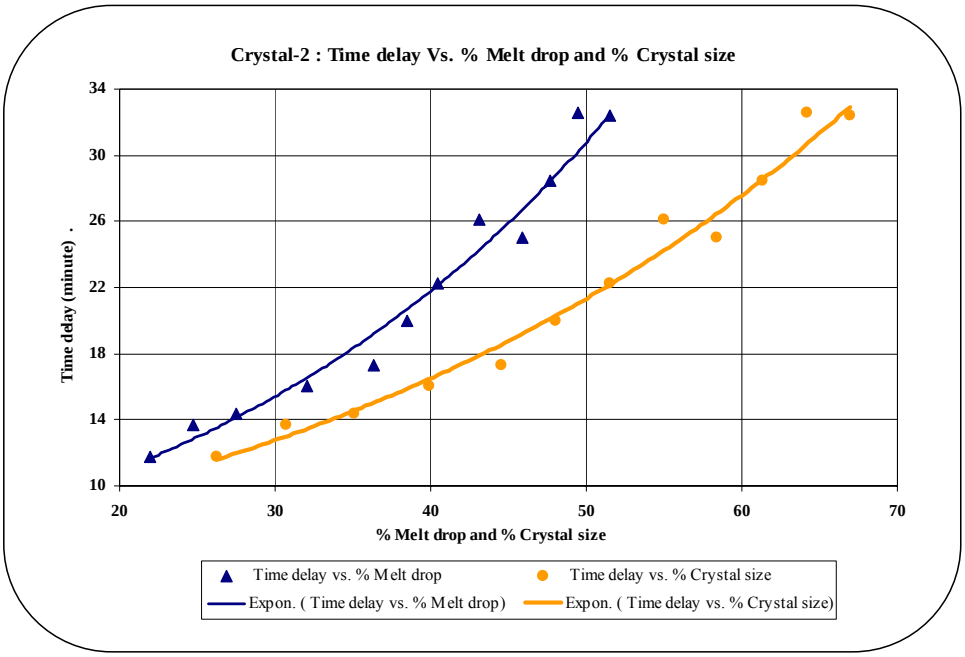

Figure 4-15: Time delay vs. % melt drop and % crystal size

4.2.6 Offline model identification based on ARMA model

We have presented earlier that the crystal growth process can be modeled as a time-varying time delay system. For the advanced adaptive control system, real-time model identification is necessary for such time-varying system. Auto regressive moving average (ARMA) model (as shown in equation (3-1)) was considered for this identification. Once the model parameter converges during the identification, for the optimal control action, the objective cost function can be minimized with constrains. Such controller is obviously advantageous compared to the conventional PID controller.

Here, only the stability of such process identification with higher orders model and time delay has been checked. The main reason of considering the higher order model is that such time varying time delay can be approximated by pade-approximation as the higher order model with constant time delay model. The change in time delay will be approximated by the change in parameters of higher order model during the identification. However, the stability of such high order model needs to be studied.

Table 4-2: Stability of the ARMA model identification

Delay		Order of the model (=A=B)					
Minute	**Model delay (d)**	**Order 3**	**Order 10**	**Order 20**	**Order 30**	**Order 40**	**Order 50**
0.00	0	0.02658	0.03026	0.05815	0.66386	17.23808	15.70202
2.00	30	0.03390	0.01753	0.01616	0.01494	0.02237	0.03026
4.00	60	0.03843	0.01759	0.01713	0.01493	0.01594	0.01549
6.00	90	0.04276	0.01756	0.01739	0.01493	0.01587	0.01573
8.00	120	0.04344	0.01755	0.01780	*0.01492*	0.01592	0.01557
10.00	150	0.04085	0.01761	0.01922	*0.01499*	0.01603	0.01552
12.00	180	0.04423	0.01760	0.02115	*0.01504*	0.01622	0.01559
14.00	210	0.06353	0.01757	0.02568	*0.01504*	0.01624	0.01556
16.00	240	0.09364	0.01757	0.04321	*0.01509*	0.01624	0.01568
18.00	270	0.04078	0.01752	0.09585	0.01506	0.01638	0.01576
19.50	300	0.02452	0.01751	0.19463	0.01494	0.01642	0.01580

For the model identification, the order of input and output were assumed to be identical ($n_a = n_b$). The delay d is assumed to be the multiple of sampling time. The process model identification was carried out from the sinusoidal test results of Crystal-2 for various delays time and presented in Table 4-2. From the Table 4-2 one can see that for $n_a = n_b = 30$ and for delay range 8 minute to 18 minute, the prediction errors were consistently lower than other models. In the other hand, for the lower order

model $n_a = n_b = 3$, the prediction errors were consistently higher. The higher order models are better choice for model identification and prediction. According to Table 4-2, the higher order $(n_a = n_b > 10)$ model identification is stable in terms of predictive error, as it remains bounded. Here, the only one step-ahead prediction error is checked. However, during the actual control system design the prediction horizon can be extended to cover the range of time delay, as the model is stable.

4.3 Initial results and motivation

The melt level and crystal size were observed changing not only the Eigen structure but also the time delay between the input and output during the crystal growth. The effect is very apparent for slow growing crystals and cannot be neglected for control system design.

The growth system considered for developing the control system is presented in section 4.1 . Initially, the growth interface was adjusted to be flat by adjusting the rotation rate. The instability or growth interface change occurs with the present system at around 40 to 42 rpm for LGT crystal growth. The optimum rotation rate was set to 35 rpm. The second test was carried out to approximate the density of the melt. The fast cooling of the melt created a void in the center of the solid material. The density of the melt was 5.63 g/cm^3 calculated from the volume of the void. The density of the solid material is 6.15 g/cm^3. In other words, the density of the melt is about 8.5% less. This difference will be used during the calculation of the growth rate.

To study how the requirement of power varies for the constant diameter as growth proceeds, a constant power test was carried out once the cylindrical diameter is achieved.

The result reveals that initially requirement of power increases and, as the melt level drops below 57%, it starts decreasing. Controller has to adjust to new set point with melt level.

Impulse test, step test and sinusoidal were also carried out to reveal the time delay and how it changes with decreasing melt level. The results indicated an exponential relation between melt level and time delay. The controller has to be designed to consider this time varying delay. The constraints on the power inputs are also identified to preserve the quality of the crystal during the growth. The real-time identification of the crystal growth process is necessary for the predictive controller. Higher order model were proposed, as they can be more adaptive with the time-varying delay. Stability of such model during the off-line identification was carried out. For 30^{th} order model, the prediction errors were consistently lower than for the other models. However, for the lower order model the prediction error was higher, which makes them unreliable for control. This indicates that the higher order models were stable.

The results extracted from these experiments were useful to the design of the controller structure discussed in the next section. The long range model predictive control strategy along with constrain and time-delay model identification was chosen to further design an advance controller for such slow growing crystals.

CHAPTER 5: DEVELOPMENT OF CONTORL SYSTEM

The objective of this study is to develop a new control system that can consider a time- varying parameter delay and constraints. In this chapter, the new control system's design and development are discussed. Based on the specification, assumption and growth requirement, the LabVIEW control program was developed. A detailed flow chart and an operation method have been developed for the real-time growth using this program. Initially, simulations were applied to rectify programming error, modify and tune the program before adapting to the real-time crystal growth. Later, difficulties related to the process model identification during real-time growth were observed. These challenges were investigated, and suitable options to address them are presented.

5.1 New controller structure

In this section, a new controller structure is presented. At first, assumptions and specifications for the proposed controller are briefly discussed followed by the controller structure and the operation method.

5.1.1 Specifications and assumptions

- As shown in Equation (2-5), the continuous time transfer function of the Czochralski crystal growth process has three poles and two zeros. However, the discrete time function with the similar structure is not a good choice due to existence of the unknown time delay for the slow growing crystals. The higher order model is preferred in this work.

- The continuous time presentation of the time-delayed model can be presented as follows. Here, the characteristic time delay, τ_d, is total delay and can be considered as a combined delay due to the delayed dynamics of the system and the measurement delay.

  $$H_D(s) = H(s) \cdot e^{-s\tau_d}$$

- For simplicity, in a discrete time representation of the growth system, the time delay is assumed as a multiple of the sampling time. Here, the order of time delay is much greater (≥ 8 min.) than the sampling time (4 sec).
- As presented earlier, the time delay varies as the melt level or the crystal size changes. The complete system dynamic is considered as a time varying time delay system. However, the time delay is mainly studied here for the control system design.
- The R.F. generator transfer function is not included in the crystal growth model. In the cascade controller structure, there is an independent controller for it. The R.F. generator has some nonlinearities and uncertainties due to its dependence on the grid supply. E.g., the controller should take proper action, like pulling out the crystal if power or generator fails, in such an event.
- Generally, the output of the growth system is taken as the growth rate, which is square function of the crystal radius. However, for the slow growing crystals, the squared error produced by this growth rate can cause unnecessary perturbation because of over controlled action. Instead, the calculated diameter, from this growth rate, is considered as an output to control the growth system.
- The unit-less conversion of the power change and the diameter (input-output) should be helpful for the model identification and the control system implementation for

different growths. The output inversion (from positive to negative) is considered to make the plant positive as response system. This should help to identify the model and to avoid any ambiguity. The feedback, in this case, is positive instead of negative.

5.1.2 New model of the controller

Figure 5-1 represents the proposed cascade controller structure for the crystal growth technique. The control structure is similar to the one discussed in chapter 2.5 Loop-2 controls the R.F. Generator power as per the supplied feedback of loop-1. Loop-1 is the primary controller for the diameter of the crystal. The control action is divided into four tasks.

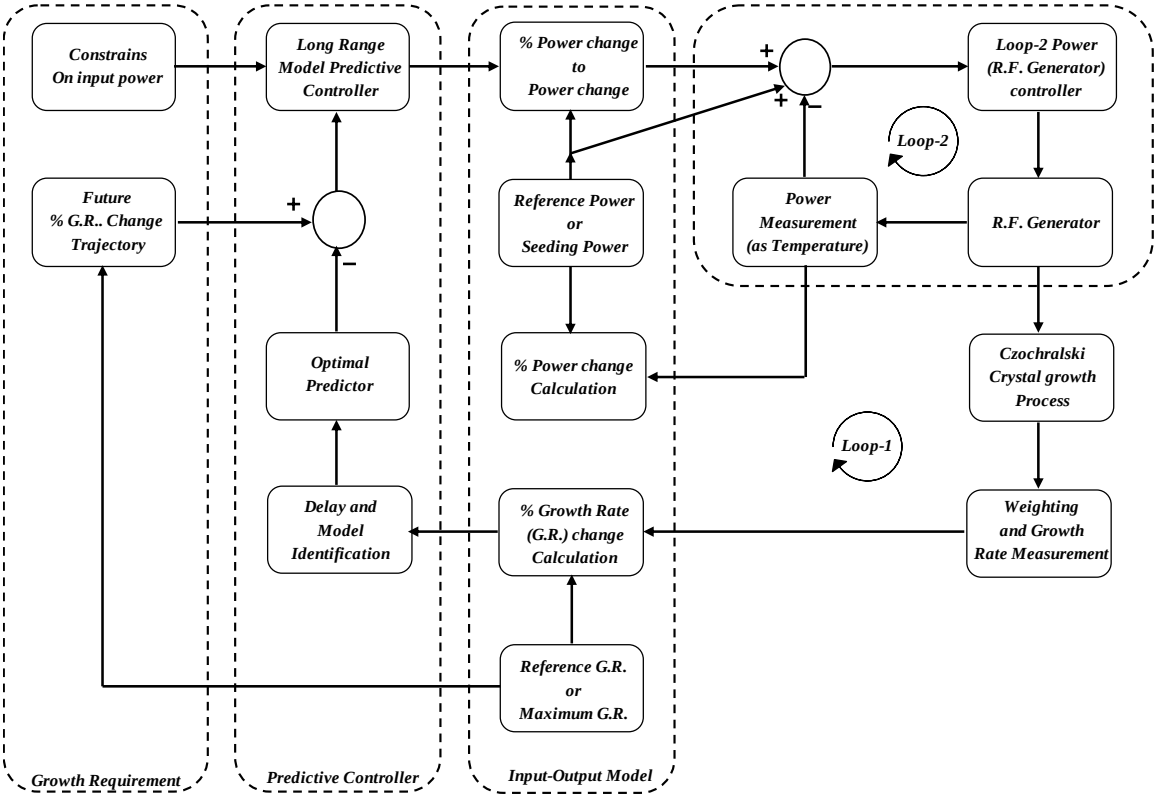

Figure 5-1: Proposed controller structure

- First is a measurement task. The computer communicates with the weighing mechanism and measures the weight of the growing crystal. The signal is then filtered and converted into approximate growth rate and diameter of the crystal as discussed in chapter 4.1.3. The computer control system also measures and filters the power output of the generator in the form of the thermocouple temperature as discussed in chapter 4.1.1.
- The second task is converting both the measurement (input of the model) and control signal (output of the model) in percentage change form as discussed in 4.2.1. The Calculated growth rate or the diameter will be converted in percentage growth rate or percentage diameter change respectively. The control signal is derived from the controller output in the percentage power change form. This control signal is a feedback to loop-2. Here, this feedback will be positive because of the inversion in the modeling as shown in the Figure 5-1.
- The third task involves identification of the model and deriving a control signal. Here, the identified model is used to predict the output of the process for the control horizon based on the delay. This predicted output is compared with the required output (trajectory) of the growth system. The proper controller action is derived using a long range predictive control technique.
- The forth task is to define the growth requirement (or trajectory) and future percentage diameter change (growth rate change) trajectory. Constraints on the set point and control signal are defined in this block.

5.1.3 Flow chart of the control software

Based on the new controller structure, the LABVIEW software was used in order to develop the controller program. Figure 5-2 shows the general flow chart of the complete control software. The program consists of not only the controller structure as described above but also the graphical user interface (GUI), where the operator can adjust and select various growth related parameters.

There are mainly three parts of the control program. These parts were derived based on the operation of the control program.

- Initialization: The program is required to do the following jobs:
    - a Clear all history parameters including the measurements, indicators and charts.
    - b Initialize all sub-programs and set default values for all parameters for measurement, control and other computational variables.
    - c Define initial parameters for the new control system like model, tuning parameter, control signal, and trajectory.
    - d Get the initial growth parameters from the operator before starting the program. These data are important for calculating diameter and set point.
    - e Start the measurement and control with default values. Wait for the measurement to be stable.
    - f Start the main program with no control signal and allow the operator to set the other process parameters. Let the program run in constant power mode to achieve stability after the seeding, before starting the automatic growth.

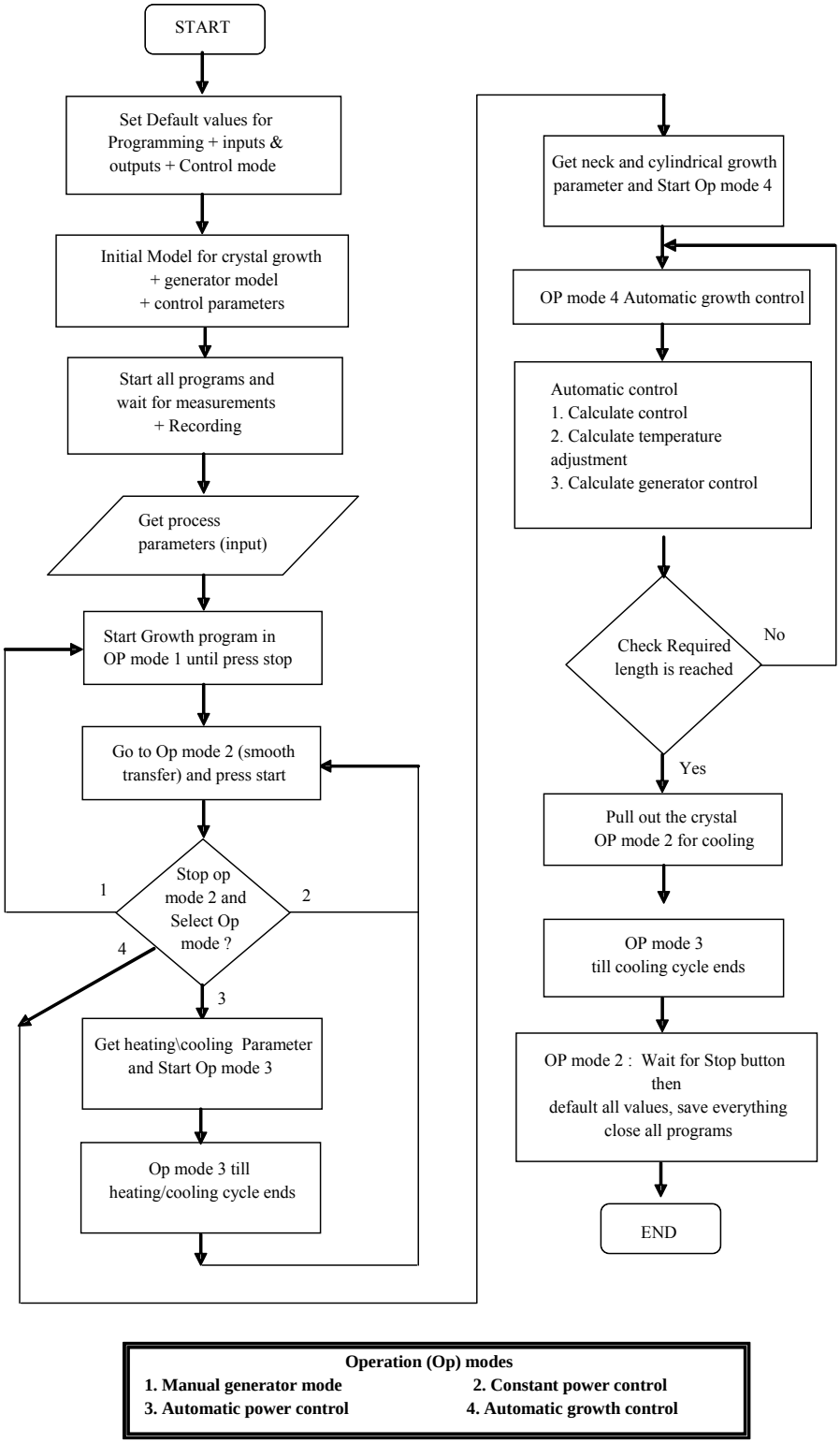

Figure 5-2: Flow chart for control program and user interface

- Heating or cooling cycle: Once the program starts, the operator needs to heat crucible to melt the chemicals. Similarly, when growth ends, after the crystal has been pulled out of the melt, the operator needs to cool down the growth system. The program is required to do the following jobs during these processes:
    a. Reset the time and power (temperature) arrays (or profile).
    b. Get the new time and power arrays from the operator.
    c. Calculate the set point and remaining time for the control program based on these arrays.
    d. Run the generator control program only to control the power. Start the profile from the present power reading and end at the final set point of the profile for the smooth operation.
- Automatic crystal growth: Once the melt is ready and the seeding is successful, the operator can start the automatic crystal growth process. Then, the program is required to do the following jobs:
    a. Calculate growth rate and diameter.
    b. Get various growth parameters for the cone and cylindrical growth part. Calculate the initial parameters for the cone and cylindrical growth for the operator to adjust and select the other growth parameters.
    c. Select the control program, set tuning parameters and start the automatic growth mode.
    d. Calculate the required trajectory, from the set point, for the program based on growth parameters and constrain.

e Calculate the control signals for the power adjustment and the generator power from the control software.

Based on this flow chart and the growth requirements, the control program was divided in four operation modes.

5.1.4 Operation modes

These four operation modes also facilitate operator to take the emergency action other than various growth related activities like seeding, heating or cooling, cone growth and cylindrical growth. The following is the description of each mode.

- Manual generator mode: This mode facilitates the operator to take emergency decision in case of a failure of the control or measurement program. The operator can directly give a manual control signal to the generator. The detail description and specification for this mode is discussed below.
    a During this mode, both control programs, diameter control program and generator control program, are stopped. However, all measurement and indicators are working. This mode can also be used to reset all calculation of the control program.
    b The program starts at this mode initially with zero control signals. Once all measurements and indicators are working normally and all required parameters are set, the operator can then switch to the control mode.
    c Transfer between manual mode to any other and vice versa has to be smooth (with out any interruption). This transfer could take some time to adjust the control signal due to control iterations. A start or stop button is needed to facilitate this transfer.

d. This mode can also be used to switch the generator control from the generator control panel to the computer. This method is necessary to rectify error or modify the program or the hardware during the growth run without a major interruption.

e. The operator can reset calculations like the calculated diameter, length and tare scale in this mode. Again, the crystal length is not calculated in this mode but growth rate measurement and diameter calculation are performed.

- Constant power mode: This mode is primarily for controlling the generator power by the control program. The operator can set power set point based on the process requirement. It is also helpful to manually adjust the power during seeding. The detail description and specification for this mode is discussed below:

    a. During this mode, the generator control program is working but the growth control program is not working. Here, control parameters for the generator control program are pre-tuned.

    b. When the manual mode is stopped after the program initialization, the program transfers to this mode. This mode serves as a default mode for all other modes. In other words, when any other operation mode ends (including the automatic growth and the automatic power) or is stopped by the operator, the control program automatically transfers to this mode. This mode can be used to reset any growth or control parameter that has been entered in automatic mode. The operator can transfer to another mode without any perturbation from this mode.

c. Like in the manual power mode, the operator can reset calculations like the calculated diameter, length and tare scale in this mode. Again, the crystal length is not calculated in this mode but the growth rate measurement and diameter calculation are calculated.

- Automatic power mode: This mode is used to automatically heat or cool the growth system. The operator can start this mode from the constant power mode. It can also be used to slowly adjust the power (temperature), if needed during the growth or seeding process.
    a. Again, similar to constant power mode, only the generator control program is working but the growth control is not working.
    b. The operator needs to define the heating or cooling profiles (time and temperature array) before starting the program.
    c. Smooth transfer from the constant power mode is required in this mode.
    d. Once it ends, program goes to the constant power mode again with smooth transfer and stays there for further action from the operator.
- Automatic growth mode: This mode is used to grow the crystal in automatic control for both the cone and cylindrical growth.
    a. The operator enters the required cone growth parameters like cylindrical diameter and height. He also selects the growth control method and control parameters before starting the automatic growth.
    b. The program should start from the present diameter as a set point and grow to the desired diameter during the cone growth. This mode can also

be helpful to adjust the crystal diameter if something goes wrong and program needs to be restarted.

c Once the cone growth ends, it transfers to the cylindrical growth.

d The program remains in this mode either the required length of the crystal cylindrical part is reached or the operator stops it. Once it ends, the program goes to the constant power mode with smooth transfer and stays there for further action from the operator. All control and growth parameters resets at the end.

e Even during the control mode, the operator can adjust the power change, which is to be added to set point power of the generator control loop. This facilitates to fine tune the growth and adjust the power, if some abrupt interruption occurs during the growth.

5.1.5 Process parameters for measurement, control and calculation

This section describes the data or parameters required by the program in order to work as desired. It also describes the measurements and calculation that the program needs to present to the operator in order to take proper action.

Initially, the operator needs to enter various process parameters that are required by the control program to measure, calculate and control the process. Figure 5-3 shows the data required (a) before starting the program (b) before the automatic power mode (c) before the automatic growth (i.e. starting the crystal growth). Similarly, the operator can also reset the crystal length, diameter (or growth rate), tare scale, and charts before starting the growth or during the constant power mode.

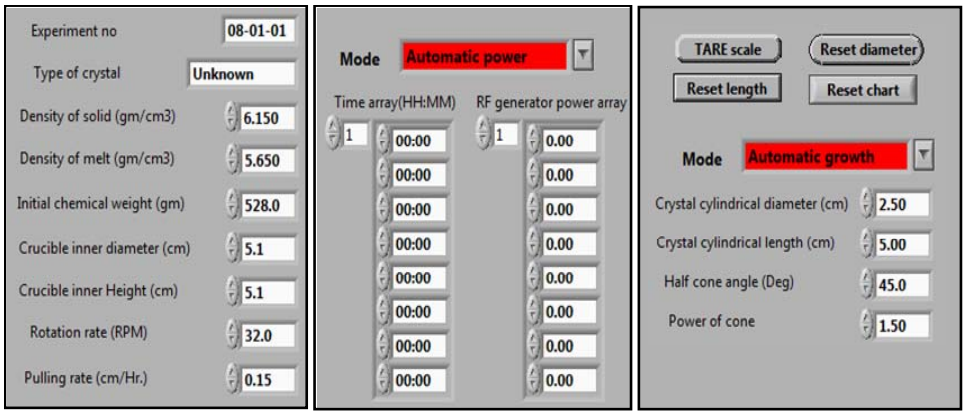

Figure 5-3: Input data: for starting the program, heating cycle and automatic growth

In addition, during the manual power mode and the constant power mode, the operator has to enter the manual control signal and the power (temperature) set point respectively based on the operation mode. The operation mode can be started and stopped using a button at any time during the process.

The control mode for the automatic growth, LRPC or PID etc., can only be selected before the growth starts. However, the control system's parameter can be tuned during the growth. It is worth mentioning here that operator also can adjust the manual power change and the diameter set point during the automatic growth to fine tune the process manually, if required. Here, the generator control signal updates every 200ms whereas the control signal for the growth control program updates every 8 seconds. It measures weight every 4 second and filter it from last two samples.

From these parameters and measurements, software calculates following three types of parameters. Figure 5-4 shows some of these variables used in the control program.

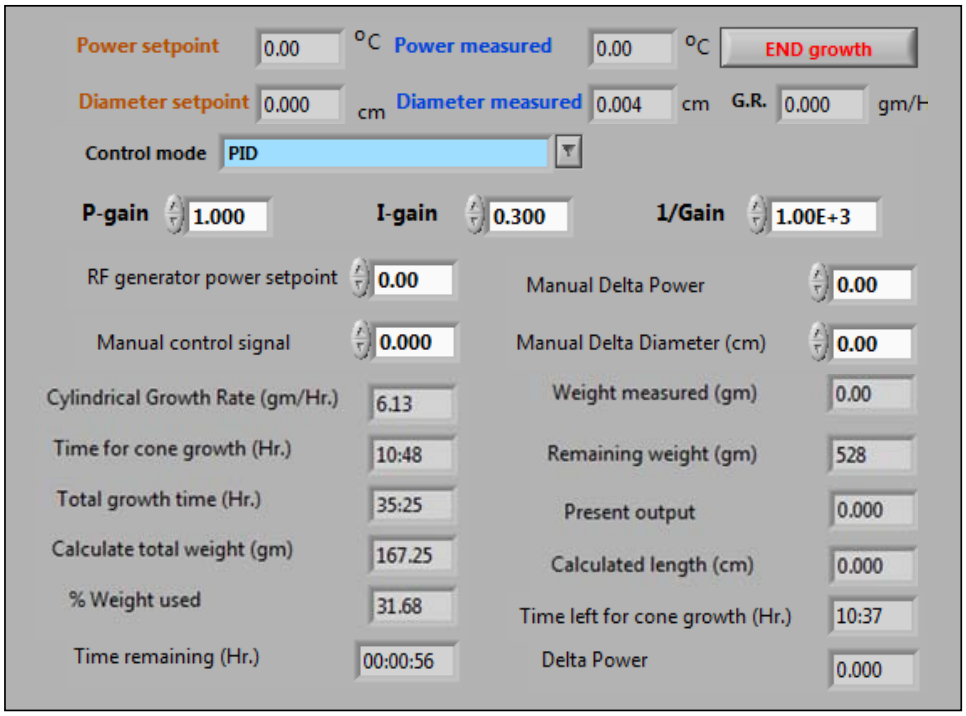

Figure 5-4: Various measurements, calculations and control parameters

General: crystal growth rate, crystal diameter, crystal calculated length, power change (temperature), present output (i.e. control signal), remaining weight, remaining time for heating or cooling cycle.

$$W_{total} = W_{cylindrical} + W_{cone} = \pi \cdot \rho_s \cdot r_{cylindrical}^2 \cdot \left(\frac{v_p \cdot t_{cone}}{3} + Lenth_{cylindrical} \right)$$

$$Time_{total} = t_{cone} + t_{cylindrical} = t_{cone} + \frac{Length_{cylindrical}}{v_p} \cdot \left(1 - \frac{r_{cylindrical}^2}{R_{crucible}^2} \right)$$

(5-1)

- Set point or trajectory program: diameter set point, temperature set point.
- Growth parameters: time remaining during cone growth, calculated growth rate for cylindrical part, present time for cone growth, total growth time, total weight and

percentage weight used. Approximate total growth time and total weight are calculated before starting the growth, to help the operator, using the equation (5-1).

5.1.6 Development of the graphical user interface and LabVIEW software

LabVIEW software is preferred in order to develop the control program. LabVIEW software using virtual instruments (VI) is more user friendly than the present MicRicon controller is. It also has some advantage over other programming language like C++. LabVIEW provides customizable controls and indicators in various formats e.g. buttons, charts, values and characters that could easily adopted with the control software. It has a benefit of running independent sequences or VI based on the requirement of the program. The development of the LabVIEW program for the crystal growth control was divided in various parts, or independent VI files, based on the objective. There are mainly five independent VIs in this project.

- Global variables and graphical user interface (GUI): GUI is a center of the program that enables the operator to use the control program effectively. GUI also allows the operator to change the operation mode, control mode and process parameters. It calculates set points for both the control programs, depending on the operation mode of the process. It connects and calls all other VIs and uses global variable VI to share various controls and indicators between them. Figure 5-5 shows GUI interface of the program before starting the program.

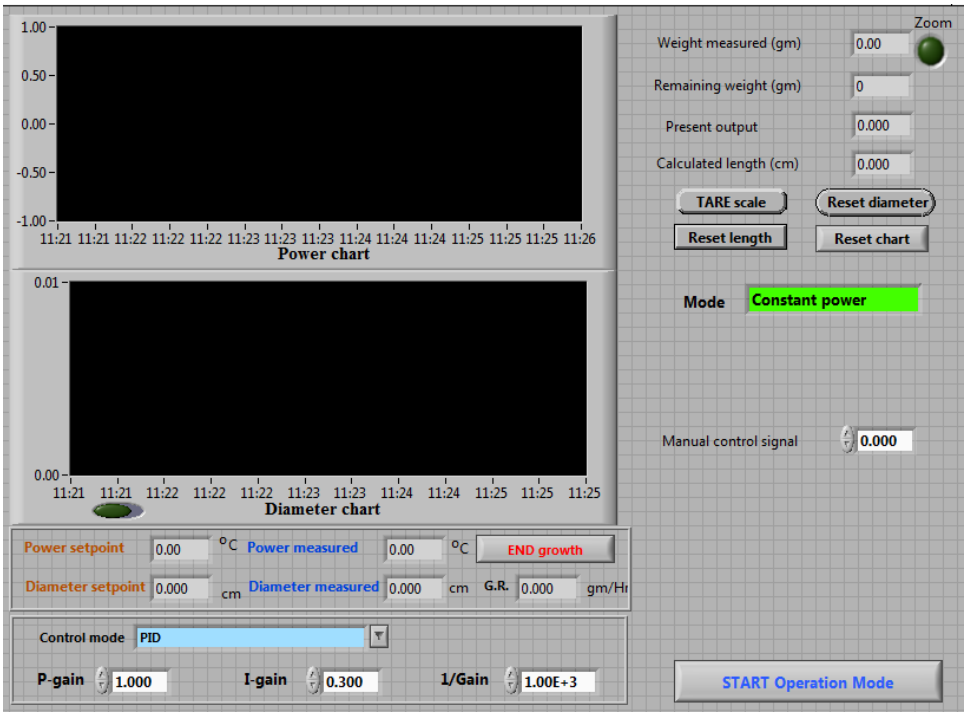

Figure 5-5: Graphical user interface of LabVIEW control program

- Input and output: This VI measures required variables, power and weight, and calculates growth rate, crystal diameter and crystal length. For simulation purposes, the process model VI is developed in place of this program.
- Generator control VI: This program calculates the generator control signal based on the error between a set point and the actual values, depending on the control mode selected by the operator. The program also adds up positive feedback, calculated form the growth control program, and present set point to calculate the new set point for the generator control as shown in Figure 5-6. High limit and low limit of the power adjustment are the constraints on the power control for crystal growth. They prevent the crucible and the growth system from overheating, if the control program does not

work normally. As shown in the figure, diameter multiplier variable works like a flag for auto (=1) and manual (=0) control program.

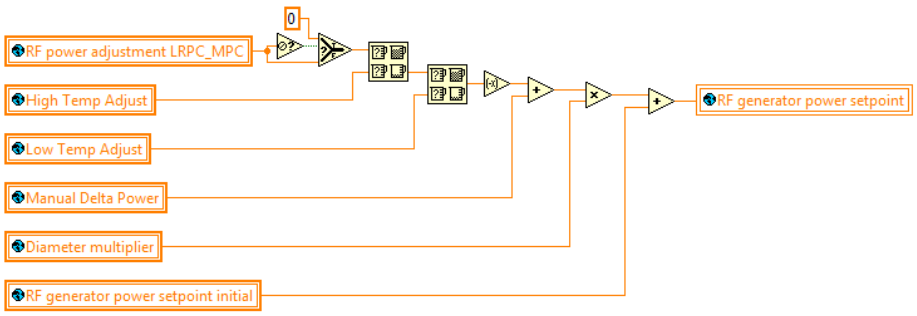

Figure 5-6: Generator set point calculation from the growth control feedback

- Growth control VI: This program calculates the control signal (or change of power) required to change the diameter of the crystal. APPENDIX-B shows the algorithm developed to calculate the control signal based on LRPC – MPC method discussed in Chapter 3.3 .
- Data recording VI: This program records all the data in a text file in a suitable format. This data can be used for later analysis.

5.1.7 Method of operation for the operator

This section describes the operation steps for the operator to grow a crystal, using the developed control program. They are divided into four tasks.

- Start the process: Open GUI program and press the run button in LabVIEW to start the program. The operator enters all initial growth parameters, as described above, on the right side of the screen and then presses the start program button. Initially, the

program starts in the manual mode and will remain there for 30 seconds to reset all the parameters, call all VIs and start measurements. At this time, the manual control signal can be used to start the generator.

- Once the "STOP Operation Mode" button enables, the operator then can transfer from manual mode to constant power mode. This process takes some time because the control program runs until the control signal reaches the manual power set point for a smooth transfer. In addition, any operation mode can be applied from the drop down control and pressing “START Operation Mode” button respectively.
- Heating or cooling process: Once in automatic power mode, the operator enters the temperature and time profile in the form of array and then presses the start button to run the profile. When the process ends, it goes back to the constant power mode. The operator can also stop the process at any time and the process will go back to the constant power mode.
- Growth process: To start the growth process, the first job is the seeding process. The operator can adjust temperature in the constant power mode. Once the seeding is successful and stable, the process is ready for the automatic crystal growth. The operator goes to automatic growth mode and enters the parameters that are needed for the cone and cylindrical growth as discussed earlier. The control mode, LRPC or PID, and initial gain parameters can also be selected before starting automatic growth. To facilitate the proper parameter selection, the operator can see various calculated growth parameters during these, as shown in Figure 5-4. The automatic growth control can be started, after this. The process starts from the cone growth and ends when the required crystal growth length of the cylindrical part is reached. During the

process, the operator can fine-tune the control system by changing the control parameters. Even during the automatic mode, the operator can adjust manual power change and diameter change without stopping the automatic control. At the end, the crystal is pulled and the automatic growth mode is stopped. The crystal is then cooled by using the automatic power mode and selecting the proper cooling profile. However, the program can be interrupted at any time during the growth and the process can be controlled from any other mode. This flexibility is good for any immediate action, if needed, during the growth.

5.2 Initial parameters for new controller

In this section, some common problems that can affect crystal growth are discussed. Later, the trajectory mapping and unit-less transformation of the control model is presented. In addition, during the initial growth new controller had some problem to control and model identification. After analyzing the data, the solution of this problem is proposed here.

5.2.1 Common problems during crystal growth

The crystal growth process is inherently unstable. In fact, some time a very stable crystal growth response can be an indication of a polycrystalline crystal rather than a single crystal. The crystal growth process is a time consuming process that makes it more vulnerable to the numerous instabilities that are uncontrollable. A slight change in any of the process parameters can create an unstable growth. In my experience in the crystal growth lab at University of Central Florida, I have faced many of these instabilities but some of them have more profound effect on the control system than the others. Here,

some of these uncontrollable uncertainties are presented to explain the effect not only on the crystal but also on the whole process.

- Power instability and the crystal growth loss: If the power fails during the crystal growth process, the molten chemical solidifies at the surface. This causes the grown crystal to be stuck with the solidified chemical in the crucible. However, due to the rotation mechanism, the grown crystal keeps rotating. In this condition, the crystal can brake from the seed. The seed holder can also be damaged. Figure 5-7 shows the crucible with the solidified crystal and the seed holder because of the power failure during the actual growth. Here, the crystal was broken from the seed holder. In another case, instead of power failure, if the power dip is observed for just few seconds then the diameter of the crystal can become unstable, which later on needs to be controlled by the controller minimizing any abrupt power correction. In addition, the power supply parameter like voltage and frequency keeps changing during the entire growth and has profound effect on the crystal quality and growth stability.
- Cooling water instability: in crystal growth laboratory, the UCF physical plant supplies chilled water. This water is used to cool the cooling water system by a heat exchanger. The temperature change of this cooling water has a very significant effect on the crystal growth. Especially, during the seeding when the temperature needs to be adjusted very carefully and maintained precisely for long time. Any changes in the chilled water temperature changes the temperature of the melt and creates instability in the growth as discussed below.

Figure 5-7: Result of power failure during the growth

a If the chilled water temperature decreases, the seeding becomes unstable and the crystal diameter starts increasing. This may initiate disturbance or defects in the growing crystal. Later, this defect can grow through out the crystal length and the crystal may become useless or cracked.

b On the other hand, if the chilling water temperature increases during the seeding, the seed starts melting and the operator may lose the seed. The operator may have to start the whole process again using another seed. Figure 5-8 shows cyclic instability of chilling water recorded during one of seeding process. In the figure, the unit of magnitude is of 5 degree Celsius/cm and the unit of speed is 2cm/h speed. The first seeding attempt is shown by a mark. The temperature of both child water (red) and cooling water (green) were stable, at this time. Later during the instability, the temperature change of 3 degree Celsius in chilled water supply resulted in

about 6 degree Celsius temperature change in cooling water supply to the growth chamber and heating coil. Multiple seeding attempts failed due to the large temperature fluctuations. In the end, the seed was lost due to melting. A new seed was installed and temperature was again adjusted for seeding. The successful seeding took about 12 h.

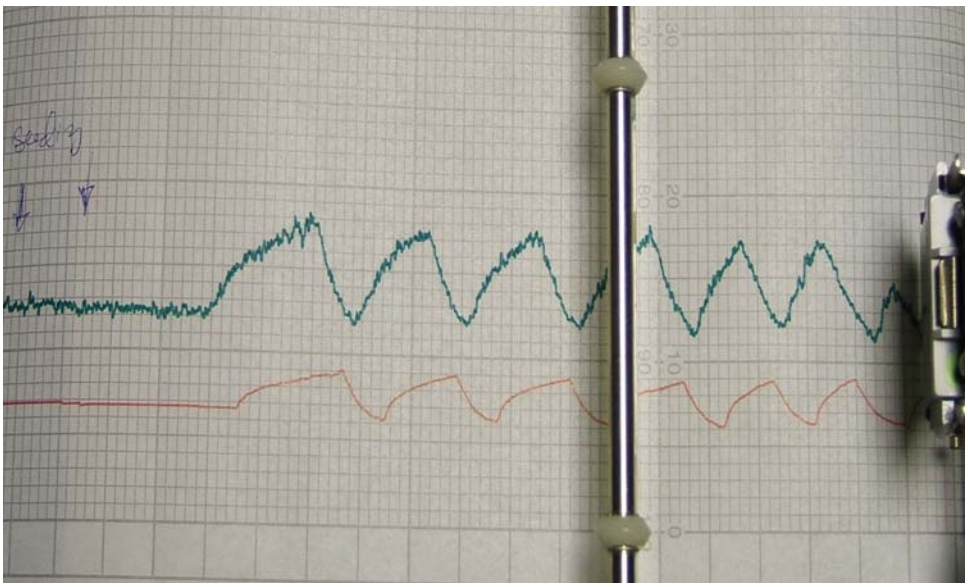

Figure 5-8: Cooling water and chilled water temperature fluctuations

- Weighing error and effect on the controller: The weighing mechanism used for the growth process has the tolerance of +/- 0.1 g. During the initial phase of the growth, this could create problem in calculating growth rate. Figure 5-9 shows the growth rate (g/h) calculated during the ideal or no growth condition for about 3 h. The calculate diameter error from this weight noise could match the approximate diameter or the growth rate required during the seeding (about 4 to 5 mm). The operator needs to keep watching the seed growth until it stabilizes at a later part of the cone growth.

Hence, the automatic growth can only be started effectively once the diameter reaches about 10 mm and growth is stabilized.

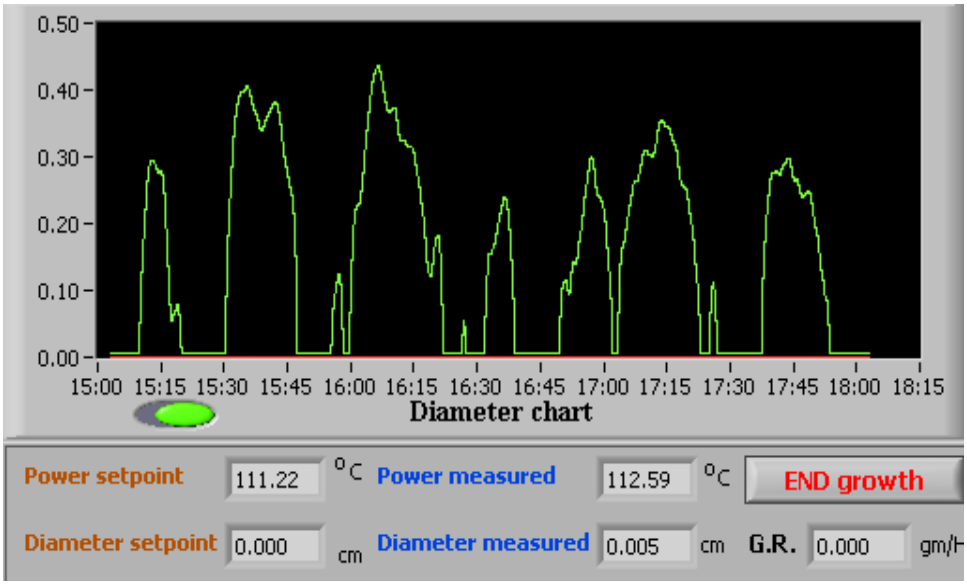

Figure 5-9: Diameter error due to weighing system noise

5.2.2 Input-output and set point calculations for control

Before presenting the result of the new control system, it is important to present a few design parameters like the future prediction, order of the model and delay. The detail description of different options and selections are presented here.

As discussed in earlier, the input-output model of the growth process was presented as a unit-less model. Here, the feedback is positive as the process is already inverted. This strategy helped to design the positive model of the process for control design. The input of the model is the power change or unit-less ΔP_{actual}. Equation (5-2) was applied to ormalize the input. Here, the operator can define maximum and minimum ΔP from the power required during seeding, $P_{seeding}$, by using variable x. The power required during

the seeding process changes with the crucible diameter. Hence, in this case, the variable x is defined by the maximum and minimum of ΔP with seeding $P_{seeding}$ for the different crucible diameter. The value of x was derived from the previous growths and analyzing the range of power change during the crystal growth. If the operator changes this variable, he may need to fine-tune the process. However, he can keep the same tuning parameter for the same diameter crucible. Similarly, the output of the process $D_{crystal}$ was normalized with the diameter of the crucible $D_{crucible}$ the maximum diameter the crystal can grow. Similarly, the set point of the process is converted in a unit-less quantity. These calculations were performed at each control instant before the control signal calculation, the unit-less model and set point parameter calculation in LabVIEW block diagram as shown in Figure 5-10.

$$\Rightarrow \Delta P_{\max} = P_{seeding} \cdot x = -\Delta P_{\min}$$

For small (1 inch) diameter crystal $x = 0.1$

For large (2 inch) diameter crystal $x = 0.2$

$$\Rightarrow \text{ i/p of the model} = \frac{\Delta P_{actual}}{\Delta P_{\max}} = \frac{\Delta P_{actual}}{P_{seeding}} \cdot \frac{1}{x}$$

$$\Rightarrow \text{ o/p of the model} = \frac{D_{crystal}}{D_{crucible}}$$

(5-2)

- The last control change $\Delta u(k)$ is needed to calculate the long range predictive control, as per Equation (3-11). However, for the long range predictive control of the crystal growth system, this parameter could create instability if the controller action is not proper for any one control instant. In addition, for the time varying system like the crystal growth, the present output is the effect of many last control signals instead of just one. To resolve this issues, $\Delta u(k)$ is calculated from the mean value of the

difference between the old input array and the new input array at any instant as shown in following figure.

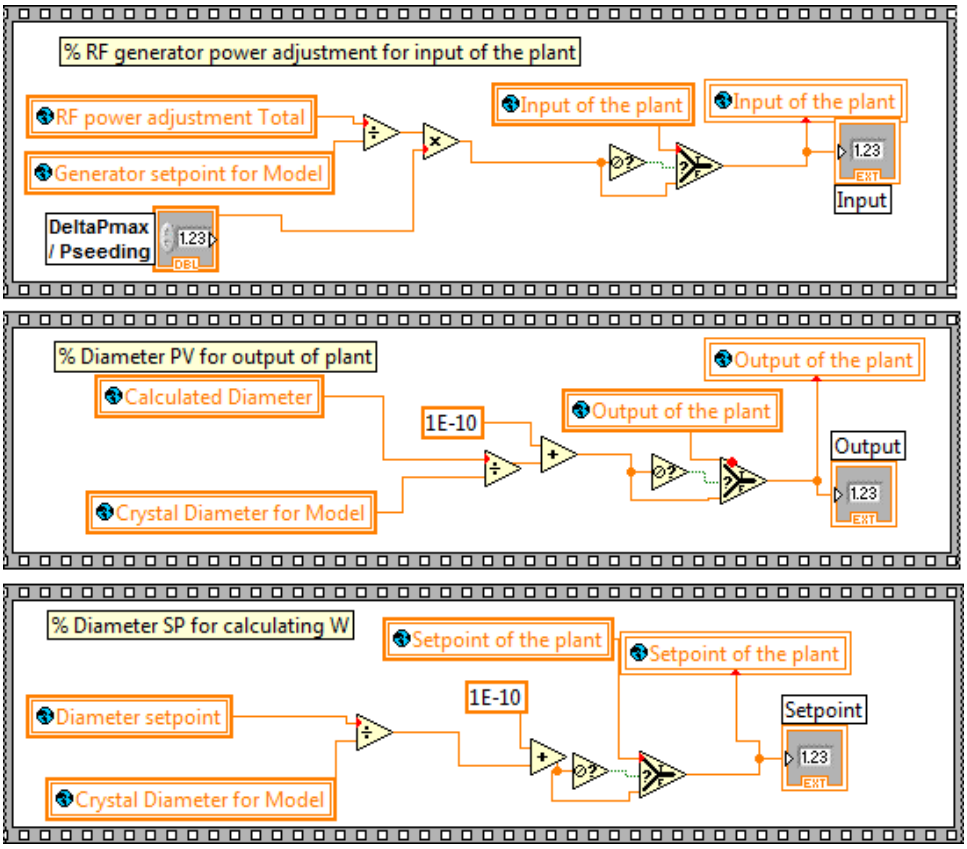

Figure 5-10: Unit-less input-output of the model and set point

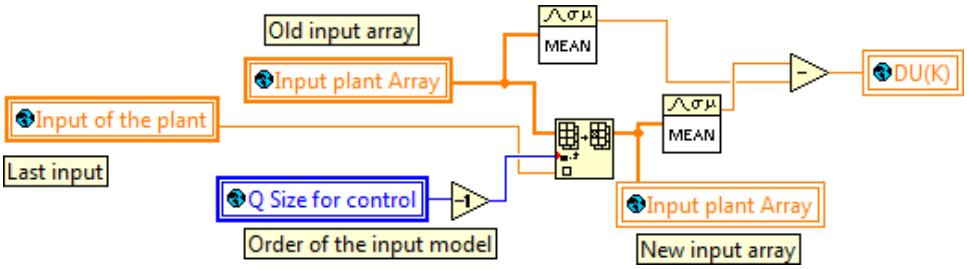

Figure 5-11: Calculation of $\Delta u(k)$ for LRPC control

5.2.3 Process model for identification and prediction

The crystal growth process is time-varying time-delay process. The identification of the unknown delay for the time-varying time-delay process in real-time is not possible. This could be an interesting future work but presently is out of the scope of this research. In this case, initially, there were only three options for the selection of the model parameters and for the model-identification for a real-time application. Each of this case was studied independently to understand the complexity and the possibility for the application on the real time Czochralski growth process. The results are discussed here.

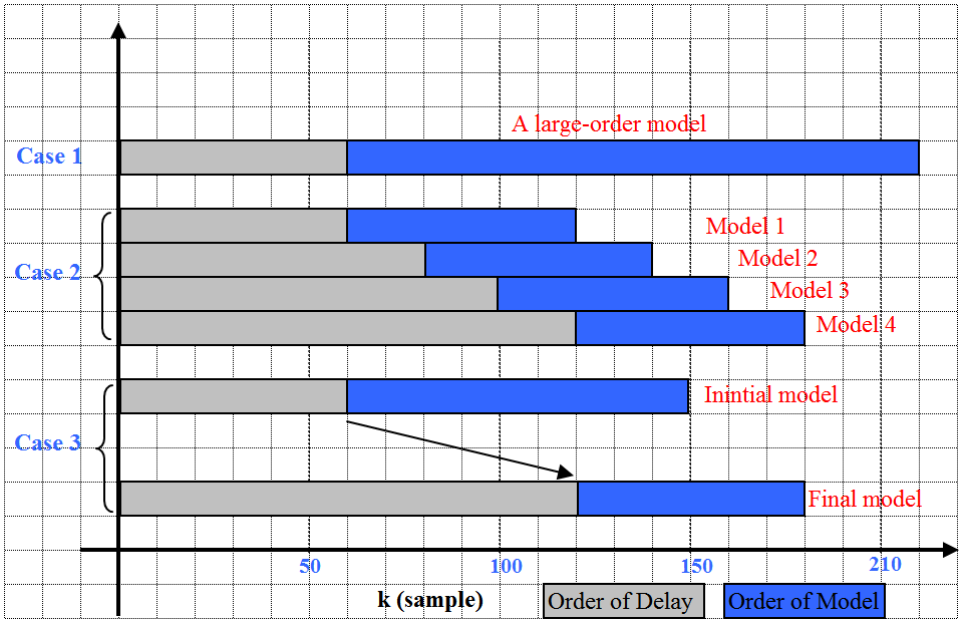

Figure 5-12: Order of delay and model for crystal growth

- A large-order model with a constant delay: In this case, the delay was assumed constant, about 60 samples i.e. 8 minutes. The model order was assumed to be covering the whole range derived in chapter 4.2.6. I.e. form 60 samples to 150

samples (from 10 to 20 minutes) as shown in the Figure 5-12. In this case, both the identification process and LRPC program needs to solve the matrix inversion and the recursive calculation to calculate the prediction and control signal. During the development of the control program, it was observed that once the order of the model is higher than 60 samples, the computational time for the complete control sequence (i.e. identification + LRPC program) increases rapidly. Table 5-1 shows the average computational time for each option measured on the actual control computer. In addition, as the order of the model increases, the total calculation error increases. This could affect the stability of the control system. Hence, this option was not a preferred choice for the real-time control system of the crystal growth process. In the future, when the computational power of computer and accuracy increases, this option could be a better and simpler choice than the other choice described here.

Table 5-1: Computation time for different model

Option	Order of Delay	Order of model	Computational time
1	60	80	5 second
	60	100	6.5 second
	60	120	8.5 second
	60	150	11 second
2	60 , 80, 100, 120	60	6 second
3	60	60	4 second

- Multiple models with the same order but different delay: In this case, four models were considered with the same order (i.e. 60 samples = 8 minutes) for the whole control range. The order of the delay for each one was considered different (i.e. from

60, 80, 100, 120 samples). Thus, the predictive horizon can be covered completely. Here, the lower order models are preferred to reduce computational time to less than 8 sec for real-time application. The gain scheduling for each model was carried out based on the relation between the delay and the length of the crystal described in chapter 4.2 . The length of the crystal was divided into three parts from initial length to final length. Figure 5-13 is a graphical representation of the gain scheduling for each model as the growth progresses. This kind of gain scheduling gives a smooth transfer to the delay-based control from one model to another. The problems related to this case are discussed here.

a In this case, the identification and LRPC program have too many variables (about 4 times than normal). The total no of calculations for control increases (four times than the earlier case at each stage of LRPC program). It increases complexity during designing and rectifying errors of the control program.

b In addition, the software shares some of the same standard subroutine Vis. This sharing could lead to confusion and control signal error.

c The operator needs to change all of the models parameters with different types of crystal growths. This could be a complicated task. Any wrong parameter selection can create a problem during real-time growth.

d If any of the identification process or the LRPC calculation becomes unstable at any stage of the growth, the error or the wrong control signal ($\Delta u(k)$) propagates to all models and their control programs.

e Crystal 4 and Crystal 5 were grown using this technique. Few simulations were also run based on this case, but they were either found to be too complex or too cumbersome for real-time operation. In the future, if one can check stability of both the program and model by some means during real-time growth then this case could become a possibility.

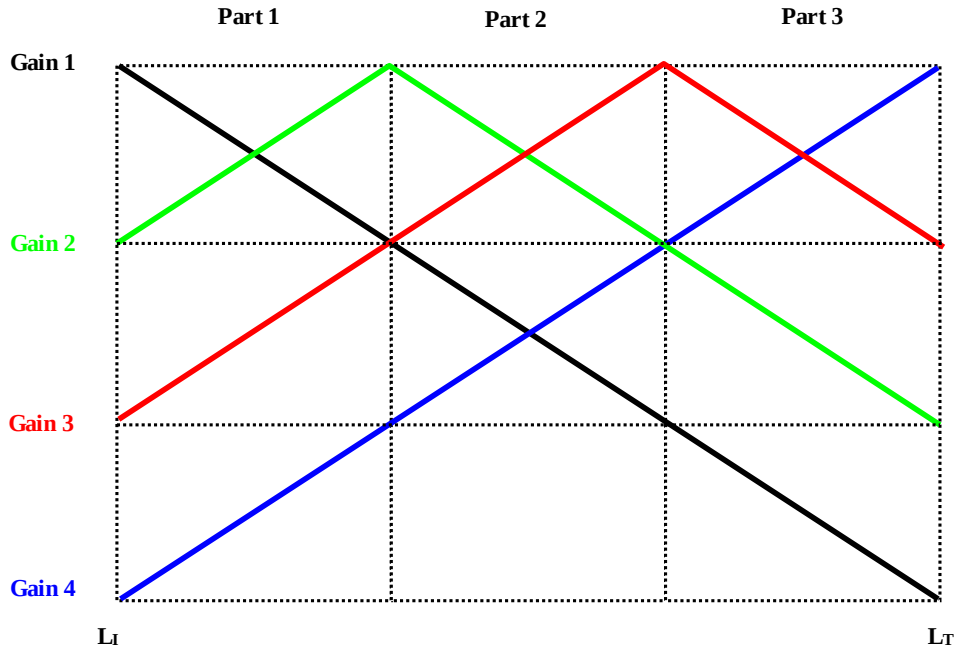

Figure 5-13: Gain scheduling for multiple model LRPC technique

- One model with the time varying predictive horizon based on the delay: The last option was to consider only one model and reduce the complexity. This model can be configured with the time varying delay. In other words, the control horizon is changing as the time delay changes with the crystal length. The control program uses a prediction based on this model to compare with the calculated trajectory. Here, the order of the model is 60 samples (8 minutes). The delay range changes as the growth

progress (function of crystal length) from 60 to 120 samples (about 8 to 20 minutes) as presented in chapter 4.2 and Figure 5-12. The model will adopt slowly with the identification process as the growth progress and delay changes. In this case, the complexity of the calculation decreases substantially. With this delay mapping, this option of one model with time-varying predictive horizon seems more suitable at present. Crystal 6 to Crystal 12 were grown from this method. The other two options need further improvement in the hardware and the program that are beyond the scope of the study at this time.

5.2.4 Data accumulation for model identification

Once the model parameter for the model identification is defined, the next step is to establish the stable model identification method. For any model identification process, some initial input-output data are required to initialize the model. For real-time model identification, these data are gathered online. The time it takes to gather this data depends upon the validation of the data, the order of input-output model and the time delay. Once the suitable data are available, the model identification process starts. Initially, the recursive model identification is not accurate. It takes a lot of iteration before the derived model is stabilized. The model is then useful for further control system calculations. All this time for gathering data and initializing iterations, the process has to be running in automatic control mode. In addition, for the crystal growth process, the input-output data seems meaningful for identification once the diameter reaches about 1 cm. For less than 1 cm diameter, the control signal and its effect on the growths is almost negligible due to weighing mechanism error. Hence, data gathered during the diameter less than 1 cm is not reliable for modeling. During this time the MRAC technique,

discussed in chapter 4.1.2, was applied for controlling the process. In other words, when the operator starts the automatic control mode, the process is controlled by MRAC technique. Once the diameter reaches 1 cm, the model identification process starts gathering the initial data and prepares the input and output arrays. The total number of the samples for data gathering and initial model identification was selected as 300 (about two times of the order of the model plus delay), which is equals to 40 minutes with 8 second per sample rate.

1. $flag_{\max} = 60 =$ Order of the model
2. Starting point: $= 5 \cdot flag_{\max} = 300;$ Ending point: $= 15 \cdot flag_{\max} = 900$
3. if $flag_{actual} < 300$
   $\Rightarrow$ LRPC gain $= 0;$ MRAC gain = 1- LRPC gain
4. if $300 \le flag_{actual} < 900$
   $\Rightarrow$ LRPC gain $= \dfrac{flag_{actual} - 5 \cdot flag_{\max}}{(15-5) \cdot flag_{\max}};$ MRAC gain = 1- LRPC gain
3. if $900 \le flag_{actual}$
   $\Rightarrow$ LRPC gain $= 1;$ MRAC gain = 1- LRPC gain

(5-3)

Once the data are available and LRPC program is ready to control the process, the software needs to transfer the control from the MRAC to LRPC smoothly. This transfer cannot be achieved in one-step. The control is transferred from the MRAC to LRPC program slowly and linearly (from 0% to 100%) as crystal grows. To achieve this goal, the gains of MRAC and LRPC were developed by applying gain scheduling. The control program takes another 600 samples (about 80 minutes) to transfer control from MRAC to LRPC technique. The time (in form of no of samples) it takes to change control from the MRAC to LRPC could be adjusted, if required, based on the type of crystal, pulling speed

and growth rate instead of 600 samples. At present, a variable named *flag* was created to track the sample number and calculates gains as shown in Equation (5-3).

5.2.5 Calculating set point trajectory

For the LRPC technique, the set point trajectory is required to calculate the total error for the control program. The starting point for this trajectory mapping is the order of time delay for the crystal growth process. The initial point $w(k+1)$ of the trajectory was considered to be the present output (percentage crystal diameter) of the process. The length (or order) of the trajectory is the length of the control horizon considered for LRPC design. The modeling data for the trajectory is presented in Equation (5-4).

$$\begin{aligned}&\text{Starting horizon} = N_1 = d_{\min} + 1\\ &\text{Ending horizon} = N_2 = d + N\\ &\text{Order of trajectory} = N_u = N = n_a + 1\end{aligned} \tag{5-4}$$

The process set point was calculated from the growth data, selected by the operator. Here, the maximum rate of diameter change for the trajectory was defined by the half cone angle as shown in Equation (5-5) to calculate the ending point, $w(k + d_{\max} + N_a)$. This rate is a constrained on the trajectory mapping and can be adjusted by the operator. The exponential factor α was adjusted to 0.98.

Figure 5-14 shows two graphs. One graph shows the trajectory ($W_{N_w \times 1}$) from the present output (0.482) to the set point (0.499). Here, 160 samples is the order (length) of the trajectory. The other graph with two pointers shows both a prediction (purple line, calculated from the model) and a trajectory (yellow line, calculated from the set point) used for the control signal calculation for 15 minutes. One can see that at one point the

prediction and the trajectory crosses each other in the graph. The error, at this point, was almost zero and hence the control signal change was near to zero.

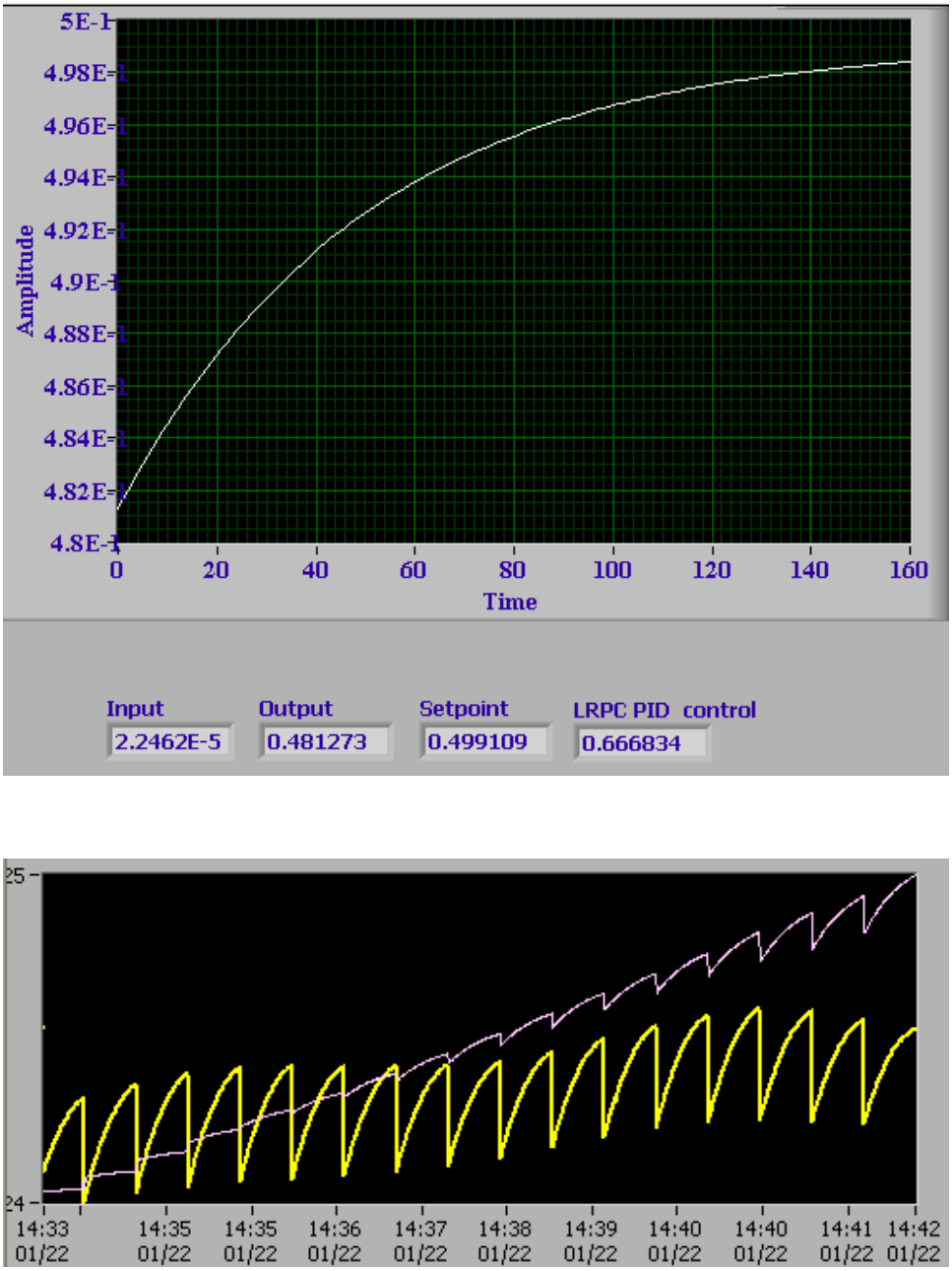

Figure 5-14: Calculation of trajectory from the set point

$$W_{N_w \times 1} = \left[w(k+1) \quad w(k+2) \quad .. \quad w(k+d_{\max}+N_a) \right]^T ;$$

Order of the trajectory $N_w = d_{\max} + N_a$,

$$w(k+i) = \alpha w(k+i-1) + (1-\alpha) r(k+i); \qquad \alpha = 0.98$$

where $w(k+1) = y(k) =$ present process output and $w(k+d_{\max}+N_a) = r(t+k)$

$$r(t+k) = y_{\text{setpoint}}(k) \;\; ; \text{if } \frac{(y_{\text{setpoint}} - y(k))}{\text{order of model} \cdot \text{sampling time}} \cdot 3600 < \dot{y}_{\max}$$

$$= \frac{\dot{y}_{\max} \cdot \text{order of the model} \cdot \text{sampling time}}{3600} \qquad ; \text{Otherwise}$$

$$\dot{y}_{\max} = 2 \cdot v_p \cdot \tan(\theta / 2)$$

(5-5)

5.2.6 Process simulation and offline tuning

Before testing the program on the real time growth system, multiple simulations are required in order to rectify error, test and tune the control software. Rectifying software error during the real time growth is not a good choice, as one may need to start the seeding or the growth again, which may take hours. The simulations can reduce this time. These simulations were also helpful at later stages for testing, tuning and verifying all calculations for the LRPC control strategy and. For simulation purposes, the initial (lower order) models (for generator model and crystal growth) were derived from the earlier growth data of Cystal-1 and presented in Figure 5-15. The properties of this simulation models are as follows:

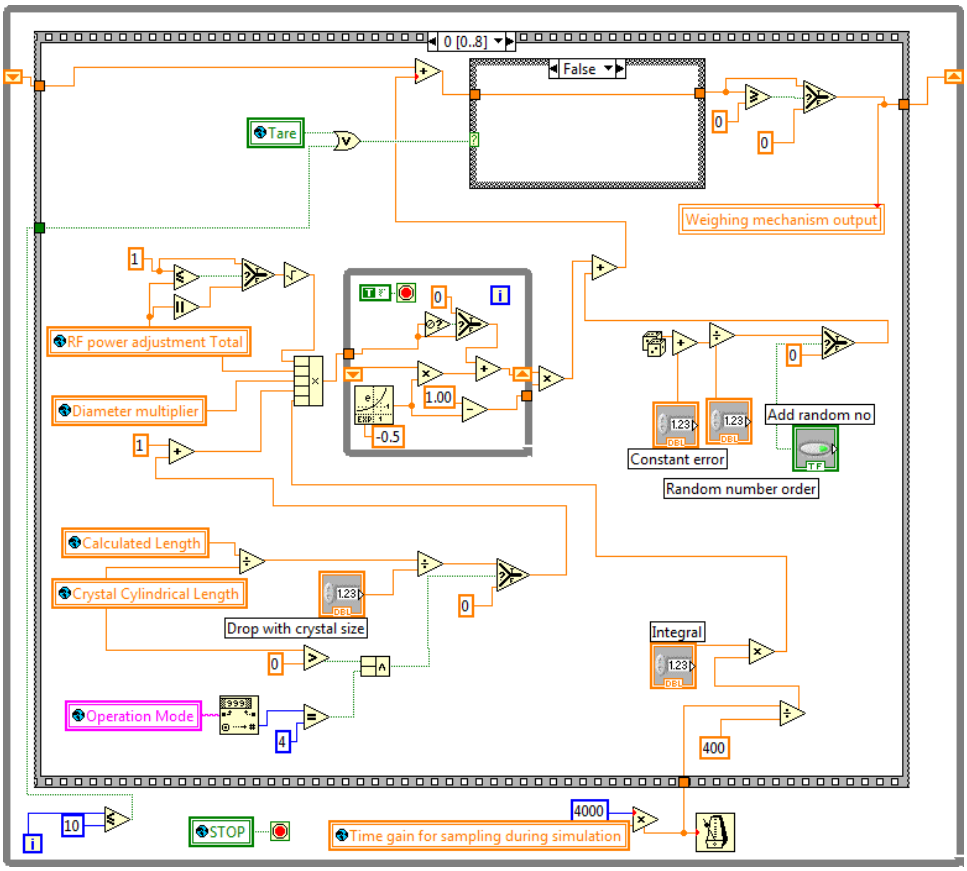

Figure 5-15: Block diagram of the crystal growth model for simulation

- The output of the generator model is considered as an input of the growth model. The growth model calculates the new weight change of simulated growth.
- This weight change is integrated with the old weight to calculate present crystal weight. This weight is passed through the normal measurement cycle for filtering and calculating the growth rate and diameter.
- Based on this calculated diameter and the set point diameter, the control program calculates the control signal ΔP. Using this ΔP and present set point, the generator control program calculates the control signal for the generator. This control signal becomes the input of the generator model. This completes the simulation.

- Some non-linearities were added to the growth model based on the experimental results discussed earlier to check the robustness of the program. First, adjustable white noise function with standard deviation and mean is added to weighing signal. In addition, the effect of power change as the melt level goes down is added in form a linear function.

5.3 Instability and model identification

After selecting the control mode and the model parameters for the identification and predication, the control program was initially tested and tuned with the simulation. The initial gain parameters for the LRPC MPC programs were tuned. These results were later tested to grow Crystal-4 and Crystal-5, as shown in Figure 5-16 and Figure 5-17 respectively, with online model identification. However, the growth system was not stable after a while. The structure of the growth system inside the furnace along with the crucible and other parameters were kept similar to the earlier growth described in Chapter 4.1.1. The set point diameter for the cylindrical portion was 33 mm. The diameter of the crucible was 55 mm and the rotation rate was kept at an optimal level of 32 rpm for the flat interface. The half cone angle for both crystals was kept constant also. The growth parameters for these crystals are shown in Table 5-2 and Table 5-3.

Figure 5-16: Crystal-4 grown with model identification

Table 5-2: Growth parameter for Crystal-4

Growth parameters for Crystal- 4			
Initial parameter		**Calculated parameter before growth**	
Material	LGT	Growth rate for cylindrical part	19.33 g/h
Crucible internal diameter	5.1 mm	Total cone growth time	9.2 h
Initial weight	515 g	Total growth time	22.6 h
Initial melt level	41.2 mm	Total weight	295 g
Crystal diameter	33 mm	% Chemical used	57%
Pulling speed	2 mm/ h	Total calculated length of crystal	54 mm
Rotation speed	32 rpm	**After growth parameter**	
Half cone angle	45^{o}	Crystal final weight	149.55 g
Power of cone	1.2	Actual Crystal length	60 mm
Cylindrical crystal length	50 mm	Actual growth time	23 h
Controller gains			
	P	I	1/ Gain
For MRAC	1	0.3	1000
LRPC-MPC Initial gain	---	---	---
LRPC-MPC After tuning	---	---	--

Figure 5-17: Crystal-5 grown with model identification

Table 5-3: Growth parameter for Crystal-5

Growth parameters for Crystal- 5			
Initial parameter		**Calculated parameter before growth**	
Material	LGT	Growth rate for cylindrical part	19.33 g/h
Crucible internal diameter	5.1 mm	Total cone growth time	9.5 h
Initial weight	515 g	Total growth time	23.2 h
Initial melt level	41.2 mm	Total weight	297 g
Crystal diameter	33 mm	% Chemical used	57.8%
Pulling speed	2 mm/ h	Total calculated length of crystal	86.55 mm
Rotation speed	32 rpm	**After growth parameter**	
Half cone angle	45^{o}	Crystal final weight	212.3 g
Power of cone	1.3	Actual Crystal length	85 mm
Cylindrical crystal length	50 mm	Actual growth time	36.8 h
Controller gains			
	P	I	1/ Gain
For MRAC	1	0.3	1000
LRPC-MPC Initial gain	---	---	---
LRPC-MPC After tuning	---	---	---

5.3.1 Results and analysis for Crystal-4 and Crystal-5

Crystal 4 was grown with the multiple model identification with multiple delay (case 2) as discussed in chapter 5.2.3. This was the first crystal that was grown using the long range predictive control method. Initially, the model reference adaptive controller controlled the crystal growth. Once the model was identified for prediction, the control was transferred to long range predictive controller, as discussed in chapter 5.2.4. As shown in Figure 5-18 , during the cone growth part, the growth was stable. During this time, the control strategy was being transferred from the MRAC to LRPC technique. The control program was able to transfer smoothly from the MRAC to LRPC before the cone growth reached about 60% of the final diameter.

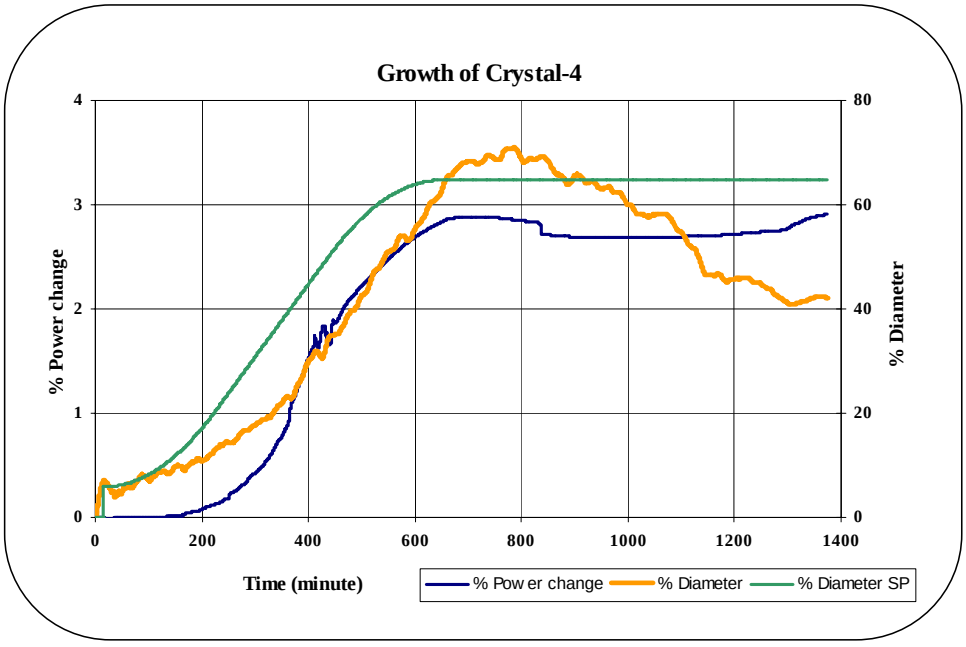

Figure 5-18: Diameter and power change graph for Crystal-4

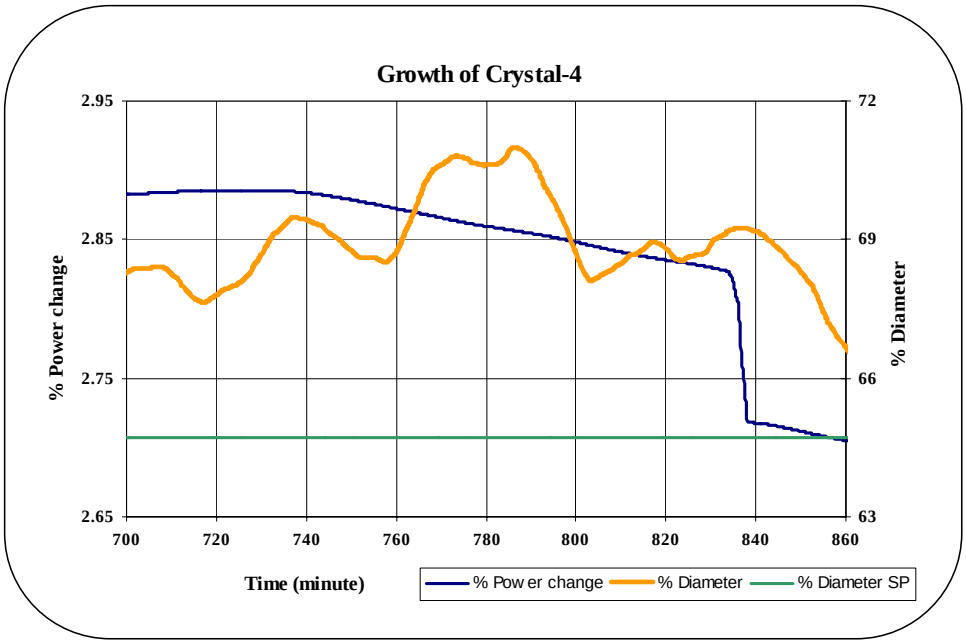

Figure 5-19: Instability in diameter and power change graph for Crystal-4

Later, when the cone growth was about to end, the controller started acting abnormally. The immediate effect on the growth system was very negligible. However, as growth continues from cone to cylindrical part, it became significant. The controller was not able to control the system and control system become almost constant as shown in Figure 5-18. The gain parameters of the controller were adjusted but were not enough as growth proceeds. It was clear that controller was not able to control the process and the control system was becoming unstable as the diameter stated decreasing. The crystal was pulled out at that stage. The final weight of the crystal was about 150 g.

The cause of this instability was not detectable during the growth. However, from the control signal calculation using the prediction system, it was clear that the prediction from the model was not proper. This caused the unstable control response. The reasons for this error in the prediction could be either the model identification or the calculation

of the control system. Using a known stable model, the simulation was run to test the calculation. The control signal calculations were normal and the control was able to transfer smoothly from the MRAC to LRPC technique. Hence, the model identification process was the main problem for the instability.

During the growth, it was not possible to study the identified model for stability. Later, the growth data gathered during the growth process was analyzed. Offline model identification was run to check the prediction and the model stability. To test the stability of the model during the model identification, a step response method was designed which can be introduced at any time during the identification. It gives the step response of the present identified model whenever interrupted during the process. The stability of the model was tested for the entire length of the grown crystal. From this analysis, the identified model was found stable initially, during the initial part of the cone growth. Near the end of the cone growth and beginning of the cylindrical growth, there were some unexpected peaks (variations) in the diameter measurement as shown in Figure 5-19. For the long-range model identification, it could cause unstable model identification.

Once the model becomes unstable, the prediction error propagates not only to the control system but also to the next identification process. The identification process was not able to derive a stable model again even though the growth was stable later. This led to control structure failure. In control system terminology, this is explained by a bifurcation theory when the process becomes unstable to stable or vice verse. Many researchers have studied the control system design for such systems. However, the model identification of the unstable process with bifurcation is yet to be explored.

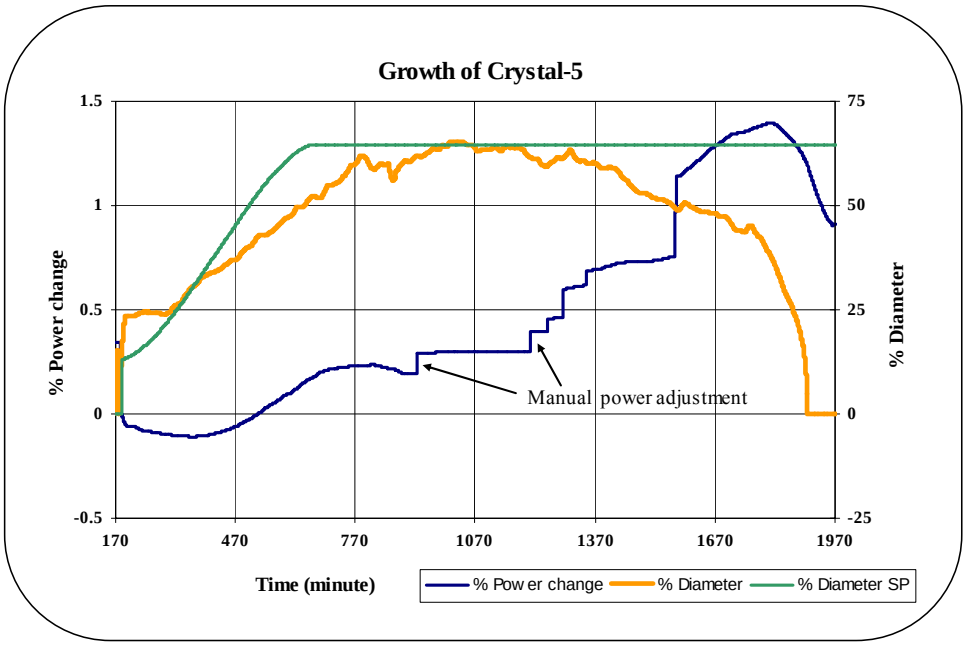

Figure 5-20: Diameter and power change graph for Crystal-5

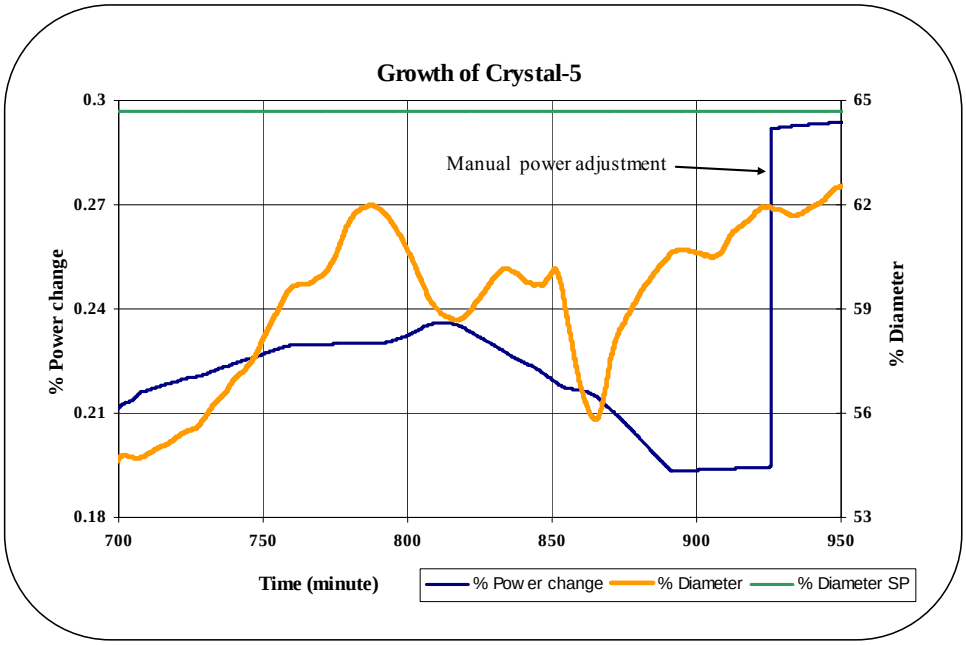

Figure 5-21: Instability in diameter and power change graph for Crystal-5

To test this hypothesis, Crystal-5 was grown with the similar growth parameters as shown in Figure 5-17. The power of cone was changed to 1.3 as shown in Table 5-3 to increase the cone growth time and achieve a stable transfer from the cone to cylindrical part. However, similar results were achieved during the growth as shown in Figure 5-20. The control was unstable near the same area as shown in the Figure 5-21. The data was gathered and analyzed for stability as discussed above. It was clear that this identification method was not able to derived stable model in case any instability in the process. For this reason, a study of partial model identification and design control system could be a better option e.g. by filtering the diameter for unstable frequency or partially defined (or bounded) model parameter. However, it is the beyond the scope of this study. The idea of real time model identification process with ability to check model stability parameter is left for future work.

5.3.2 Predefined model for long range predictive control

The main objective of this study was to incorporate the delay in the control system and predictive horizon. The time delay variation during the growth is more important factor than the model itself. For prediction, one can apply a predefined model that is derived from the old growth. In fact, multiple models, derived from different crystal region, could be an option but not preferable. At this point only one stable growth model, derived from comparing previous growth data with the stable model of the filter, was used to define the control process. (i.e. indirect control instead of direct control). The step response parameters for the actual growth like rise-time and settling time were compared with derived model for stability. Figure 5-22 and Figure 5-23 shows the step response of the derived model and parameter for the time response. Figure 5-24 and

Figure 5-25 shows the bode plot for magnitude and phase for this model respectively. The settling time is about 80 samples (i.e. 10.67 minutes) and rising time is about 75 samples. The effect of model variation with the growth can be compensated with the gain scheduling and the time varying delay for control horizon. The time-delay were removed as it was already considered in the mapping. The new control structure and testing are discussed in a later chapter.

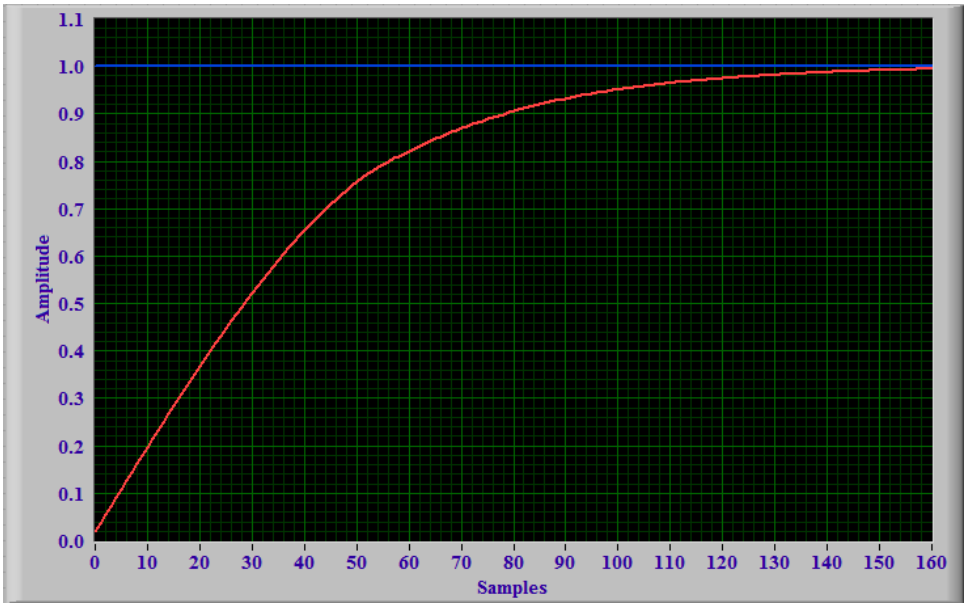

Figure 5-22: Step response of stable model

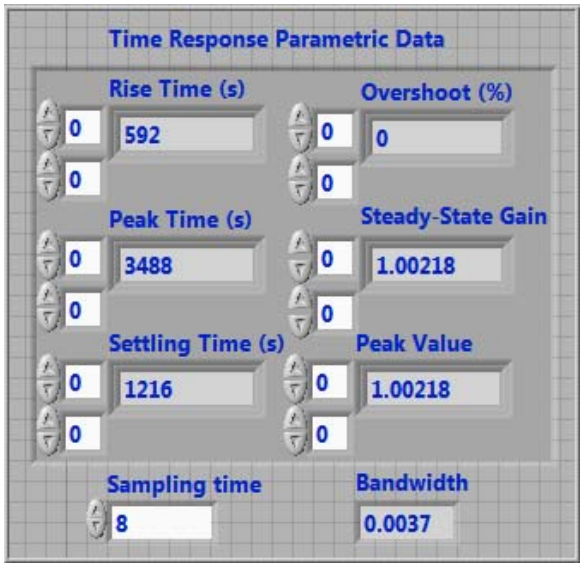

Figure 5-23: Time response parametric data for the model

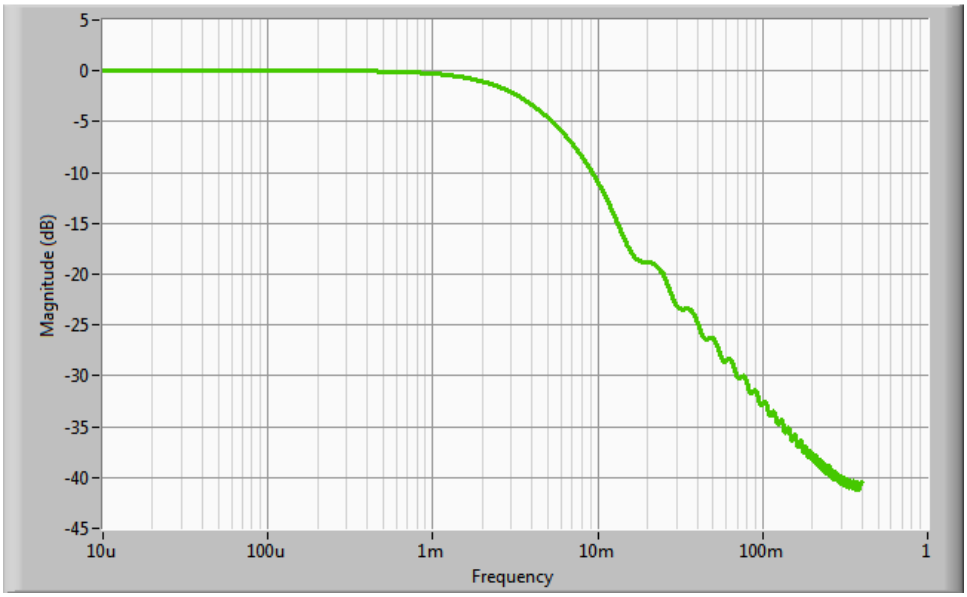

Figure 5-24: Magnitude: bode plot for the derived model

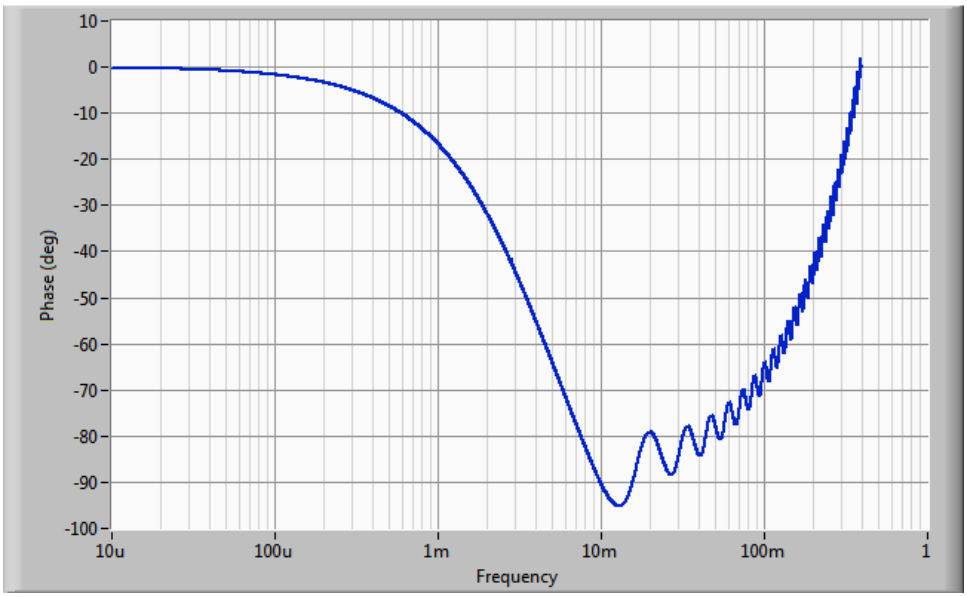

Figure 5-25: Phase: bode plot for the derived model

CHAPTER 6: IMPLEMENTATION OF LRPC CONTROL

In the last chapter, the initial result for the LRPC control system with the online model identification was discussed. The problem of the unstable model identification during the growth, if there is any disturbance in the growth, made the proposed control strategy unsuitable for the real time crystal growth. The other alternative was to apply a pre-derived stable model of the crystal growth for the control system. In other words, an indirect control strategy was adopted instead of an earlier proposed direct control strategy.

In this chapter, this indirect control strategy with a new control model is presented. Later, an another control strategy named LRPC PID, other than LRPC MPC discussed in Chapter 3, was also considered for the study. The LRPC PID is similar to LRPC MPC. However, it calculates a control signal using PID instead of MPC technique from the error between the prediction (done by the model) and trajectory (calculated from the set point).

6.1 Modified control model

The assumptions for the new control system remain the same as presented earlier in section 5.1.2. Following are the main differences in a new controller structure.

- The third task has been changed. Instead of the model identification, a predefined model is used to calculate the prediction based on the LRPC technique.
- Automatic changeover of the main control technique from the MRAC to LRPC is discussed in the last chapter needs to be tested again. However, as the model is already pre-derived, there is no need to use MRAC initially and later transfer to

LRPC slowly during the cone growth. If this transfer is not needed, it cab be removed from the control structure.

- To compensate the effect of using only one model instead of the time-varying model of crystal growth, the time varying delay mapping and gain mapping are considered for prediction. These mappings were divided in ten parts depending on the length of the crystal grown as shown in following Figure 6-1. These mapping were derived from the earlier experimental results of crystal 1 to 3.
- The control parameters for the model and delay and the trajectory mapping are similar discussed in chapter 5.3 . The control horizon for trajectory was 240 samples (or control instants). Figure 6-1 also shows the other controller parameter like a and l along with the order of the denominator N_a and numerator N_b. These values were tuned during simulation and real-time growth.

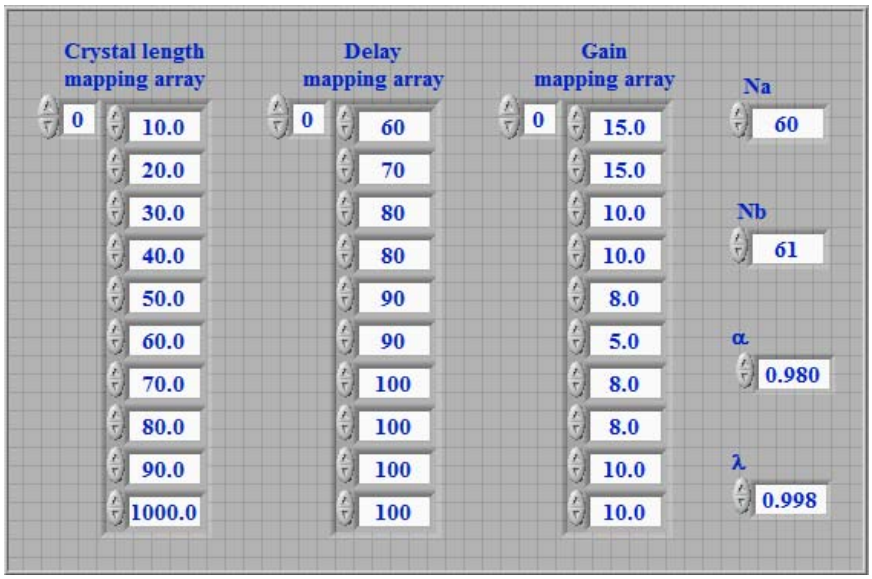

Figure 6-1: Gain and delay mapping and controller parameter

- Here, the delay increases as the melt level decreases or the crystal length increases. As the crystal length changes, software considers new delay and gain based on above mapping. The software uses this delay to compare the difference between the trajectory and prediction.
- The gain mapping is to adjust the controller gain as the crystal growth progress and the melt level goes down. Generally, the gain does not change much during the initial part of the growth. However, when the melt level goes down, the controller needs to adjust the power change faster than usual, even though the delay is increasing. The gain was slowly decreasing during the initial part of cylindrical growth. At 50% of the cylindrical length, the gain becomes constant. When the length reaches about 70%, the gain starts increases because of very low melt level. Fine-tuning for these parameters was done during the actual growth.

At this point, the complete control structure was known. The simulation and tuning were carried out before testing on the actual growth. Other process parameters for the growth, like optimum rotation, pulling speed and cylindrical diameter, still need to be adjusted in terms of stability. The effect of instabilities also needs to be tested during the growth to check the stability of the control system. For that reason, a total six crystals were grown (three for each control technique). The growth parameters, results and observations are discussed for each crystal growth in the next sections. At the end, a large-diameter crystal was grown to check the final control system.

6.2 Long range predictive PID control and crystal growth

Traditionally, the PID controllers have been in use for many processes. However, the application to the time delayed process has not been studied extensively. Here, the sake of comparison, a long range predictive PID control system is also considered for the crystal growth process. The controller structure and other specification are similar to the LRPC-MPC based controller.

6.2.1 Introduction of PID control

In this section, a long range predictive PID control (LRPC- PID) is presented. It is similar to the long range model predictive control (MPC). The only difference is in the control signal calculation for the prediction horizon. It calculates control signal using PID technique, which consists of three basic terms, P (proportional), I (integral), and D (derivative). However, instead of using the present error term only, this control considers the error between the trajectory and the predicted output of the system for the prediction horizon. That means each prediction point has an independent error and a controller with it. The benefit of such control strategy is that it can incorporate the delay of the system irrespective of the order of the system. The optimal tuning of PID gains can be achieved during the actual growth or by comparing them with the MPC control technique. Detailed description and explanation is discussed in [16]. In general, the control signal ($\Delta u(k)$) can be calculated from the following equation, which is analogues to the equation (3-11).

$$u(k) = k_p \cdot e(k) + k_i \cdot \sum_{i=1}^{k} e(k) + k_d \cdot (e(k) - e(k-1)$$

$$e(k) = \sum_{i=1}^{k} (w(k+i) - \hat{y}(k+i \mid k))$$

= Total error between predicted output and trajectory over the control horizon

(6-1)

For crystal growth process, only the P and I components are necessary. The derivative term can create unnecessary disturbance during instability. Hence, D term is neglected during the control system design. Once the software was ready and tested on simulation, the next step was to test and tune for the real-time crystal growth. Three crystals were grown using this technique. In addition, various process parameters, like pulling speed, and diameter, were adjusted to make process stable.

6.2.2 Crystal-6 growth by LRPC-PID

Crystal-6 was the first crystal grown using LRPC-PID technique. Figure 6-2 shows the grown crystal. Initial process parameters, calculated parameters and final parameters are shown in Table 6-1. Following are the observation and results of this growth.

- Initially, the seeding process was stable. Seeding diameter was about 3 mm. During the cone growth, the diameter of the crystal was increasing smoothly. Total calculated time for cone growth was 10 h with the half cone angle 45 degree, and puling speed of 2 mm/h. The cone growth was controlled by MRAC program, which was later transferred to the LRPC –PID program.

Figure 6-2: Crystal-6 growth by LRPC-PID

Table 6-1: Process parameter for Crystal-6

Growth parameters for Crystal- 6			
Initial parameter		**Calculated parameter before growth**	
Material	LGT	Growth rate for cylindrical part	19.33 g/h
Crucible internal diameter	5.1 mm	Total cone growth time	10.2 h
Initial weight	515 g	Total growth time	23.5 h
Initial melt level	41.2 mm	Total weight	299 g
Crystal diameter	33 mm	% Chemical used	58.0%
Pulling speed	2 mm/ h	Total calculated length of crystal	87.6 mm
Rotation speed	32 rpm	**After growth parameter**	
Half cone angle	45^{o}	Crystal final weight	212.3 g
Power of cone	1.4	Actual Crystal length	106 mm
Cylindrical crystal length	50 mm	Actual growth time	37.45 h
Controller gains			
	P	I	1/ Gain
For MRAC	1	0.3	10000
Before starting PID	1.5	0.5	50000
After starting PID	1.3	0.4	50000

- The cone growth took around 15 h to reach the cylindrical diameter that is approximately 30 degree cone angle. The cone growth was stable until the crystal diameter reached to cylindrical diameter (33 mm). At the end of the cone growth, there was some uncertainty and diameter increased rapidly. From the grown crystal, near end of the cone growth, the crystal developed crack internally. It could be due to the unstable flat interface. The diameter set point could have been slightly too high for the present rotation rate (32 rpm).
- The crystal growth was stable after the cone growth. However, the crystal diameter decreased at around 75% of the melt level (about 20 h). Some inclusions/voids were visible inside the grown crystal.
- Once the growth interface and growth became unstable, the control software could not stabilize the crystal diameter by adjusting the generator power. As shown in the graph, percentage power change was about 3%. The normal power change should be around 1%.
- At 50% of the melt level, the diameter decreased again and decreased continuously. The growth was completely unstable even though the total power change was about 6%. This could be due to polycrystalline growth or the set point of the crystal diameter was high, which resulted in unstable growth interface.
- After about 38 h, the crystal growth was aborted. It took about 14 h more time than calculated.

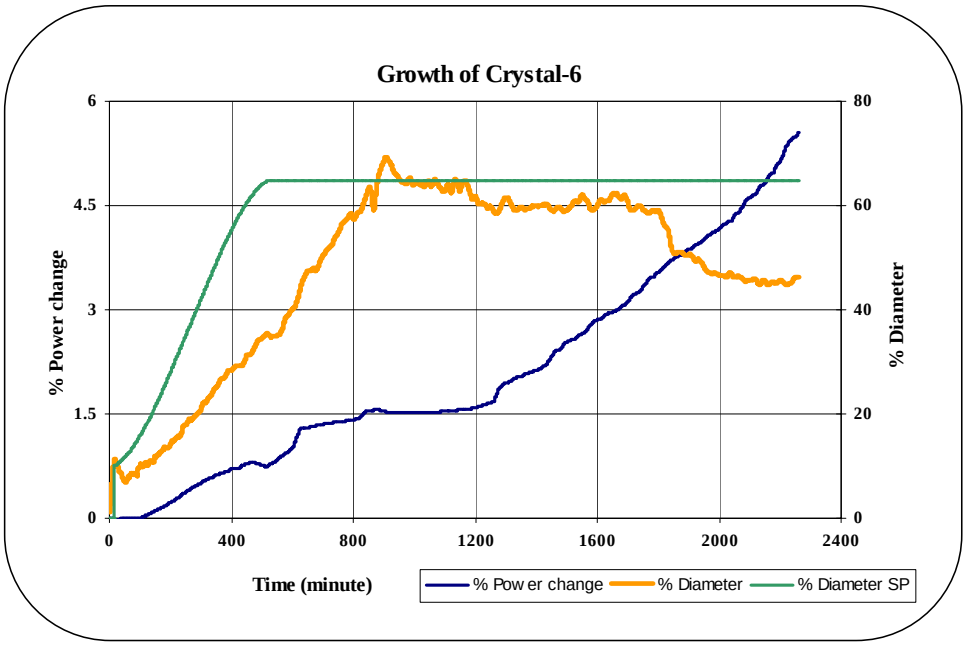

Figure 6-3: Diameter and power change graph for Crystal-6

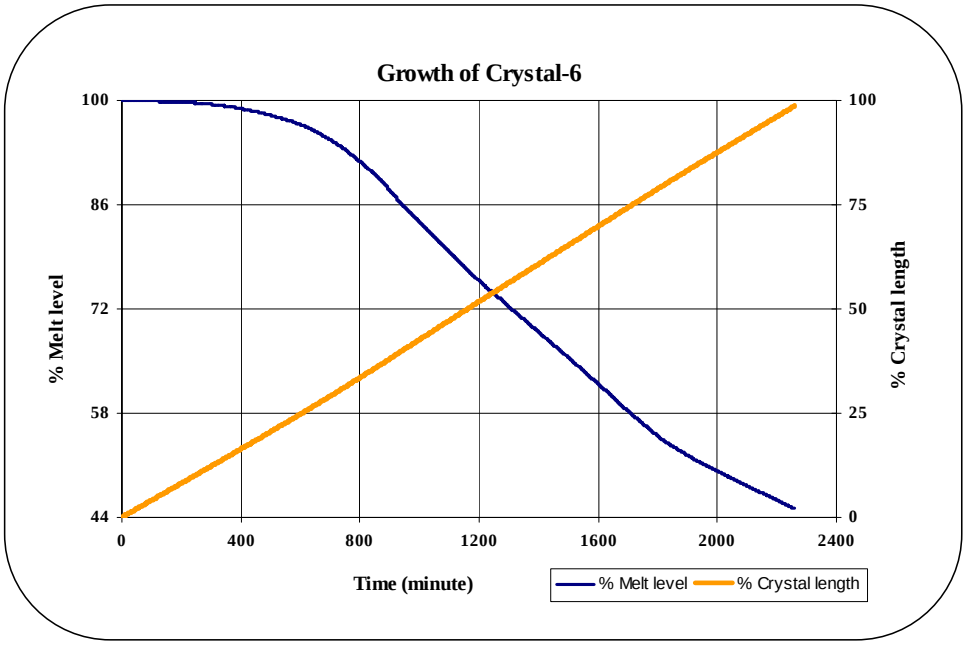

Figure 6-4: Crystal length and melt level graph for Crystal-6

6.2.3 Crystal-7 growth by LRPC-PID

Crystal-7 was again grown using LRPC-PID technique. Figure 6-5 shows the grown crystal. From the results of the last growth, diameter set point for the crystal was reduced to 28 mm from 32 mm. The power of the cone was also increased to make the cone to cylinder transfer smoother. The total time of cone growth was reduced to 9 h This reduced the total calculated weight also. Other growth parameters, calculated parameters and final parameters are shown in Table 6-2. Following are the observation and results of this growth.

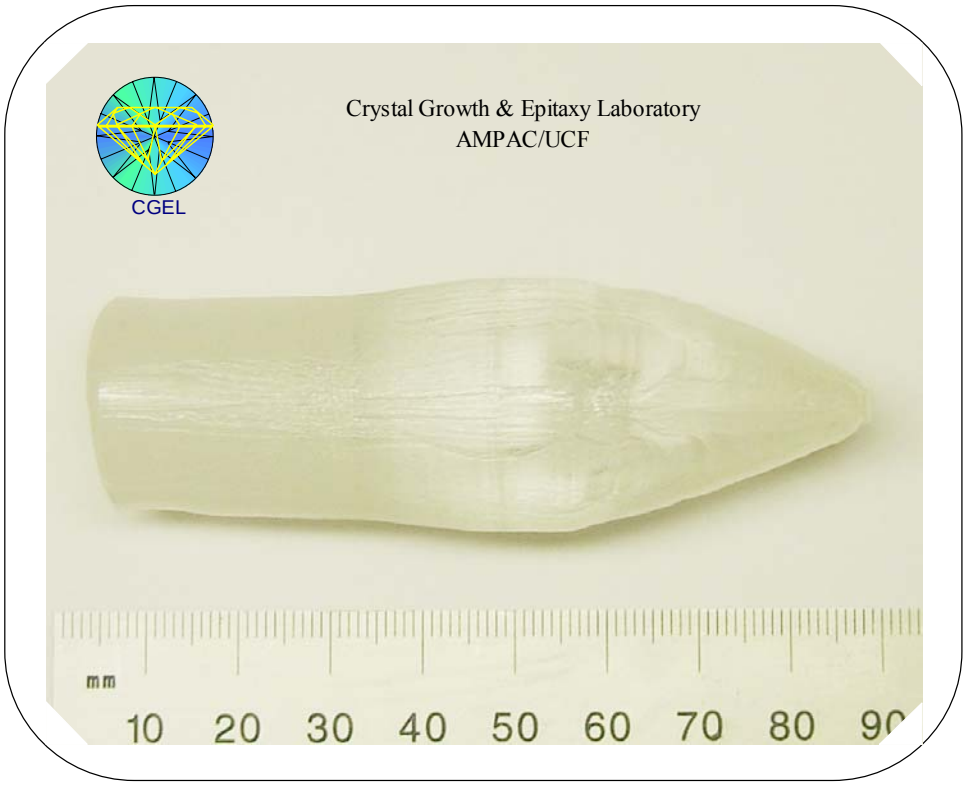

Figure 6-5: Crystal-7 growth by LRPC-PID

Table 6-2: Process parameter for Crystal-7

Growth parameters for Crystal- 7			
Initial parameter		**Calculated parameter before growth**	
Material	LGT	Growth rate for cylindrical part	11.27 g/h
Crucible internal diameter	5.1 mm	Total cone growth time	9 h
Initial weight	515 g	Total growth time	25.5 h
Initial melt level	41.2 mm	Total weight	212.2 g
Crystal diameter	28 mm	% Chemical used	41.0%
Pulling speed	2 mm/ h	Total calculated length of crystal	62 mm
Rotation speed	32 rpm	**After growth parameter**	
Half cone angle	45^{o}	Crystal final weight	188.65 g
Power of cone	1.5	Actual Crystal length	80 mm
Cylindrical crystal length	50 mm	Actual growth time	27.1 h
Controller gains			
	P	I	1/ Gain
LRPC-MPC Initial gain	1	0.4	50000
LRPC-MPC After tuning	1	0.35	50000

- The growth model for the prediction was already derived before the growth. Hence, LRPC –PID control system can be applied during initial growth without MRAC, if it is pre-tuned. Here during the actual growth, MRAC program was controlling the growth during the initial part of the growth. However, in this growth, instead of a smooth transfer from the MRAC to LRPC-PID technique, an instant transfer (one-step transfer) was opted during the growth (at time t= 175 minute). This instant transfer caused a jump in control signal (power change) but had nominal effect on the crystal diameter.
- After the seeding, the calculated seeding diameter was about 6 mm (20% of final diameter). This indicates that the seeding was not proper as can be seen by Figure 6-5. However, the starting point of the set point for crystal diameter was kept at the actual diameter. During the cone growth, crystal growth was stable and crystal grew at a 30 degree half cone angle. It took about 10 h to reach at the cylindrical diameter.

- Near the end of the cone growth, the diameter overshoot was observed, similar to the last growth. The controller adjusted the control signal. At one point, the control signal became negative and remained negative for about 5 h In other words, the crystal was growing at the same power as of seeding, which is unusual but indicates the controller was working normally. The crystal diameter remained high for about 9 h. The defects were clearly visible inside the crystal in this region. The growth interface was not stable. To stabilize it, the crystal diameter of the rotation rate had to be adjusted.
- Again, in the actual crystal, a crack was developed during the end of the cone growth, similar to the last growth. The reason could be due the diameter jump and seeding problem or higher value of the crystal diameter for the rotation rate.
- Later at 75% of the melt level, the crystal diameter decreased and kept decreasing for the remaining growth. Due to this instability, the crystal was pulled out earlier than calculated. The final melt level was 60%; where as the weight of the crystal was about 189 g.
- The gain tuning for PID controller was carried out online. It was clear from the error and control signal calculations that the controller was working properly.

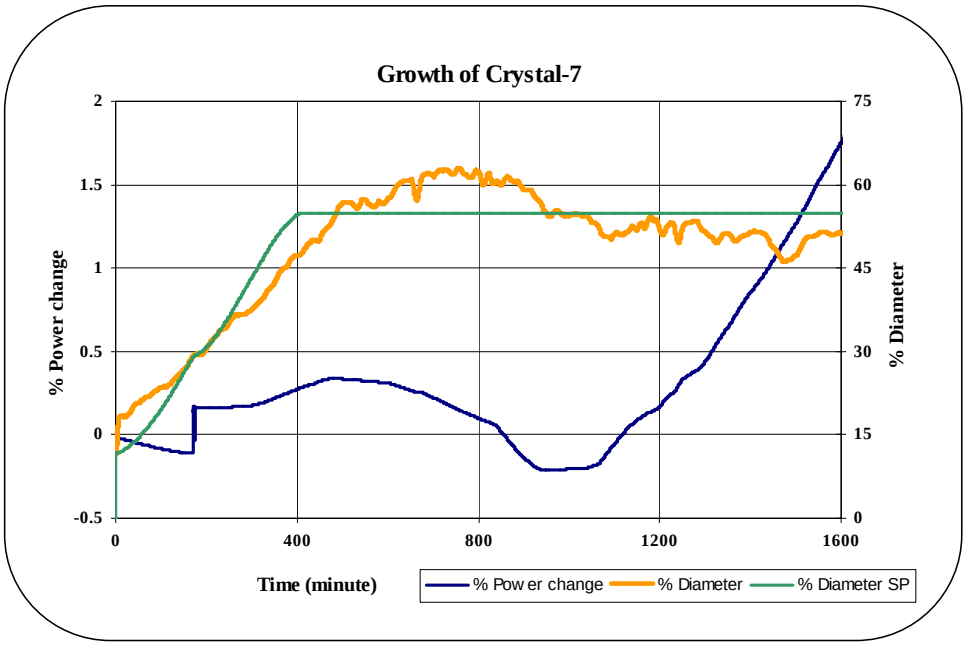

Figure 6-6: Diameter and power change graph for Crystal-7

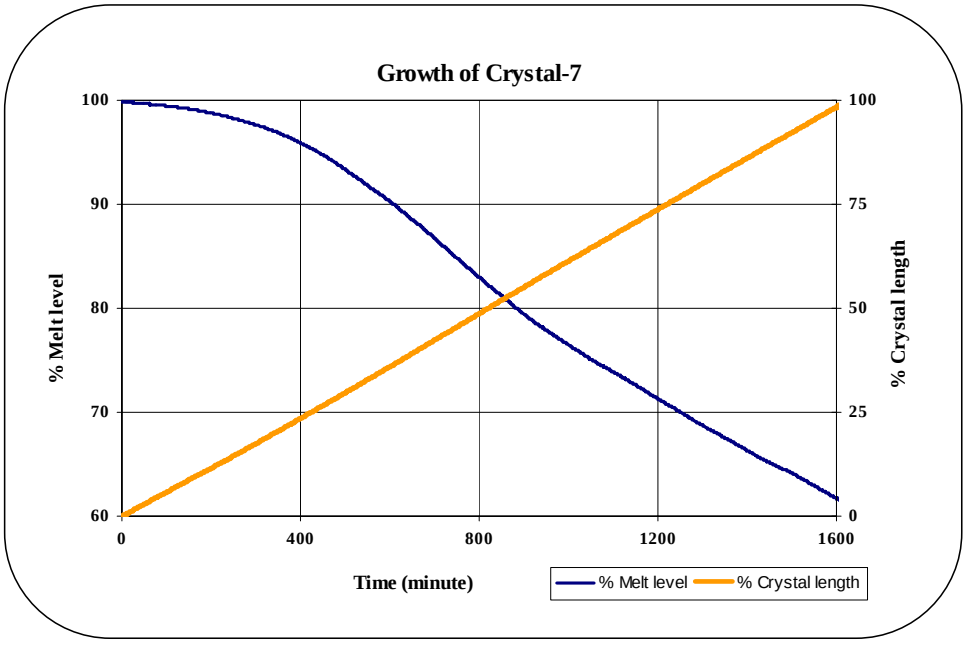

Figure 6-7: Crystal length and melt level graph for Crystal-7

6.2.4 Crystal-8 growth by LRPC-PID

During the last crystal growth, the crystal diameter was adjusted to reduce instability and eliminate cracks but still there were instability and cracks. This time, instead of crystal diameter, the rotation rate was decreased to 25 rpm from 32 rpm. This could help to stabilize the interface shape by making it convex instead of flat. Crystal-8 was grown using LRPC-PID technique. Figure 6-8 shows the grown crystal. Other growth parameters, calculated parameters and final parameters are shown in Table 6-3.

- For this growth, only LRPC-PID control was considered. The MRAC control is not needed when the model identification process was not applied for real time growth.

Figure 6-8: Crystal-8 growth by LRPC-PID

Table 6-3: Process parameter for Crystal-8

Growth parameters for Crystal- 8			
Initial parameter		**Calculated parameter before growth**	
Material	LGT	Growth rate for cylindrical part	11.27 g/h
Crucible internal diameter	5.1 mm	Total cone growth time	9 h
Initial weight	515 g	Total growth time	25.5 h
Initial melt level	41.2 mm	Total weight	212.2 g
Crystal diameter	28 mm	% Chemical used	41.0%
Pulling speed	2 mm/ h	Total calculated length of crystal	62 mm
Rotation speed	25 rpm	**After growth parameter**	
Half cone angle	45^{o}	Crystal final weight	225.13 g
Power of cone	1.5	Actual Crystal length	90 mm
Cylindrical crystal length	50 mm	Actual growth time	30.6 h
Controller gains			
	P	I	1/ Gain
LRPC-PID Initial gain	1	0.35	50000
LRPC-PID After tuning	1	0.3	50000

- For the small diameter crystal and crucible, adjusting the seeding temperature could take hours and small error in that can result in the seeding process failure. Generally, seeding temperature at the center of the melt is adjusted just above the melting temperature so that it can support a stable growth interface. However, for the small diameter crucible even a small change in the control signal causes large temperature change due to the poor inductive coupling with the coil and high operating frequency compared to the large diameter crucible. Here, the seeding temperature was little lower and hence seeding diameter rose to about 6 mm as shown in the Figure 6-9.
- Even though the starting diameter for the cone growth was high, the starting set point diameter for the growth was kept to the diameter of the seed (3mm). This could help to adjust the temperature and control the cone growth. Hence, the control signal became negative to adjust the diameter during cone growth period. The crystal diameter kept rising steadily. The actual crystal grew with 30 degree half cone angle and took 10 h to reach the cylindrical diameter.

- The cone growth was too stable, a sign of polycrystalline growth. Some abnormality was observed at the seeding point, which created a polycrystalline growth. The cracks could be due to some impurities during seeding process or due to not properly etched seed. The crystal is useless and had some abnormality during the cone growth as shown in the Figure 6-8.
- All though the crystal was polycrystalline, the crystal diameter increased more than the cylindrical diameter set point. It remained higher for about 6 h. The control signal swing back to negative after a small positive cycle.
- To check how control system behaves, when there is any abnormality in weighing mechanism, a manual perturbation was applied at time t= 1280 minute. This kind of problem can happen during the actual growth due to unsymmetrical crystal growth or problem in seeding, pulling or rotation mechanism. The control should not cool down or heat up the furnace rapidly and destroy the grown crystal. At t= 1280 minute, the diameter measurement was interrupted for about 20 minutes as shown in the Figure 6-11. Due to the long range predictive programming and constrain on the trajectory, the control system was stable and there was no abnormal cooling.
- At last, the crystal growth became unstable. The polycrystalline growth was visible from the observation window. It was pulled out after about 30.6 h.
- Total power change for the diameter control was about 1%. This indicates that the control system performance was satisfactory.
- Due to the low rotation rate, the convex shape of the growth interface is visible at the end of the crystal. However, the shape is not enough convex for the stable growth interface.

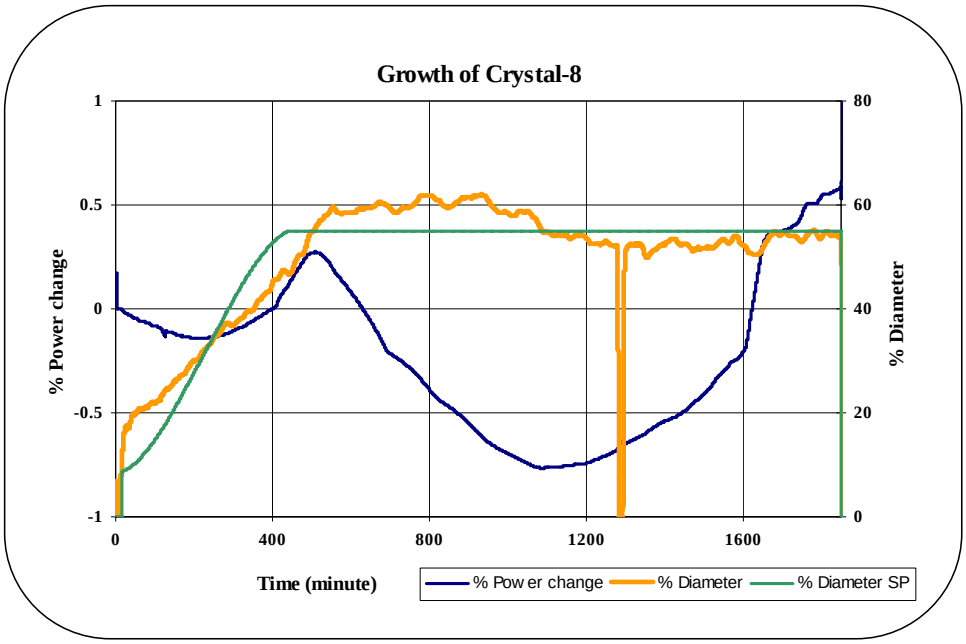

Figure 6-9: Diameter and power change graph for Crystal-8

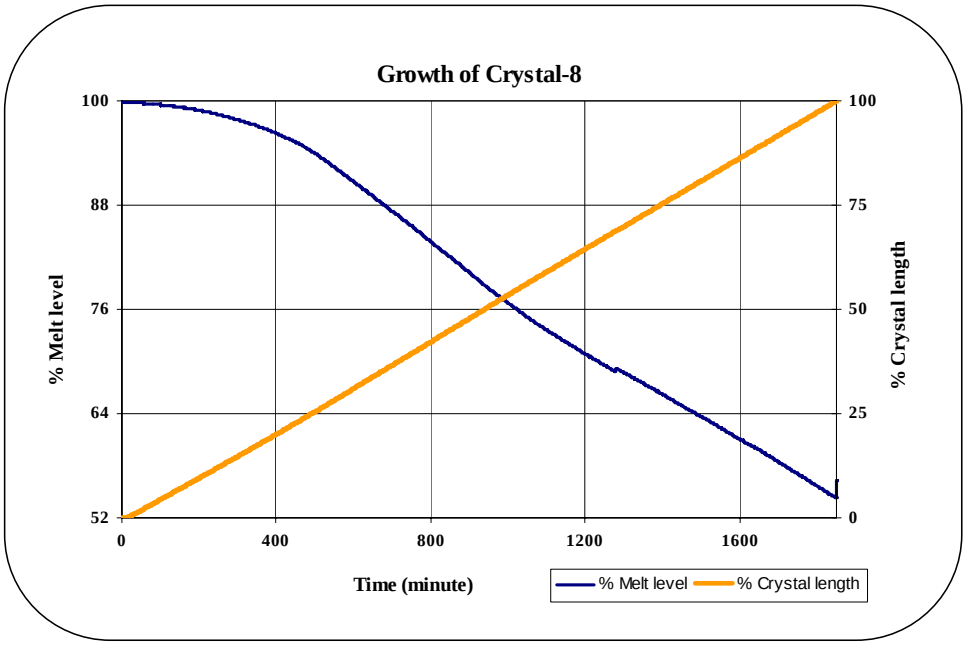

Figure 6-10: Crystal length and melt level graph for Crystal-8

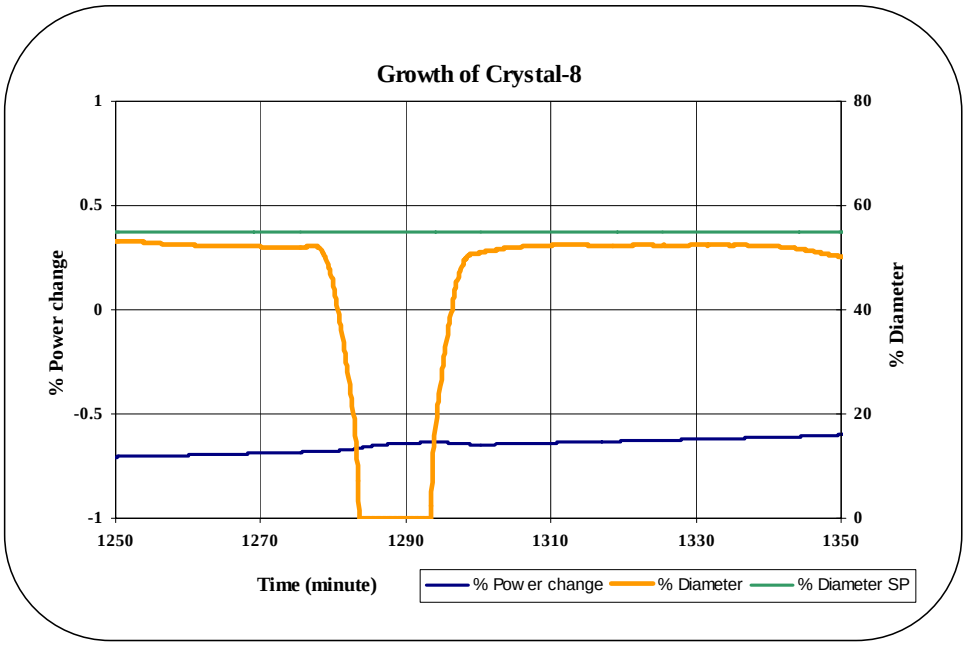

Figure 6-11: Effect of weighing mechanism error on the control system

After, analyzing these three-crystal growths and studding the response of the control system for different conditions, it is clear that long range predictive control with PID technique was satisfactory and better than conventional PID control. There were still few process parameters to be adjusted. The ratio of the crystal cylindrical diameter with crucible diameter is an important for the stability of cylindrical growth. The ratio is called ballpark number. This ratio depends upon the heat transfer for the growth system. In addition, the multiplication factor of the cylindrical diameter and rotation rate is important for the stability of the interface and crystal quality. The factor depends upon material's maximum stable crystallization rate at particular rotation rate. The next step was to test LRPC-MPC control system.

6.3 Long range predictive MPC control and crystal growth

Once the development, testing and tuning of the LRPC-MPC completed, it was applied for the real time growth system. Total three crystals were grown using this technique. Again, various parameters, like pulling speed, diameters, were also required to fine-tune to make process stable. Here, each crystal growth process is explained independently with process parameter, growth and results.

6.3.1 Crystal-9 growth by LRPC-MPC

Crystal-9 was the first crystal grown using LRPC-MPC technique. Figure 6-12 shows the grown crystal. Initial process parameters, calculated parameters and final parameters are shown in Table 6-4.

- During the last crystal growth, the crystal rotation rate was reduced to prevent cracking and to stabilize the growth interface. To optimize the interface shape further, the cylindrical diameter of the crystal was reduced to 26 mm. In addition, the power of the cone growth was increased to about 1.6. These reduced the total time of the cone growth to 8.4 h.
- The seeding process was difficult and the seeding diameter was about 6 mm once the seeding stabilized. The set point of stating of the cone growth was kept at 3 mm. Hence, the control signal during the initial part becomes negative. The cone growth continued for another 10 h. The actual cone growth angle was about 30 degree. This indicates that the growth parameters were still not optimized for the growth. The pulling speed also affects the maximum cone growth angle.

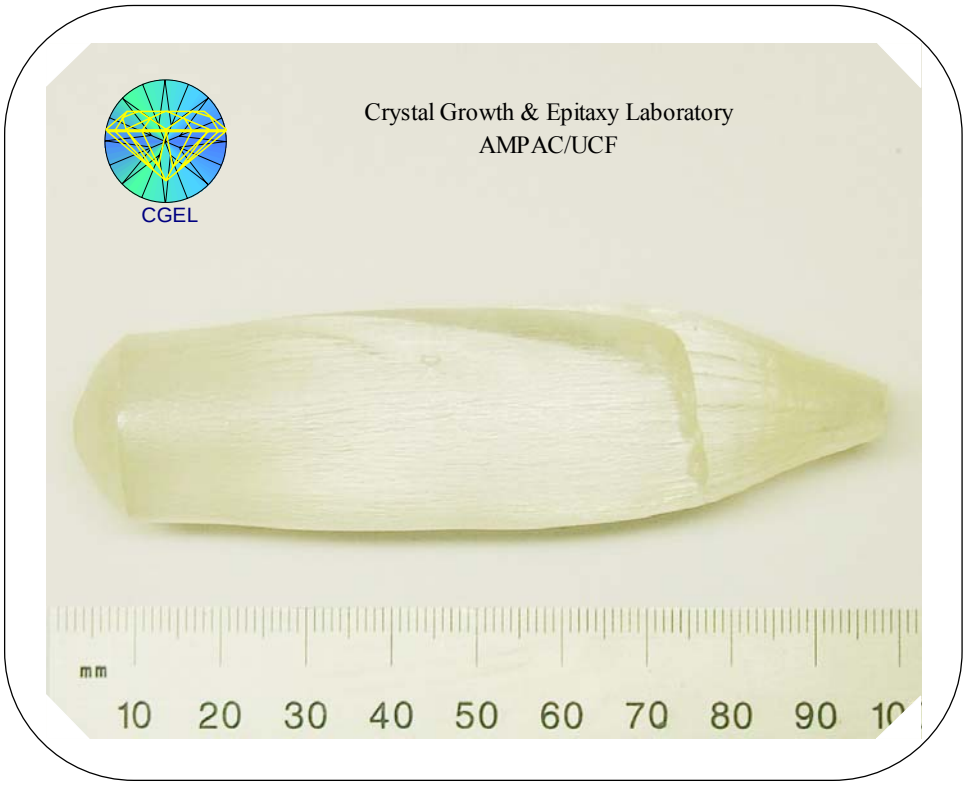

Figure 6-12: Crystal-9 growth by LRPC-MPC

Table 6-4: Process parameter for Crystal-9

Growth parameters for Crystal- 9			
Initial parameter		**Calculated parameter before growth**	
Material	LGT	Growth rate for cylindrical part	9.11 g/h
Crucible internal diameter	5.1 mm	Total cone growth time	8.42 h
Initial weight	515 g	Total growth time	26.38 h
Initial melt level	41.2 mm	Total weight	182.23 g
Crystal diameter	26 mm	% Chemical used	35.4%
Pulling speed	2 mm/ h	Total calculated length of crystal	69 mm
Rotation speed	25 rpm	**After growth parameter**	
Half cone angle	45^{o}	Crystal final weight	209.24 g
Power of cone	1.6	Actual Crystal length	93 mm
Cylindrical crystal length	50 mm	Actual growth time	30.13 h
Controller gains			
	P	I	1/ Gain
LRPC-MPC Initial gain	--	--	900
LRPC-MPC After tuning	--	--	800

- There was a diameter overshoot at the end of the cone growth again. However, it was comparatively smaller than the earlier crystals. The controller changed the power set point of the generator to adjust the crystal diameter. However, due to the constraints on the trajectory, the controller did not change power rapidly like in the PID control system. One can also see that before the diameter actually went beyond the set point the controller started decreasing the power change. This is due to the model prediction. The crystal growth remain in overshoot state for another 15 h. but the output of the controller did not change more than 1%. This again shows the stability of the controller for a long time.
- The delay and gain mapping with the crystal height were tuned earlier from the simulation and older growth data. They were not adjusted during the growth. The gain parameter for the LRPC-MPC has only one variable (1/gain) and was also pre-tuned before the growth. During the actual growth, it was fine-tuned as shown in Table 6-4. Tuning LRPC-MPC parameter compared to PID control is simple for the operator.
- When the melt level dropped below 60%, the diameter started decreasing rapidly. The controller could not adjust even though the gain parameter were higher at the end of the crystal growth. This rapid decrease in the diameter was observed in last three crystals even thought the crystal diameter and the rotation rate were reduced. There could be another factor, like complex heat-mass transfer. The dynamics for the small crucible should be changing rapidly for the low the melt level. Here, the growth continued until the 60% of the melt level drop. Instead of 60%, the growth should run until the melt level drops to 50% only. This affects the yield of the crystal growth for

the small diameter crucible. This yield factor should be considered not only during the required crystal parameter but also during the design of crucible.

- The crystal was pulled out after 30 h growth time. The total weight of the crystal was 210 g. From the grown crystal, the convex shape of the growth interface is can be observed, which is desirable for the stability of the crystal growth. There was no crack near the end of the cone growth. In addition, defects were not visible throughout the crystal length. However, there was a crack in the crystal that was developed during the cooling cycle of the crystal.

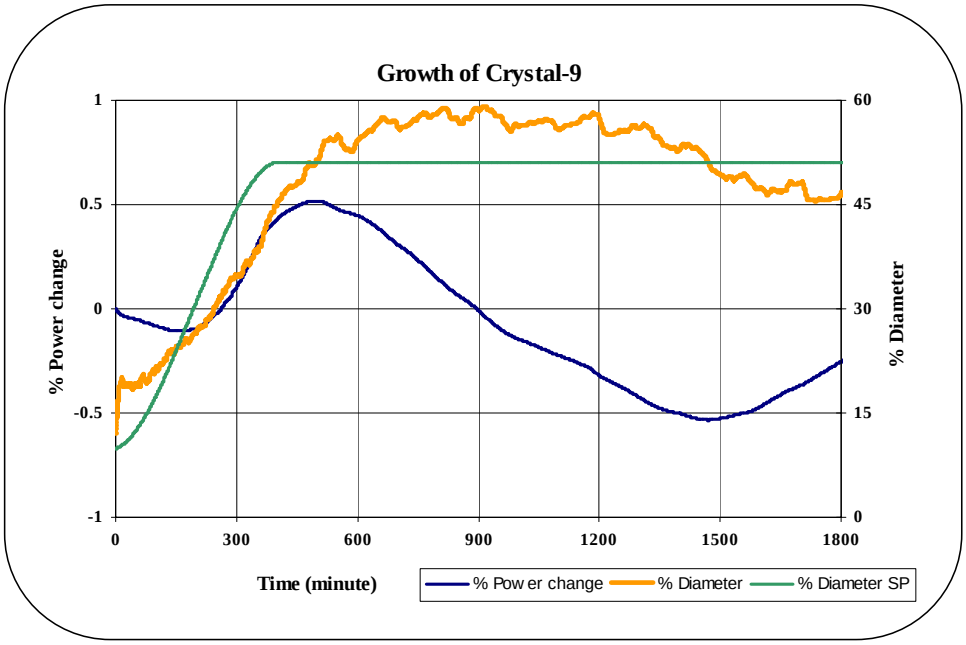

Figure 6-13: Diameter and power change graph for Crystal-9

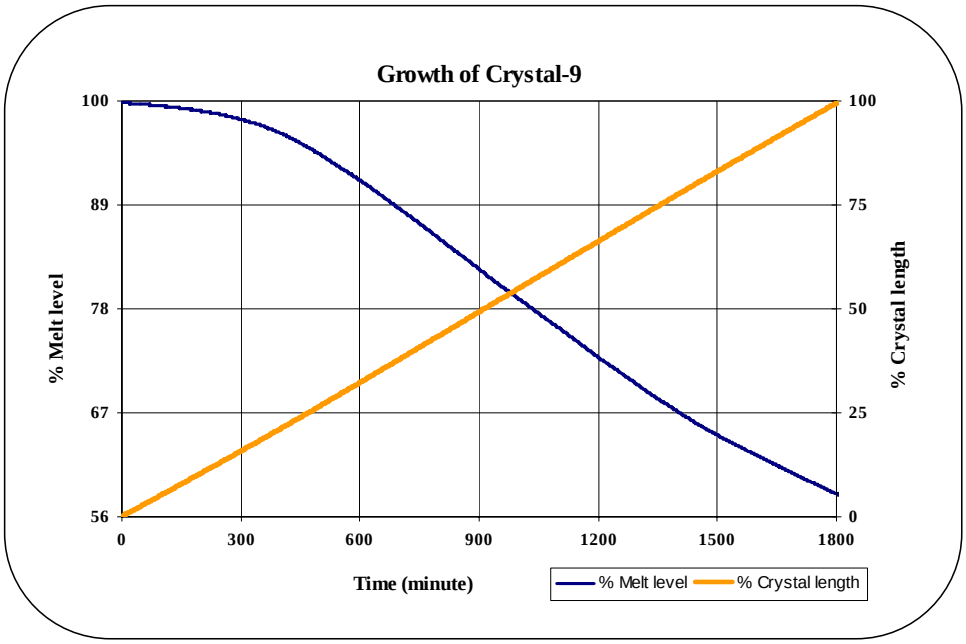

Figure 6-14: Crystal length and melt level graph for Crystal-9

Finally, the controller was working normally and the crystal quality was also improved compared to the earlier growths. However, some growth parameters like diameter, pulling speed and rotation speed still need to be optimized during the next growths to prevent overshoot.

6.3.2 Crystal-10 growth by LRPC-MPC

The crystal growth process requires not only good control but also optimization of growth parameters during the growth. As per the results of the last growth, the crystal quality and control system have shown good improvement. However, the crystal diameter again increased near the end of the cone. This could be due to the high pulling speed or half cone angle. Decreasing the pulling speed reduces the maximum growth rate that can be very crucial during the end of the cone growth where growth rate increases rapidly

(exponentially if diameter increases linearly). Decreasing pulling speed also makes the growth process slower. The total growth time for crystal growth increases. In other words, controller also gets more time to control process. The higher crystal rotation rate and crystal cylindrical diameter set point could also be the problem as they define not only the growth interface but also the heat transfer in the melt and the crystal. Reducing both should decrease the convection pattern in the melt and could improve the crystal quality. The stable convection pattern may also help to stabilize the growth even at the low melt level. In control point of view, varying any of these parameters, including the pulling speed, does not change the model derived. Hence, the operator does not need to define the model again. However, fine-tuning may be required.

Figure 6-15 shows Crystal-10 grown using LRPC-MPC technique. Initial process parameters, calculated parameters and final parameters are shown in Table 6-5. The pulling speed was decreased to 1.5 mm/h. The power of the cone was increased to 1.6, to compensate the effect of low pulling speed. The total time for the cone growth was increased to 10.47 h. with a maximum growth rate of about 6.13 g/h. The total percentage chemical used dropped to 32.5% as the set point diameter for the cylindrical part was reduced to 25 mm. The rotation rate was adjusted to 16 rpm.

- The seeding was better than last two times. The seeding diameter was about 4.5 cm. The length of the seed crystal decreased with every growth. Here, the remaining seed crystal is kept attached to the original crystal.

Figure 6-15: Crystal-10 growth by LRPC-MPC

Table 6-5: Process parameter for Crystal-10

Growth parameters for Crystal- 10			
Initial parameter		**Calculated parameter before growth**	
Material	LGT	Growth rate for cylindrical part	6.13 g/h
Crucible internal diameter	5.1 mm	Total cone growth time	10.47 h
Initial weight	515 g	Total growth time	35.24 h
Initial melt level	41.2 mm	Total weight	167.23 g
Crystal diameter	25 mm	% Chemical used	32.5%
Pulling speed	1.5 mm/ h	Total calculated length of crystal	72.3 mm
Rotation speed	16 rpm	**After growth parameter**	
Half cone angle	45^{o}	Crystal final weight	203 g
Power of cone	1.5	Actual Crystal length	110 mm
Cylindrical crystal length	50 mm	Actual growth time	42.4 h
Controller gains			
	P	I	1/ Gain
LRPC-MPC Initial gain	---	---	800
LRPC-MPC After tuning	---	---	700

- The cone growth took about 13 h to end with the final diameter reaching about 8% higher than set point diameter. The controller was adjusting control signal to change the power of the generator. Unlike, last experiment, the crystal diameter started decreasing with the control signal. This indicates that growth parameters were adjusted near to the optimum values. The overshoot in the diameter may be due to the half cone angle. Analyzing the last several growths, the cone growth was actually growing with about 30 degree half cone angle instead of 45 degree. This can be adjusted during the next growth.
- After 8 h, the controller was able to adjust the crystal diameter near the set point diameter. The slow response of the controller is mainly due to the two constraints that were designed in the controller structure. First during the trajectory mapping, a constraint was put on the maximum rate of change for the diameter. The second constraint is applied on the rate of change of control signal during the growth. This helps to protect the control signal going out off bound and having an abnormal jump. These two constraints also help to conserve the quality of the crystal.
- The crystal was allowed to grow more than the predefined length to see how the controller behaves with the melt level drop. With the reduced rotation rate, crystal diameter and pulling speed, the controller was able to maintain the diameter set point even at low melting level. Unlike earlier growths, diameter did not decreased at the end of the growth. The growth continued for about 42 h with 40% melt level drop.
- The growth interface was more convex than the last crystal mainly due to the decrease in rotation rate.

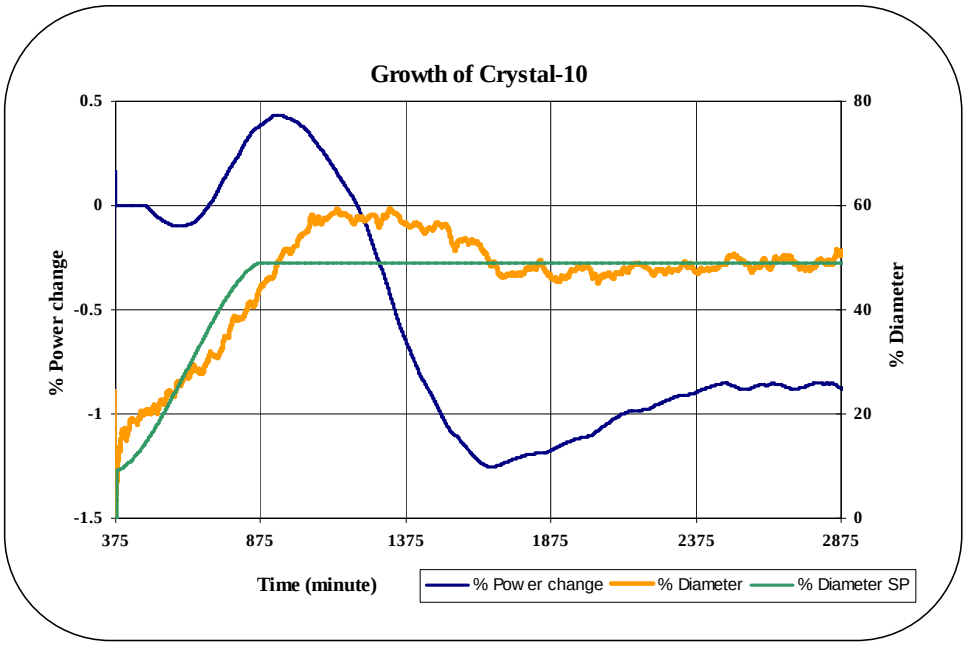

Figure 6-16: Diameter and power change graph for Crystal-10

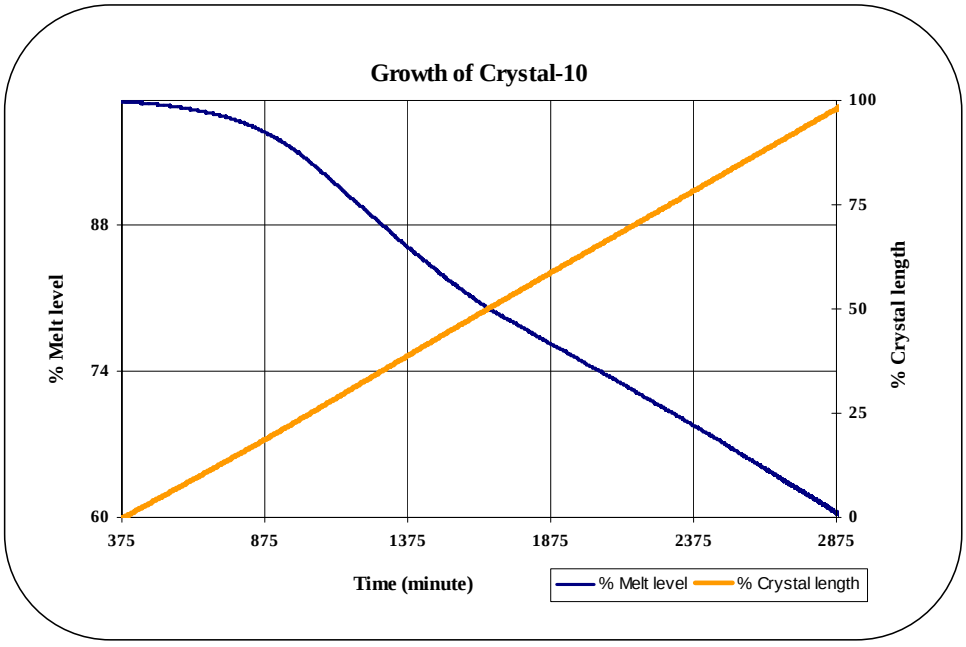

Figure 6-17: Crystal length and melt level graph for Crystal-10

From this growth experiment, the optimum growth parameters mainly rotation rate, diameter set point and pulling speed were achieved. However, to reduce the diameter overshoot near the cone growth, the half cone angle has to be optimized.

6.3.3 Crystal-11 growth by LRPC-MPC

Figure 6-18 shows Crystal-11 crystal grown using LRPC-MPC technique. Initial process parameters, calculated parameters and final parameters are shown in Table 6-6. The half cone angle was reduced to 30 degree to slow the cone growth. The power of the cone was reduced to 1.4 to compensate the slower cone growth. The total calculated time for the cone growth was increased to 17.57 h with the maximum growth rate of about 6.13 g/h. The total percentage Chemical used increased to 35% as the cone growth was extended for about 7 h.

- Again, the seeding was not the idle one. The cone growth continued for about 18 h, which matched calculated time. i.e. the actual half cone angle was also 30 degree.
- A diameter overshoot was again visible near the end of the cone growth. It decreased significantly compared to last growths and lasted for only 5 h. This is a significant improvement. The controller was able to adjust the diameter back to the normal set point.
- The crystal growth remained stable after the diameter reached back to the set point. No striation or crack or growth abnormality is visible on the grown crystal.
- The maximum power change was about 0.75% of the seeding power, which is very small and indicates stable control performance.

- The crystal was grown 5 h more than previously calculated, to see how the melt level drop affects the crystal growth. A small crack on the outside the crystal was observed due to some impurities in the melt. However, it did not propagate through the crystal.

After all these growth, the performance of the LRPC-MPC controller was satisfactory. Other crystal growth parameters were also optimized to grow stable small diameter single crystal.

Figure 6-18: Crystal-11 growth by LRPC-MPC

Table 6-6: Process parameter for Crystal-11

Growth parameters for Crystal- 11			
Initial parameter		**Calculated parameter before growth**	
Material	LGT	Growth rate for cylindrical part	6.13 g/h
Crucible internal diameter	5.1 mm	Total cone growth time	17.57 h
Initial weight	515 g	Total growth time	42.34 h.
Initial melt level	41.2 mm	Total weight	178.06 g
Crystal diameter	25 mm	% Chemical used	34.6%
Pulling speed	1.5 mm/ h	Total calculated length of crystal	80.92 mm
Rotation speed	16 rpm	**After growth parameter**	
Half cone angle	30^{o}	Crystal final weight	201.8 g
Power of cone	1.4	Actual Crystal length	100 mm
Cylindrical crystal length	50 mm	Actual growth time	47.82 h
Controller gains			
	P	I	1/ Gain
LRPC-MPC Initial gain	---	---	700
LRPC-MPC After tuning	---	---	750

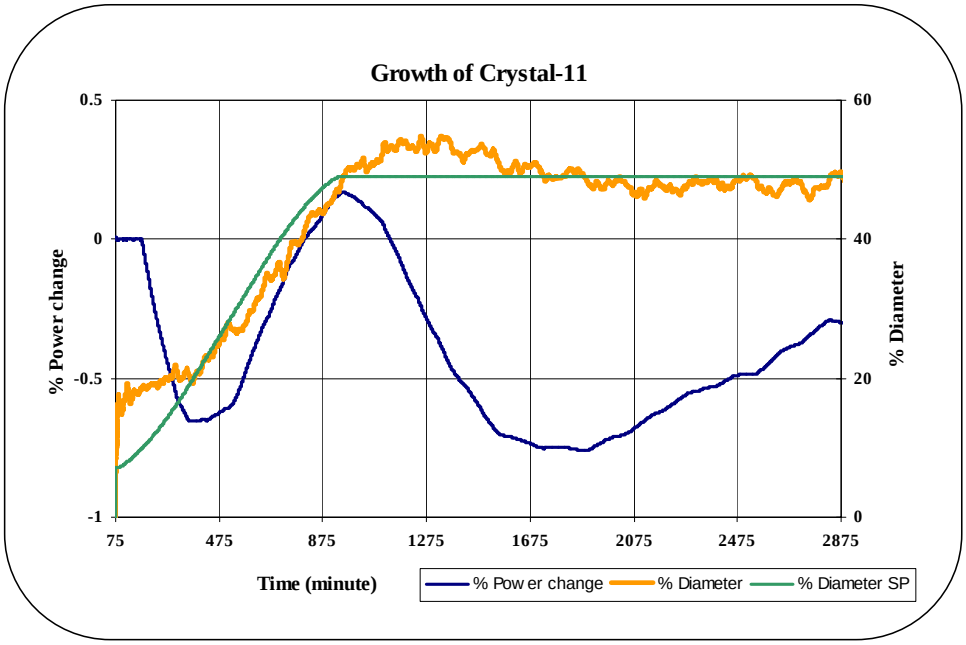

Figure 6-19: Diameter and power change graph for Crystal-11

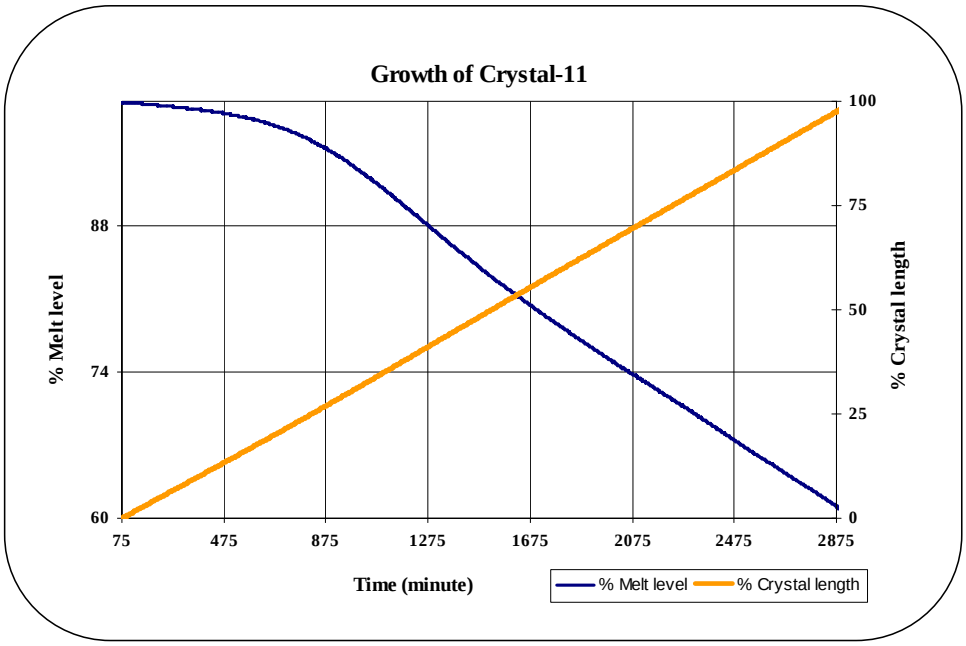

Figure 6-20: Crystal length and melt level graph for Crystal-11

6.3.4 Crystal-12 growth by LRPC-MPC

Once all testing and tuning for the small crystal was over and control system was satisfactorily stable, it was time to test it for the large diameter (5.1 mm) growth. Figure 6-21 shows Crystal-12 grown using LRPC-MPC technique. The initial process parameters, calculated parameters and final parameters are shown in Table 6-7.

- The growth parameters like the pulling speed, rotation rate, and half cone angle were all pre-optimized during earlier growths using the Micricon controller. The optimization work for large diameter crystal was not related to this study. The optimum half cone angle is 45 degree. The optimum pulling speed is about 1 mm/h. The total cylindrical crystal length is 10 cm. The maximum growth rate for the 5.1 mm diameter crystal was 19.31 g/h. The percentage chemical use for large diameter crystal was about 65% with the approximate weight of 1298 g.

- The seeding process for a large diameter crystal is comparatively easier than the small diameter. This is mainly due to the low convection pattern in the melt and higher surface area of the melt, which causes a high temperature gradient. Also for the large diameter crucible, the magnetic coupling frequency for the same temperature is much lower due the higher crucible surface area for conduction. This makes the power adjustment easier to control and tune. In addition, the visibility during the seeding is better than the small diameter crystal. One can see the bright ring around the seed after the seeding and adjust power before actually pulling the crystal. Here, the seeding process was like an ideal one and was very stable. The seeding diameter was around 4 mm.
- The cone growth took about 55 h with about 45 degree half-cone angle. Here, the crystal was actually following the set point curve throughout the cone growth. In fact, there was no diameter jump at the end of the cone growth like for the small crystal growth. It is worth mentioning that the control system, along with cone growth mapping discussed earlier helped, to reduce the facet formation during the cone growth and cone was comparatively smoother than the crystal of Figure 2-4.
- The crystal kept growing until at one point a small diameter variation was observed (at time t=3750 min). The percentage power change (or control signal) was continuously increasing from cone growth to this moment (time t=3750 min). It also represents that time delay is changing with the melt level changes.

Figure 6-21: Crystal-12 growth by LRPC-MPC

Table 6-7: Process parameter for Crystal-12

Growth parameters for Crystal- 12			
Initial parameter		**Calculated parameter before growth**	
Material	LGT	Growth rate for cylindrical part	19.31 g/h
Crucible internal diameter	9.0 mm	Total cone growth time	55 h
Initial weight	2020 g	Total growth time	110 h
Initial melt level	mm	Total weight	1298 g
Crystal diameter	51 mm	% Chemical used	64.3%
Pulling speed	1 mm/ h	Total calculated length of crystal	80.92 mm
Rotation speed	16 rpm	**After growth parameter**	
Half cone angle	45^{o}	Crystal final weight	1261 g
Power of cone	1.4	Actual Crystal length	16 mm
Cylindrical crystal length	100 mm	Actual growth time	81.35 h
Controller gains			
	P	I	1/ Gain
LRPC-MPC Initial gain	---	---	750
LRPC-MPC After tuning	---	---	750

- At time t=3750, the crystal diameter suddenly started increasing as shown in Figure 6-23 . The diameter overshoot for about 1 h. After this, a negative cycle (diameter reduction) was observed for another 1 h. The diameter increase is also visible on the actual crystal. There could be three reasons for this diameter instability.
- First, there was some nitrogen gas instability during the replacement of the gas bottles, which generally takes about 20-30 minutes. The nitrogen pressure and flow dropped suddenly inside the growth chamber, the partial pressure of the oxygen increases. The crystal coloration and the remaining melt coloration is due to oxidation of the iridium crucible, which describes the presence of oxygen inside the chamber. Later to flush out the oxygen and protect the crucible, the flow of nitrogen was increased to 10% than normal. This could have caused the diameter fluctuation.
- The growth structure of the large diameter system could be another reason. The initial melt level was about 58 mm. Once the diameter starts increasing, the melt level drops. However, the melt level drop is slower than the crystal pulling speed. Hence, at

one point, the crystal starts coming out of the crystal. When it does, the heat transfer and mass transfer changes dramatically. The heat conduction inside the crystal increases whereas heat loss from the melt decreases. This could create diameter instability. Here, when the crystal length was about 75% and the melt level dropped to about 50%, the grown crystal was actually coming out of the crucible.

- Also, as the melt level drops, total heat conduction from the crucible to melt decreases. This causes melt to cool down little bit. Generally, the control system keeps cooling down the crucible to sustain constant diameter for the initial part of the growth. However, as the melt-level drops and the melt starts cooling down, the control system starts heating up the generator again at one point. This causes the change of direction of the control signal as can be seen in the Figure 6-23. At this point overall control system and growth system is very sensitive to any perturbation. The melt level at that time was about 50%.
- The controller was able to overcome the diameter instability observed at t=3750 minute. The growth was again stable after that. The crystal was pulled out after 81 h of growth time.
- There are some cracks at the end of the crystal due to the stresses. Near the end of the growth, the crystal growth interface was touching at the bottom of the crucible. The total chemical of 63% was used during the growth. Hence, the remaining melt level was about 18 mm, which is almost equal to the height of the convex growth interface.
- For the control point of view, the model for prediction, the gain and delay mapping and the controller gain were kept similar to the last small diameter crystal. The only parameter changed was x as per the Equation (5-2). This is the advantage of

normalizing all parameters insider the control system. In practice, one can grow small crystal to tune and identify the model of the crystal and apply it to the large diameter crystal. This could reduce tuning time, the cost of chemical and increase the large diameter crucible effective life. It is worth mentioning that all of the small crystals were grown from the old left over chemicals and old polycrystalline crystals. The large diameter crystal was grown with new chemical.

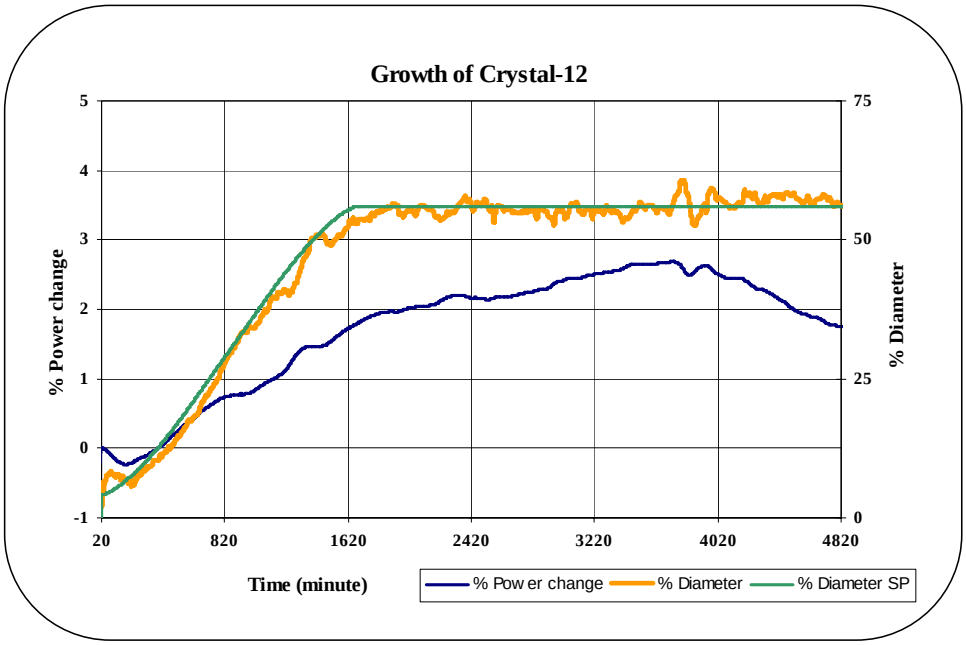

Figure 6-22: Diameter and power change graph for Crystal-12

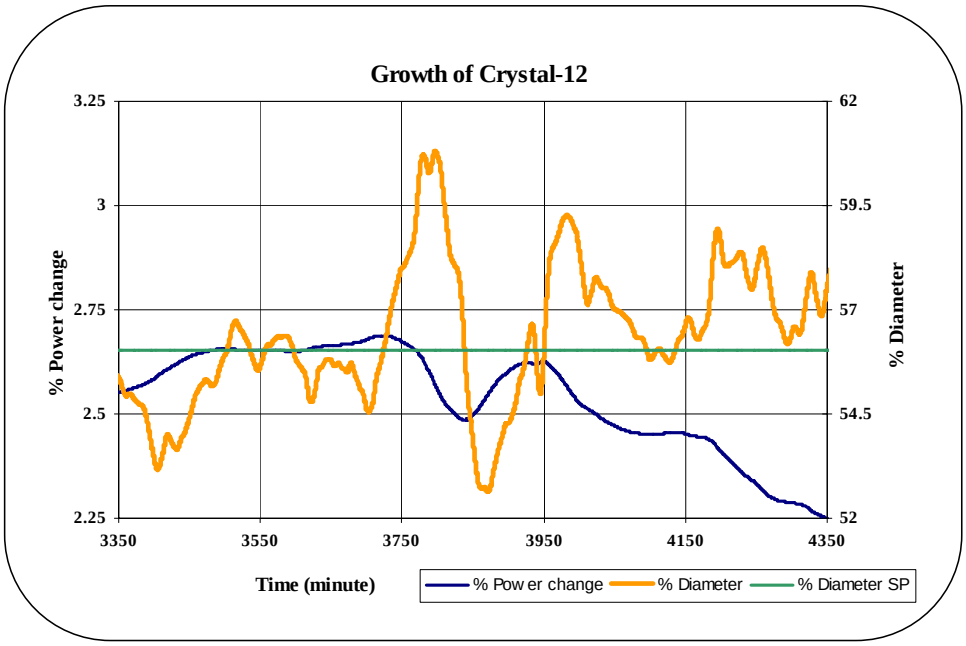

Figure 6-23: Diameter and power change graph for Crystal-12 at t=3750 min

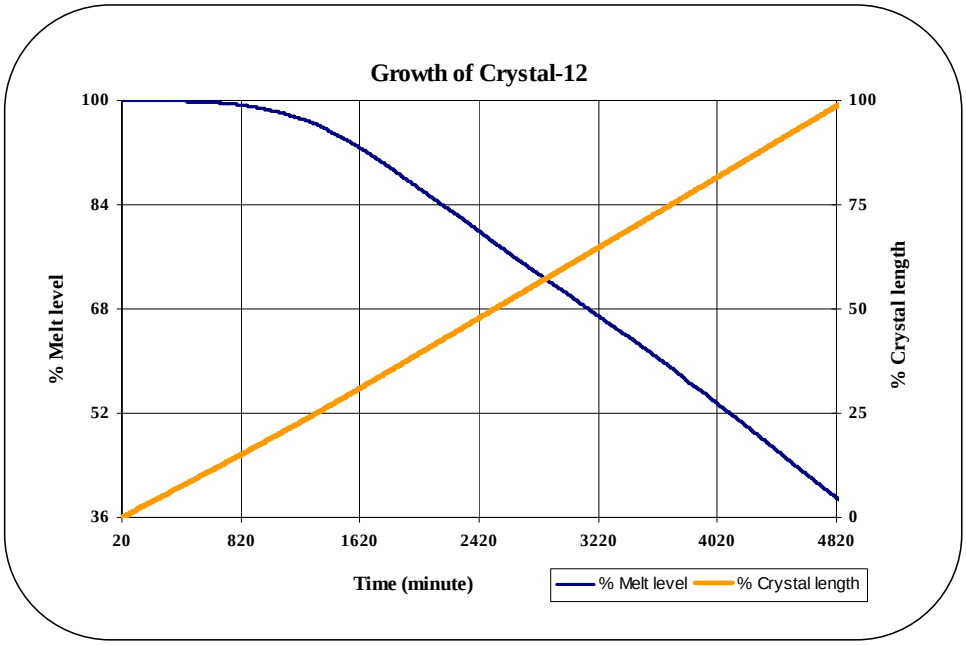

Figure 6-24: Crystal length and melt level graph for Crystal-12

After, analyzing these three crystals and growing a large diameter crystal using LRPC-PID, it was clear that the LRPC-MPC technique was better than the conventional PID control. For the small diameter crystal growth, various growth parameters were adjusted such that the growth becomes controllable. This is the first time a crystal growth dynamics was defined as a time varying delayed process. The results are promising and can lead to further optimization and design of a better control system to improve the crystal property and the growth performance.

CHAPTER 7: CONCLUSION

7.1 Conclusion

The crystal growth by Czochralski growth is a batch process. The process parameters change as the crystal grows. This is due to the change in heat and mass transfer dynamics of the growth system as the melt level decreases (or crystal length increases). These dynamics govern the growth stability and the thermal conditions at the growth interface, which in turn affects the crystal quality. The optimizations of the process parameters for such changes are very important for the repeatability and yield of the crystal.

For slow growing crystals, like LGT studied here, the delay between the system response and the control signal change is large and cannot be neglected. Conventional PID control does not consider this delay and creates sluggish response, which is not suitable for the growth of high-quality oxides. The objective of this work was first to identify the time delay and then study how this time delay changes as the melt level decreases and the crystal length increases during the growth. Once this has been identified, the variable time delay can be incorporated inside the control system by model prediction technique. Another aspect of the crystal control is to identify the model and model parameters that can be used for the prediction. Once these parameters are established, the long range model predictive control system can be designed to grow the crystals.

This work was divided in three parts:

- A few crystals were first grown to study the time delay throughout the crystal growth. It was found that as the crystal grows and the melt level decreases, the time-delay between the control signal change and the significant growth response, was increasing. Hence, the process model can be described as time-varying time delay model. The effective time delay was found between 8 to 20 minutes, which was later considered for the control design.
- The data gathered during the growth experiments, were analyzed for order of the model and the prediction accuracy. The large order model that covers the response was more accurate than small order model. However, during the real time model identification, the identification process was unstable for any small perturbation. Later, only pre-derived model with the suitable order was considered for control system design.
- The new control systems, LRPC-PID and LRPC-MPC, based on long-range predictive techniques, were developed and tested in real-time crystal growth. Both control systems performed satisfactorily after tuning them with delay and gain mapping. The constraints on the control signal and predictive horizon were also adjusted for crystal growth stability. At the end, a large diameter crystal was grown with the same control system to prove its effectiveness for any crystal growth.

It is important to mention that it is the first time that the delay factor was considered in the control system design for Czochralski crystal growth. In addition, it is the first time that different control models were compared in a single study and by using one crystalline material. This did allow to gain extensive knowledge on how and when the different models can (or cannot) be used. From our experiments, we could

demonstrate that the delay in response is a function of time, e.g. time-varying delay. In the following, the main aspects studied during this work, and main recognitions/results are summarized:

- The crystal growth was presented as the time-varying time delay process
- The time delay was shown as a function of the melt level or crystal height.
- The order of the process model for the prediction was defined.
- Failure of the real-time model identification process was studied. A pre-derived stable model was derived from the old growth data for the long range prediction.
- A unit less representation of the process model was derived so that the same control system could be applied to other diameter crystal growths of the similar material.
- The prediction horizon and mapping of the trajectory for the complete control horizon were designed. The time delay mapping and gain mapping with respect to crystal height was also adopted for control system.
- The constraints on the trajectory and control system were applied for stability.
- The lower order model was developed for simulation and pre-tuning of the process.
- The long range model predictive control system was developed using LRPC-PID and LRPC-MPC technique with time-varying horizon as time delay changes.
- Real-time implementation of the control system for testing and tuning of process parameter and control parameter was carried out.

7.2 Future work

This work was an initial work towards developing an advanced multiple models, parameters and constraints based predictive control. For the crystal growth, such

controller can not only control the growth process but also helps the operator to optimize the control to preserve the crystal quality in case of disturbance. The future work topics are divided in two parts as discussed here:

- Real-time model-identification and control:
    a. Instead of deriving a complete model during the real-time model identification, a suitable partial model identification method would be a better choice to derive a stable model. The model can be bounded in terms of settling time, stability, gain and other transient response parameters. These bounds can be calculated from the experiments. These bounds can change as the melt level changes during the growth and not the whole model. A recursive estimation of such higher order model with above bounds would be helpful in many real-time applications other than just a crystal growth process.
    b. Such process model can also be represented as a Fuzzy model. The identification of fuzzy model on real time process would also be a good area for further research. A fuzzy controller for the long range prediction and application to crystal growth can also be studied.
    c. Identification of unknown delay for time-varying delayed process would also be another topic of research. It has wide a range of applications and benefits to the control system and modeling area.
- Hysteresis and multiple model, parameter and constraints based predictive control:
    a. Hysteresis modeling: The crystal growth is a time delayed process. The heat generation dynamics and the heat loss dynamics creates hysteresis

loop in the response. This hysteresis not only changes with the melt level but also with the input (control signal) of the system. In other words, for larger input (control signal) the hysterias loop is small where as for small input, the process has higher hysterias region (wide). The multiple models of hysteresis for the different melt level and the input could be very helpful to control the process. Currently, the study of hysteresis system and control technique is an emerging research area in the control system. Applying this theory would be beneficial to improve the crystal growth control.

b Multiple parameters: Instead of presenting growth process as a single input and single output (SISO) model, other process parameters can be considered to develop a multi-input and multi-output control system. E.g. the pulling speed, rotation rate, crucible and crystal temperature, crystal and crucible position, magnetic field and atmospheric condition. The multi-input multi-output control system design can be different from the linear-cascade structure considered in this study.

c Multiple Constraints: The relation of the defect generation and the change in the temperature could help to develop various constraints that can minimize these defects. This time only two constraints were tested. The first one was on the controller speed by the controlling trajectory and the other one was on the limit of the control system output. Identification of the other constraints for preserving the quality of the crystal during the growth would be very important.

APPENDIX-A: ELECTRICAL AND INSTRUMENTATION DETAILS

The Controller unit is presented in Figure 4-1. Here, the description and setting of each component of this unit is discussed for the reference. There are mainly for components of this unit that are two National Instruments card for analog and digital input and output, motor controller and weight measurement system.

- NI multifunction card: AT-MIO-16E

This E Series device is a configured for an SCXI chassis (DAQ Card), which houses two other SCXI cards as shown in following figures. The first is SCXI-1121 with controller block SCXI-1328 for measuring thermocouple temperatures of R.F. Generator (Device 2, Channel 0) and cooling water system (Device 2, Channel 4) in differential mode. It also filters out the noise and amplifies the signals as per the preset notches inside the card.

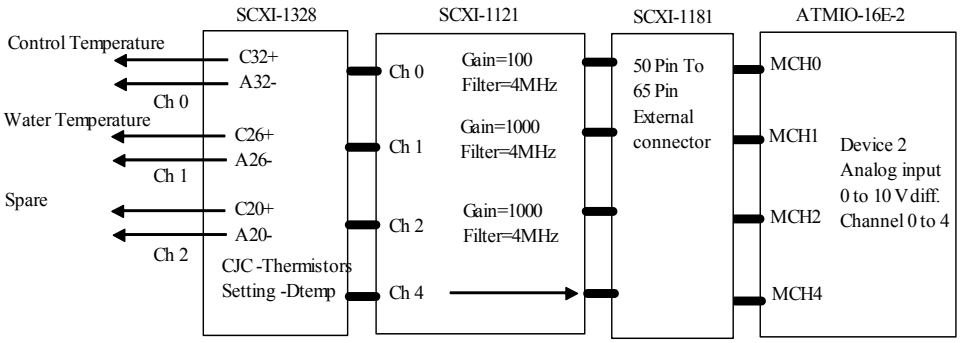

The E Series device also has two channels of Analog Output (AO) voltage with selectable reference and range using software. In present configuration, it is used to control Generator power (Device 2, Channel 1). The control signal is unipolar (0V to +10V).

- Motor control circuit

Max-100 servo motor drives are configured for adjusting the speed of rotation and pulling motor. Another AC motor is used for fast pulling. Magnetic coupler, which works on 90 V DC, is utilized to connect and disconnect the pulling servomotor as per the requirement. Solid-state relays are used to control the High current AC relay, which controls the devices. The complete connection diagrams are shown in following figures.

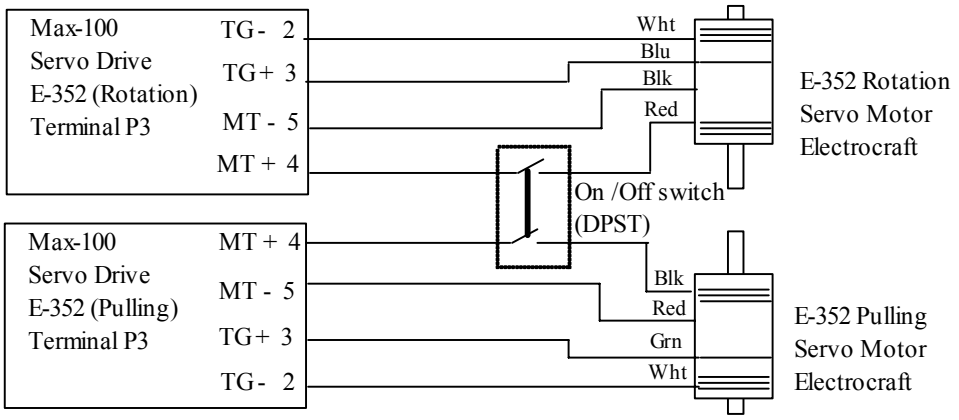

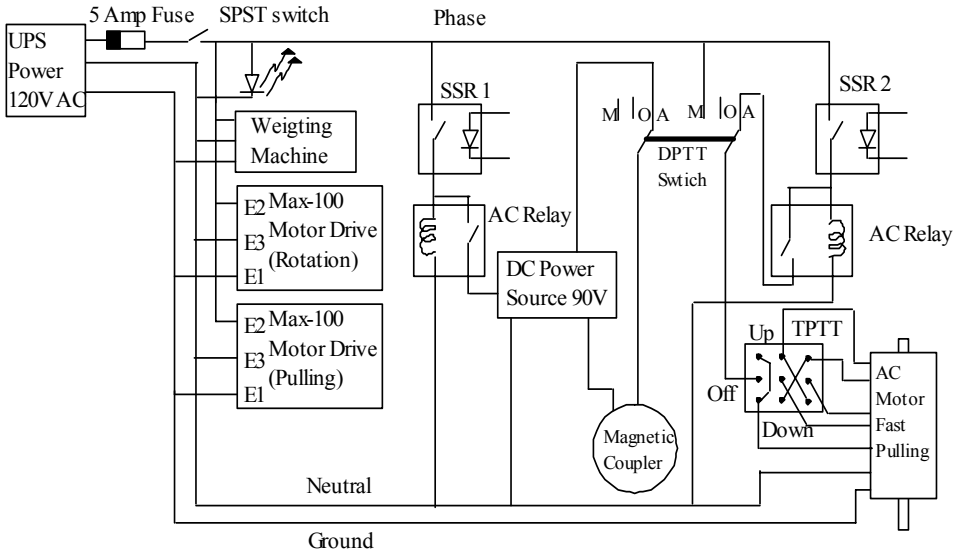

- Connector diagram weighing machine

Digital weight scale is used to measure the weight of crystal. This scale is connected to computer using RS-232 serial port (No. 0) as shown in the figure with following configuration. Baud Rate: 1200; Data bits: 7; Stop bits: 0; Parity: 1

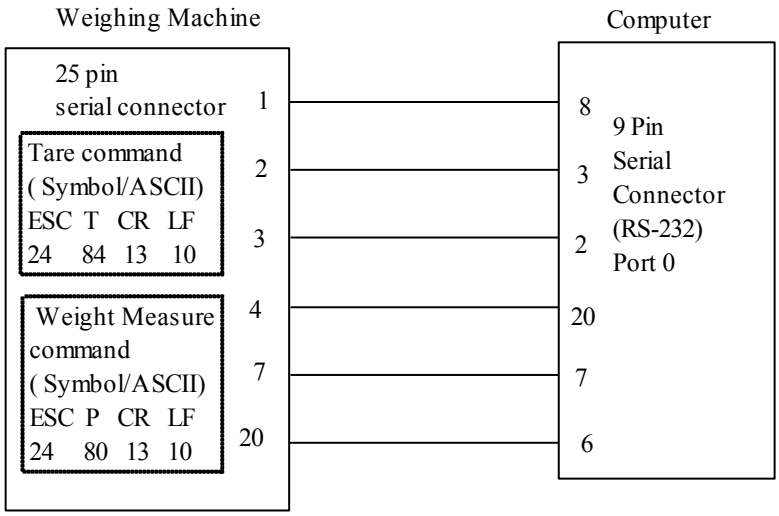

APPENDIX-B: ALGORITHEM FOR LRPC MPC TECHNIQUE

1. Calculate G matraix

$\rightarrow$ for $i = 0$ to $n_a \Rightarrow\ g_i = -\sum_{j=1}^{i} a_j \cdot g_{i-j} + \sum_{j=0}^{i} b_j$ = Vector

$\rightarrow$ for $\forall i < 0\ \Rightarrow\ g_i = 0$

2. Calculate F and G'_{d+i} matraix

$\rightarrow$ First row of $f_{i,j} \Rightarrow i = 0$

for $j = 0$ to $n_a - 1$ $\Rightarrow$ $f_{0,j} = a_j - a_{j+1}$

for $j = n_a$ $\Rightarrow$ $f_{0,n_a} = a_{n_a}$

$\rightarrow$ First row of $f_{i,j} \Rightarrow i = 1$ to $n_a - 1$

for $j = 0$ to $n_a - 1$ $\Rightarrow$ $f_{i,j} = f_{i-1,j+1} + (f_{i-1,0}) \cdot f_{0,j}$

for $j = n_a$ $\Rightarrow$ $f_{i,n_a} = (f_{i-1,0}) \cdot f_{0,n_a}$

3. Calculate G'_{d+i} matraix

$\rightarrow$ for $i = 0$ $\Rightarrow$ $G'_d = b_{n_b}$

$\rightarrow$ for $i = 1$ to n_a $\Rightarrow$ $G'_d = b_{n_b} \cdot f_{i-1,0}$

4. Calcualate P matrix: $P = [\delta G^T G + \lambda I]^{-1}$

$\rightarrow$ initialize $\delta(j) = (\alpha)^{n_a - j}$; $\lambda(j) = \lambda \cdot (\alpha)^{n_a - j}$

$\rightarrow$ $P^{-1}(k) = \lambda I \ \Rightarrow\ P_0(k) = 1/\lambda I$

$\rightarrow$ for $j = 1, ..., n_a$ with $h(k+1) = \delta r_j$

$\rightarrow$ $P_j = P_{j-1} - P_{j-1} \cdot h \cdot \left(1 + h^T \cdot P_{j-1} \cdot h\right)^{-1} \cdot h^T \cdot P_{j-1}$

$\rightarrow$ $P_{n_a} = [1 \quad .. \quad 1][\delta G^T G + \lambda I]^{-1}$

5. Calculate K matrix : $K = \left[\text{ First row of matrix } P_{n_a}\right] G^T$

$\rightarrow$ $K_i = \sum_{j=0}^{i} P_j \cdot g_{i-j}$ for $i = 1, ..., n_a$

6. Calculating control signal

$\rightarrow$ $\Delta u_{1\times 1}(k) = \delta K_{1\times N_a} (W - f)_{N_a \times 1}$

$\rightarrow$ $u(k) = u(k-1) + \Delta u(k)$

REFRENCES

[1] DTJ. Hurle, "Crystal Pulling From the Melt", Springer-Verlay, 1993.

[2] DTJ. Hurle, "Control of Diameter in Czochralski and Related Crystal Growth Techniques", Journal of Crystal Growth 42, 1977, Page 473-482.

[3] N. Kobayashi, "Heat Transfer in Czochralski Crystal Growth". In Preparation and Properties of Solid State Materials, Ed. WR Wilcox, Dekker, New York, 1981.

[4] B. Chai, J. L. Leafucheur, Y.Y. Ji and H. Qiu, "Growth and Evaluation of Large Size LGS ($La_3Ga_3SiO_{14}$), LGN ($La_3Ga_{5.5}Nb_{0.5}O_{14}$) & LGT ($La_3Ga_{5.5}Ta_{0.5}O_{14}$) Single Crystal", IEED International Frequency Control Symposium, 1998, Page 748-760.

[5] Hyoung Jung, Jung Min Ko, Kwang Bo Shim, Tsuguo Fukudu and Keun Ho Auh, "Influence of Starting Melt Composition on $La_3(Ta_xGa_{1-x})Ga_5O_{15}$ Crystal Grown by Czochralski Method", Journal of Crystal Growth 200, 2000, Page 275-280.

[6] S.V. Tsivinsky, "Dislocation Density in Pure Crystal Grown from Melts", Kristall und Technik 10, 1975, Page 5-35.

[7] C.D. Brandle, "Czochralski Growth of Oxides", Journal of Crystal Growth 264, 2004, Page 593-604.

[8] M.A. Gevelber and G. Stephanopoulos, "Dynamics and Control of the Czochralski Process-I", Journal of crystal growth 84, 1987, 647-668.

[9] M.A. Gevelber, G. Stephanopoulos and M.J.Wargo, "Dynamics and Control of the Czochralski Process-II", Journal of crystal growth 91, 1988, 199-217.

[10] M.A. Gevelber, M.J. Wargo and G. Stephanopoulos, "Advanced Control Design Considerations for the Czochralski Process", Journal of crystal growth 85, 1987, 256-263.

[11] DTJ Hurle, "Dynamics, Stability and Control of Czochralski Growth", Journal of Crystal Growth 128, 1993, Page 15-25.

[12] J.P. Wilde, Lamberturs Hesselink and Robert S. Feigelson, "Diameter Stabilization of Czochralski-grown $Sr_{0.61}Ba_{0.39}Nb_2O_6$ (SBN) Crystals Using Real-time Computer Control", Journal of Crystal Growth 113, 1991, Page 337-359.

[13] M.D. Aggarwal, R. Metzl, W.S Wang and J. Choi, "A Versatile Czochralski Crystal Growth System with Automatic Diameter Control", Review of Scientific Instruments 66, n 7, July 1995, Page 3939-3942.

[14] M. Malek-Zavarei and M. Jamshidi, "Time-Delay Systems: Analysis, optimization and applications", North-Holland Systems and Control series – 9, Elsevier Science publishing, Netherland, 1987.

[15] P.B. Deshpande and R.H. Ash, "Elements of Computer Process Control", ISA, 1981.

[16] E.F. Camacho and C. Bordons, "Model Predictive Control in the Process", Springer-verlay, 1995.

[17] K.J. Åström, and B. Wittenmark, "Adaptive Control", Addison - Wesley, Massachusetts, 1989.

[18] L. Ljung, "System Identification: Theory for the User", Printice-Hall, Englwood cliffs, N.J., 1987.

[19] G. Favier, D. Dubois and C. Rougerie, "A Review of k-step ahead Predictors", IFAC Proceeding on System Identification Parameters Estimation 2, 1988, Page 887-893.

[20] D.W. Clarke, C. Mohtadi and P.S. Tuffs, "Generalized Predictive Control Part 1 and 2", Automatica 23-2, 1987, Page 137-160.

[21] D.W. Clarke, "Advances in Model-based Predictive Control", Oxford University Press, Oxford, 1994.

[22] J.R. Gossner, B. Kouvaritakis and J.A. Rossiter, "Stable Generalized Predictive Control with Constraints and Bounded disturbances", Automatica 33, 1997, Page 681-700.

[23] T. Alvarez and C. Panda, "Handling Infeasibility in Predictive control", Computers and Chemical engineering 21, 1997, Page 577-582.

[24] R.M.C De Keyser, Ph. G.A. Van de Velde and F.G.A Dumortier, "A Comparative Study of Self-adaptive Long Range Predictive Control Methods", Automatica 24-2, 1988, Page 149-163.

[25] R.M.C. De Keyser and A. Van Cauwenberghe, "Extended Prediction Self-adaptive Control", IFAC Symposium on Identification and System Parameter Estimation", 1985, Page 1255-1260.

[26] D.W. Clarke and L. Zhang, "Long-range Predictive Control using Weighting-sequence Model", Proceeding IEE – 134, Pt-D, 1987, Page 187-195.

[27] W. Bardsley, G.W. Green, C.J. Holliday and DTJ Hurle, "The Weighing Method of Automatic Czochralski Crystal Growth-I", Journal of Crystal Growth 40, 1977, Page 13-20.

[28] W. Bardsley, G.W. Green, C.J. Holliday and DTJ Hurle, "The Weighing Method of Automatic Czochralski Crystal Growth-II", Journal of Crystal Growth 401, 1977, Page 21-28.

[29] G.C. Joyce, DTJ Hurle and Q.A.E. Vaughan, "Novel Development of the Weighting Method for Automatic Czochralski Crystal Growth of Semiconductors", Journal of Crystal Growth 100, 1990, Page 11-25.

[30] Nikolai V. Abrosimov, Vladimir. N. Kurlov and Sergei. Rossolenko, "Automated Control of Czochralski and Shaped Crystal Growth Process using Weighing Techniques", Progress in Crystal Growth and Characterization of Materials, 2003, Page 1-57.

[31] DTJ Hurle, G.C. Joyce, M. Ghassempoory, A.B. Crowely and E.J. Stern, "The Dynamics of Czochralski Growth", Journal of Crystal Growth 100, 1990, Page 11-25.

[32] J.J. Derby and R.A. Brown, "On the Dynamics of the Czochralski Crystal Growth", Journal of Crystal Growth 83, 1987, Page 137-151.

[33] Roberto Irizarry-Rivera and Warren Seider, "Model-predictive Control of the Czochralski Crystallization Process", Journal of Crystal Growth 178, 1997, Page 593-633.

[34] Michael Gevelber, Danielle Wilson and Ning Duanmu, "Modeling Requirements for Development of an Advanced Czochralski Control System", Journal of Crystal Growth 230, 2001, Page 217-223.

[35] Antonios Armaou and Panagiotis Christofides, "Crystal Temperature Control in the Czochralski Crystal Growth Process", Process System Engineering, AIChE Journal 47, n-1, January 2001, Page 79-106.

[36] Haihong Qiu, "Development of a Computer Control System with Self-tuning Growth Rate Control for the Czochralski Crystal Growth Process", PhD Thesis, University of Central Florida, 1997.

[37] J.J. Derby and R.A. Brown, “Thermal-Capillary Analysis of Czochralski and Liquid Encapsulated Czochralski Crystal Growth”, Journal of Crystal Growth 75, 1986, Page 227-240.

[38] K. Rieding, “Autonomous Liquid Encapsulated Czochralski Growth of Single Crystal GaAs by Intelligent Digital Control”, Journal of Crystal Growth 89, 1988, Page 435-446.

[39] Peter Sveshtarov and Marvin Gospodinov, “The Effect of the Interface Shape on Automatic Czochralski Weight Diameter Control System Performance”, Journal of Crystal Growth 113, 1991, Page 186-208.

[40] S.H. Lee, V.J. Kim, S.H. Cho and E.P. Yoon, “The Influence of the Czochralski Growth Parameters on the Growth of Lithium Niobate Single Crystals”, Journal of Crystal Growth 125, 1992, Page 175-180.

[41] Christine Klemenz, Jun Luo and Dhaval Shah, In: 29th International Conference on Advanced Ceramics and Composites, Cocoa Beach FL, 2005.

[42] J. Luo, D. Shah, C.F. Klemenz, M. Dudley, H. Chen, Journal of Crystal Growth 287 (2006) p. 300-304.

[43] Dhaval S. Shah and Christine F.Klemenz, In: IEEE International Frequency Control Symposium (2006) p. 196-200.

[44] H. Stao, M. Kumatoriya and T. Fujii, “Control of the Facet Plane Formation on Solid-Liquid Interface of LGS”, Journal of Crystal Growth 242, 2002, Page 177-182.

[45] Dhaval S. Shah, “Application of Model Reference Adaptive Control for Czochralski Crystal Growth Technique”, MS Thesis, University of Central Florida, 2004.

[46] M.S. Grewal and A.P. Andrews, “Kalman Filtering: Theory and Practice”, Printice Hall, Englwood Chiffs, NJ, 1993.

[47] H. Akaike, “A New Look at Statistical Model Identification”, IEEE Transaction on Automatic Control 19, no 6, 1974, Page 716-723.

[48] G. Schwarz, “Estimating the Dimension of a Model”, Analytical Statistics 6, no-2, 1978, Page 461-464.

[49] Sarkar, P.P. Kanjilal, “On a Method of Identification of Best Subset Model from Full AR Model”. Communications in Statistics –Theory and Methods – 24, No-6, Page 1551-1567.

[50] P. Young, “Recursive Estimation and Time Series Analysis, an Introduction”, Springer-verlag, Berlin, 1984.

[51] R.R. Hocking, “Development in Linear Regression Methodology 1959-1982”, Technomatrics-25, no 3, 1983, Page 219-249.

[52] S. Boyd, L El Ghaouni, E. Feron and V. Balakrishnan, “Linear Matrix Inequalities in Systems and Control Theory”, SIAM books, 1994.

[53] G.J. Bierman, “Factorization Method for Discrete Sequential Estimation”, Academic Press, New York, 1977.

[54] Wai Gao, Miao Lei Zhou, Yuan Chun Li and Tao Zhang, “An Adaptive Generalized Predictive Control of Time-Varying Delay System”, Proceeding of the Third International Conference on Machine learning and Cybernetics, Shanghai, 26-29, August 2004, Page 878-881.

[55] Zheng and Feng, “Identification of Stochastic Time Lag Systems in the Presence of Colored Noise”, Automatica 26, 1990, Page 769-779.